



LEHIGH  
UNIVERSITY

Library &  
Technology  
Services

The Preserve: Lehigh Library Digital Collections

# The Determination Of Moment Distribution Constants Of Members With A Variable Moment Of Inertia.

## Citation

ONDRA, OTAKAR. *The Determination Of Moment Distribution Constants Of Members With A Variable Moment Of Inertia*. 1955, <https://preserve.lehigh.edu/lehigh-scholarship/graduate-publications-theses-dissertations/theses-dissertations/determination-31>.

Find more at <https://preserve.lehigh.edu/>

*This document is brought to you for free and open access by Lehigh Preserve. It has been accepted for inclusion by an authorized administrator of Lehigh Preserve. For more information, please contact [preserve@lehigh.edu](mailto:preserve@lehigh.edu).*

# DOCTORAL DISSERTATION SERIES

Publication No. : 15,332

**AUTHOR:** Otakar Ondra, Ph. D., 1955  
Lehigh University

**TITLE:** THE DETERMINATION OF MOMENT  
DISTRIBUTION CONSTANTS OF  
MEMBERS WITH A VARIABLE MOMENT  
OF INERTIA

University Microfilms, Ann Arbor, Michigan

THE DETERMINATION OF MOMENT DISTRIBUTION CONSTANTS  
OF MEMBERS WITH A VARIABLE MOMENT OF INERTIA

by

Otakar Ondra

A DISSERTATION

Presented to the Graduate Faculty

of Lehigh University

in Candidacy for the Degree of

Doctor of Philosophy

Lehigh University

1955

Approved and recommended for acceptance  
as a dissertation in partial fulfillment of the requirements  
for the degree of Doctor of Philosophy.

Sept. 30, 1955

Wm. J. Eney  
Professor in Charge

Accepted, September 30, 1955

Special committee directing the doctoral work  
of Mr. Otakar Ondra

Ferdinand P. Beer Chairman

C. D. Jensen

E. Russell Toombs Jr

C. A. Shook

W. J. Eney

### ACKNOWLEDGMENT

The author wishes to acknowledge a debt he owes to Professor William J. Eney, pioneer, inventor, and authority in the field of mechanical methods of stress determination.

This debt dates back to the time when the author, then a resident graduate student at Lehigh University, was first introduced by Professor Eney to the analysis of statically indeterminate structures by means of elastic models. Professor Eney's leadership, inventiveness and keen discernment in the solving of complex problems of structural analysis were unfailing sources of inspiration and incentive to the author in his own teaching career and in the pursuit of this investigation.

More recently, Professor Eney, despite his numerous other duties as administrator, director of research, and educator, accepted the role of mentor of this dissertation. His many constructive suggestions, his genuine interest, and the unstinted time he devoted to this paper and the author are gratefully acknowledged and deeply appreciated.

## TABLE OF CONTENTS

	Page
SYNOPSIS - - - - -	1
I - INTRODUCTION - - - - -	2
II - BEAMS - - - - -	5
1. General	5
2. Carry-Over Factor	6
3. Stiffness Factor	11
4. Modified Stiffness Factor	12
5. Relationship between the Stiffness Factor and the Pressure Solid	14
Example 1 - Deepened Beam. Carry-Over and Stiffness Factors	17
Example 2 - Haunched Beam. Carry-Over and Stiffness Factors	19
6. Making and Weighing the Model	21
7. Verification of Experimental Data and Results	24
8. Fixed End Moments in Beams	27
Example 3 - Deepened Beam. Carry-Over and Stiffness Factors; Fixed End Moments	32
9. Fixed End Moment	35
10. Fixed End Moments. Uniformly Distributed Load	37
11. Influence Lines for Fixed End Moments	38
12. Moments Caused by Impressed Distortions	39
13. Shear Stiffness and Flexibility	41
14. Correlation between Model and Prototype	43
Example 4 - Deepened Beam. Absolute Stiffness Factors; Moments Due to Impressed Distortions; Absolute Shear Stiffness	44

	Page
15. Accuracy of the Experimental Method	48
III - SYMMETRICAL ARCHES - - - - -	52
1. General	52
2. Carry-Over Factor	53
3. Stiffness Factor	57
4. Experimental Determination of Carry-Over and Stiffness Factors	61
5. Equivalent Arch Models	65
Example 5 - Deepened 120° Circular Arch. Carry-Over and Stiffness Factors	71
6. Modified Stiffness Factor	74
Example 6 - Elliptical Arch of Constant Moment of Inertia. Carry-Over and Stiffness Factors; Modified Stiffness Factor	76
7. Accuracy of the Experimental Method	77
8. Fixed End Moments	80
9. Influence Lines for Thrust, Shear and Fixed End Moment	82
Example 7 - Elliptical Arch. Influence Lines for Reactions	85
10. Discussion of the Semi-Experimental Method	93
11. Fixed End Moment	94
Example 8 - Elliptical Arch. Fixed End Moment	94
IV - THE EFFECT OF IMPRESSED DISTORTIONS IN SYMMETRICAL ARCHES - - - - -	95
1. Lineal Displacement	95
2. Rotation	96
3. Thrust Stiffness	96
Example 9 - Elliptical Arch. Effects of Settlement, Rotation, Temperature Change, Rib Shortening	98

	Page
4. Discussion	100
5. Arch Fixed at One End and Hinged at the Other	101
6. Arch Hinged at Both Ends	104
7. Discussion	105
V - CONCLUSION - - - - -	106
VI - APPENDIX. Analytic Solutions of Examples 1 to 9	109
Bibliography	129
Vita	130



## SYNOPSIS

This paper describes and illustrates an experimental method of determining the moment distribution constants for beams and symmetrical arches with variable moments of inertia.

The method does not rely upon the use of deformer-type gages or other special instruments such as are used in the well known experimental methods developed by G. E. Beggs, W. J. Eney, and others. It is based on the concept of a three-dimensional  $M/EI$  solid whose properties are functions of the loads, slopes, and deflections of the statically indeterminate member which it represents. It is shown that each of the moment distribution constants is a function of a ratio  $J/Q$  which also defines the location of the center of gravity of the  $M/EI$  solid. This ratio is evaluated experimentally by weighing the solid and by the use of statics. Mathematical integration or the approximate summation process are replaced by weighing, resulting in considerably simpler calculations and a greater reliability of results in comparison with standard methods of analysis.

Once the moment distribution constants are known the Cross method of balancing moments is relatively simple to apply.

## I - INTRODUCTION

1. The Problem Defined. - In applying the moment distribution method of analysis to a given problem several factors or constants must be determined before the process of balancing moments can be carried out. In general, these constants include fixed end moments due to loads, carry-over, stiffness and distribution factors, thrust stiffness, flexibility, etc. In the case of beams with a constant moment of inertia the determination of these factors presents no difficulties inasmuch as they are simple functions of the span, moment of inertia, modulus of elasticity, etc., of the member considered.

For beams with variable moments of inertia and arches of either constant or variable moment of inertia the determination of the moment distribution constants is generally difficult. This is especially true of arches where complex functions involving integral calculus must be evaluated. In practice, the approximate summation process is frequently substituted for mathematical integration, or graphics are used. Although the work is greatly simplified, the necessary tabular computations or graphic constructions are cumbersome and time-consuming. Moreover, the various methods of analysis are closely related to each other so that it is generally impossible to check results by an algebraically independent method.

The experimental method of mechanical analysis applied by the late Professor G. E. Beggs of Princeton University, and the more recent general methods of determining moment distribution constants developed by Professor W. J. Eney of Lehigh University<sup>(1)</sup>, constitute a noteworthy simplification of the problem.

2. The Method. - It will be shown in chapters II, III and IV of this paper that the moment distribution constants for members with constant or variable moments of inertia exhibit a common parameter  $J/Q$  in which  $J$  and  $Q$  are the second and first moments, respectively, of the integral  $A = \int \frac{ds}{EI}$ , in which  $ds$  is an infinitesimal element of length measured along the longitudinal axis of the member and  $EI$  is its flexural stiffness.

It will be recalled that in hydrostatics an analogous ratio  $J/Q$  defines the location of the so-called center of pressure upon a submerged plane surface exposed to hydrostatic pressure of the liquid above it. Since hydrostatic pressure increases linearly with the depth of submersion, the relationship between the magnitude of the resultant hydrostatic pressure and the size and configuration of the submerged area may be represented by a wedge-shaped "pressure solid" whose base is the area under consideration and whose altitudes vary linearly.

---

<sup>(1)</sup> W. J. Eney, "Fixed Ended Moments by Cardboard Models," *Engineering News-Record*, December 12, 1935.

In the conjugate beam, neutral point, and column analogy methods of analysis of restrained members, the  $M/EI$  or the  $M$  - diagram is used as a load acting upon a fictitious beam, cut-back structure, or analogous column section. In all three of these methods the bending moment  $M$  varies linearly with the  $x$ -distance referred to one end of the member. In the conjugate beam and the neutral point methods the integral  $\int \frac{M}{EI} ds$  is conceived as a two-dimensional diagram so that in a general case the variation of the ordinates  $M/EI$  is no longer linear. The moment-area method is closely related to the conjugate beam method. In the column analogy method, the reciprocal of flexural stiffness  $EI$  is conceived as a width so that  $M$ ,  $ds$ , and  $1/EI$  constitute a three-dimensional orthogonal coordinate system. The integral  $\int \frac{M}{EI} ds$  is represented by a load of linearly varying intensity acting upon an area  $A = \int \frac{ds}{EI}$ .

In the following chapters the moment distribution constants are expressed as functions of the ratio  $J/Q$ , and the analogy between the "pressure solid" and the load diagram is utilized in determining the required load-slope-deflection relationships.

## II - BEAMS

1. General. - The variation of the moment of inertia in beams and girders may be achieved in several ways. In structural steel rolled sections the web is usually kept constant and the variation of  $I$  is obtained by using cover plates of different lengths arranged in stepwise fashion. In built up steel girders the web may be varied and the flange kept constant, or both may be varied. Members made of reinforced concrete may have a variable cross section and a constant percentage of reinforcement or vice versa, or both the outside dimensions and the steel concentration may be varied.

Steel and concrete members with non-parallel intrados and extrados (curved and markedly haunched beams, etc.) may have the appearance of what is architecturally known as an arch. From the viewpoint of the designer the term "arch" is misleading inasmuch as it is impossible to draw a sharp distinction between a "curved beam" and a "flat arch." The latter produces a greater amount of lateral thrust against the abutments and its stability depends upon the lateral resistance of the supporting abutments or walls. Curved beams with a small radius of curvature (hooks, etc.) in which shearing stresses and deformations are of primary importance are not included in either classification.

2. Carry-Over Factor. - By definition, the carry-over factor of a flexural member is the ratio of the moment induced at the fixed end of the member to the moment causing rotation at the other simply supported end. In Fig. 1a, a beam simply supported at a and fixed at b is subjected to a moment  $M_a$  at a,

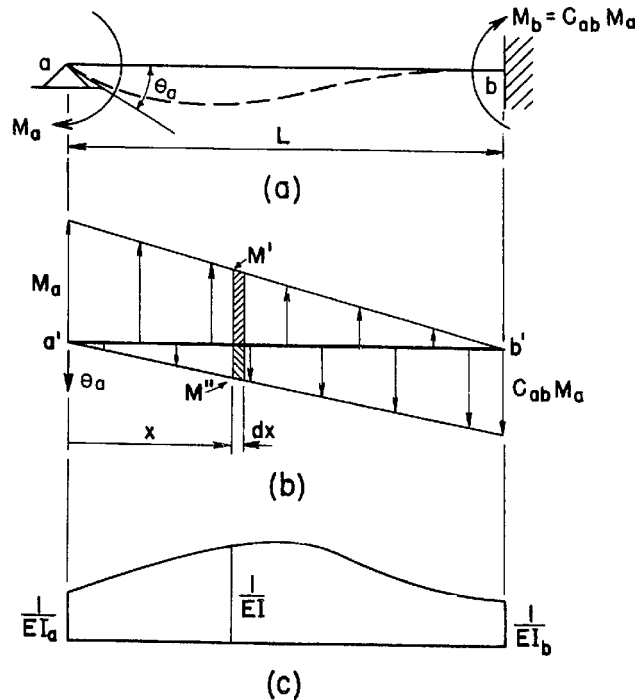


Fig. 1

causing a moment  $C_{ab} M_a$  at b, in which  $C_{ab}$  is the carry-over factor from a to b. The bending moment diagram for beam ab is drawn in Fig. 1b and Fig. 1c shows the variation of the  $1/EI$ -values of the beam along its span. In the conjugate beam method of analysis the  $M/EI$ -diagram is the load applied to a fictitious beam a'b' having the same span  $L$  as the real beam. the shears in this fictitious or conjugate beam correspond to the slopes of the real beam ab, and the bending moments correspond to its deflections. Accordingly, the conjugate beam in Fig. 1b is simply supported at a' and free at the other end b'.

The equilibrium of the conjugate beam requires that the sum of moments of the loads about any point be zero.

Taking moments about  $\underline{a'}$ , the condition of equilibrium is

$$-\int_{a'}^{b'} \frac{M' dx}{EI} x + \int_{a'}^{b'} \frac{M'' dx}{EI} x = 0 \quad \text{Eq. 1}$$

But 
$$\frac{M'}{L-x} = \frac{M_a}{L}$$

Substituting for  $M'$  and  $M''$  in Eq. 1,

$$-\frac{M_a}{L} \int_{a'}^{b'} \frac{(L-x) x}{EI} dx + \frac{C_{ab} M_a}{L} \int_{a'}^{b'} \frac{x^2}{EI} dx = 0$$

whence

$$C_{ab} = \frac{L \int_{a'}^{b'} \frac{x dx}{EI} - \int_{a'}^{b'} \frac{x^2 dx}{EI}}{\int_{a'}^{b'} \frac{x^2 dx}{EI}} \quad \text{Eq. 2}$$

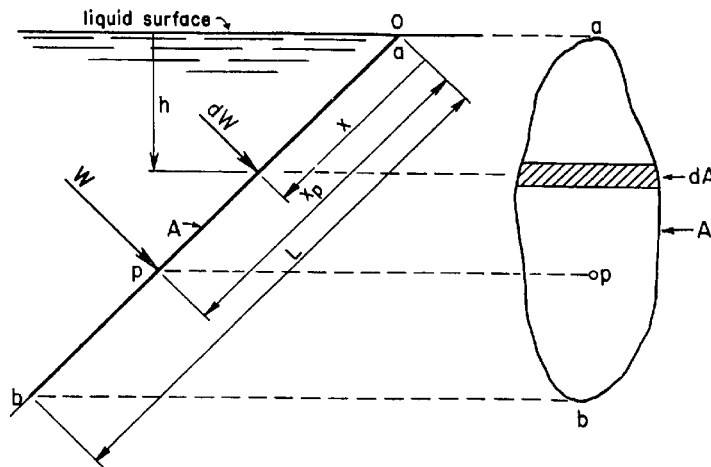
Introducing the notation

$$\left. \begin{aligned} \int_{a'}^{b'} \frac{dx}{EI} &= A \\ \int_{a'}^{b'} \frac{x dx}{EI} &= Q \\ \int_{a'}^{b'} \frac{x^2 dx}{EI} &= J \end{aligned} \right\} \quad \text{Eqs. 3}$$

Eq. 2 becomes

$$C_{ab} = \frac{LQ - J}{J} = \frac{Q}{J} L - 1 \quad \text{Eq. 4}$$

Fig. 2 represents a plane surface  $ab$  submerged in a liquid with a free surface. Its area  $A$  is subjected to



hydrostatic pressure forces whose resultant  $W$  passes through the so-called center of pressure,  $p$ . By taking the sum of moments of elemental forces  $dW$  about axis  $O$  it can be readily

Fig. 2

shown that the center of pressure is located at a distance

$$x_p = \frac{J}{Q} \quad \text{Eq. 5}$$

in which  $x_p$  is referred to axis  $O$ , and  $J$  and  $Q$  are the second and first moments, respectively, of area  $A$  about the same axis.

Since the unit pressure forces vary linearly with the depth of submersion  $h$ , the total force  $W$  on area  $A$  may be

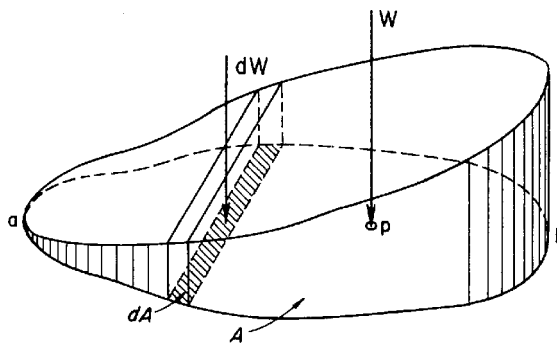


Fig. 3

represented by the weight of a solid whose base has the same configuration and area as the surface  $ab$  and whose altitudes vary linearly. Such a "pressure solid" is shown in Fig. 3.



Fig. 4 represents the elevation of the pressure solid shown in Fig. 3. Let the solid be simply supported at a

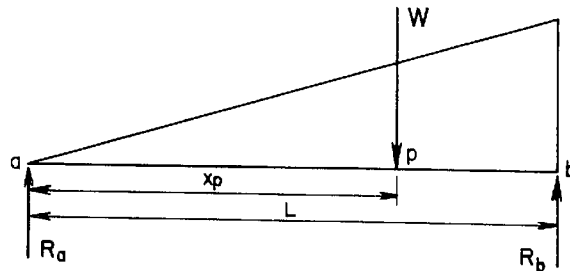


Fig. 4

and b. Taking the sum of moments of forces about the center of pressure p,

$$R_a x_p = R_b (L - x_p)$$

$$\text{or } x_p = \frac{R_b L}{R_a + R_b}$$

But

$$R_a + R_b = W$$

so that

$$x_p = \frac{J}{Q} = \frac{R_b L}{W} \quad \text{Eq. 6}$$

Since quantities  $J$  and  $Q$  in Eqs. 4 and 6, respectively, are identical functions of areas  $A$ , the carry-over factor given by Eq. 4 may be expressed in terms of the pressure solid forces, that is,

$$C_{ab} = \frac{Q}{J} L - 1 = \frac{W}{R_b} - 1 = \frac{R_a}{R_b} \quad \text{Eq. 7}$$

If the beam has a constant moment of inertia, the body force (or resultant pressure) is located at a distance  $x_p = \frac{2}{3} L$ , and the carry-over factor is

$$C_{ab} = \frac{W \frac{L}{3}}{W \frac{2L}{3}} = \frac{1}{2}$$

An alternate derivation of Eq. 7 is based on Maxwell-Mohr reciprocal theorem and the conjugate beam properties.

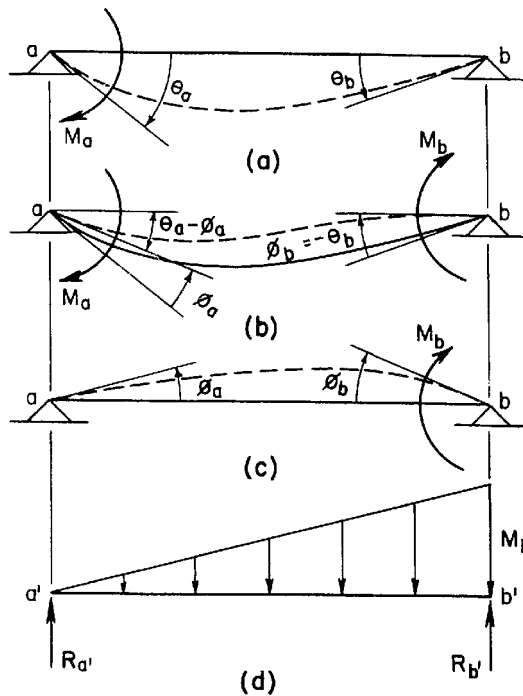


Fig. 5

In Fig. 5a, the beam is simply supported at a and b. An arbitrary moment  $M_a$  is applied at a causing end rotations  $\theta_a$  and  $\theta_b$  as shown. In Fig. 5b, an additional moment load  $M_b$  is applied at b, inducing rotations  $\phi_b$  and  $\phi_a$  at ends b and a. Let the magnitude of  $M_b$  be such that  $\phi_b = -\theta_b$  so that the net rotation at b caused by  $M_a$  and  $M_b$  is zero.

According to Maxwell-Mohr theorem of reciprocal rotations (an application of the more general reciprocal theorem <sup>2)</sup>),

$$M_b (-\theta_b) = M_a (\phi_a)$$

Since  $\theta_b = -\phi_b$ ,

$$\frac{M_b}{M_a} = \frac{\phi_a}{\phi_b}$$

Since moment  $M_b$  prevents the rotation at b that would be induced by moment load  $M_a$  applied at a, it is the fixed end moment at b. It follows that the ratio of the two moments is the carry-over factor from a to b,

$$C_{ab} = \frac{M_b}{M_a} = \frac{\phi_a}{\phi_b} \quad \text{Eq. 8}$$

<sup>2)</sup> See derivation in "Statically Indeterminate Structures" by L.C. Maugh, page 11.

It may be concluded from the definition of the angle changes  $\phi_b$  and  $\phi_a$  that if an arbitrary moment  $M_b$  is applied at b (Fig. 5c), the ratio  $\phi_a/\phi_b$  is the carry-over factor from a to b. The magnitude of  $M_b$  is immaterial inasmuch as no restrictions were placed on the magnitude of  $M_a$  at the outset of the derivation.

Rotations  $\phi_a$  and  $\phi_b$  correspond to shears at a' and b' in the conjugate beam caused by the  $M/EI$  diagram used as a load. Expressing the total load as  $\int \frac{1}{EI} M dx$  where  $M$  varies linearly as is shown in Fig. 5d, the concept of the "pressure solid" (or three-dimensional conjugate beam) is evolved by visualizing the  $1/EI$ -values as variable widths of its base area  $\int \frac{dx}{EI}$ . The ratio  $R_{a'}/R_{b'}$  is the carry-over factor from a to b.

3. Stiffness Factor. - The stiffness factor at the simply supported end of a flexural member is defined as the moment required to rotate that end through a unit angle while the other end is held fixed. In Fig. 1a,  $M_a$  is the stiffness factor  $S_a$  at a when  $\theta_a$  is a unit angle in radian measure.

Taking the sum of moments about b' in Fig. 1b,

$$-\theta_a L + \int_a^b \frac{M' dx}{EI} (L-x) - \int_a^b \frac{M'' dx}{EI} (L-x) = 0$$

or

$$-L + \frac{S_a}{L} \int_a^b \frac{(L-x)^2}{EI} dx - \frac{C_{ab} S_a}{L} \int_a^b \frac{(L-x)x}{EI} dx = 0$$

from which

$$S_a \left[ L^2 \int_a^b \frac{dx}{EI} - 2L \int_a^b \frac{x dx}{EI} + \int_a^b \frac{x^2 dx}{EI} - C_{ab} \left( L \int_a^b \frac{x dx}{EI} - \int_a^b \frac{x^2 dx}{EI} \right) \right] = L^2 \quad \text{Eq. 9}$$

In terms of Eqs. 3 and 4 the last equation becomes

$$S_a \left[ L^2 A - 2LQ + J - \frac{L^2 Q^2 - LQJ}{J} + LQ - J \right] = L^2$$

which reduces to

$$S_a = \frac{I}{A - \frac{Q^2}{J}} \quad \text{Eq. 10}$$

If the moment of inertia of the beam is constant Eq. 10 yields

$$S_a = \frac{I}{\frac{I}{EI} L - \frac{\left( \frac{I}{EI} L \frac{L}{2} \right)^2}{\frac{I}{3} \frac{I}{EI} L^3}} = \frac{4EI}{L}$$

4. Modified Stiffness Factor. - The modified stiffness factor  $S'_a$  is the moment which must be applied at a to rotate that end through a unit angle while the other end b is simply supported.

When b is a simple support, the carry-over factor from a to b is zero so that Eq. 9 reduces to

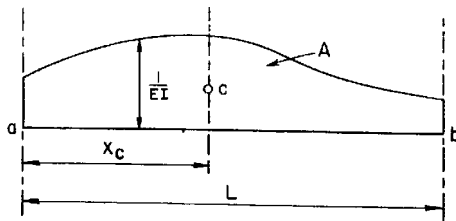
$$S'_a \left[ L^2 A - 2LQ + J_a \right] = L^2 \quad \text{Eq. 11}$$

in which  $J_a = J$  is the second moment of area  $A$  about the vertical axis through  $\underline{a}$ .

Applying the parallel-axis theorem of second moments of area  $A$ ,

$$\left. \begin{aligned} J_a &= J_c + A x_c^2 \\ J_b &= J_c + A (L - x_c)^2 \end{aligned} \right\}$$

where  $J_a$  and  $J_b$  are the second moments of  $A$  about axes



through  $\underline{a}$  and  $\underline{b}$ , respectively,

$J_c$  is the second moment of  $A$  about the centroidal axis of  $A$ ,

and  $x_c$  is the distance of the

centroid of  $A$  from  $\underline{a}$  (Fig. 6).

Fig. 6

Eliminating  $J_c$  from the last two equations,

$$J_a = J_b - AL^2 + 2ALx_c$$

and substituting for  $J_a$  in Eq. 11,

$$S'_a [-2LQ + J_b + 2ALx_c] = L^2$$

But  $2ALx_c = 2LQ$

Therefore, the modified stiffness factor at  $\underline{a}$  is

$$S'_a = \frac{L^2}{J_b} \quad \text{Eq. 12}$$

If the beam has a constant moment of inertia, Eq. 12 yields

$$S'_a = \frac{L^2}{\frac{1}{3} \frac{1}{EI} L^3} = \frac{3EI}{L} = \frac{3}{4} S_a$$

5. Relationship between the Stiffness Factor and the Pressure Solid. - Fig. 7a represents a deepened beam for which it is

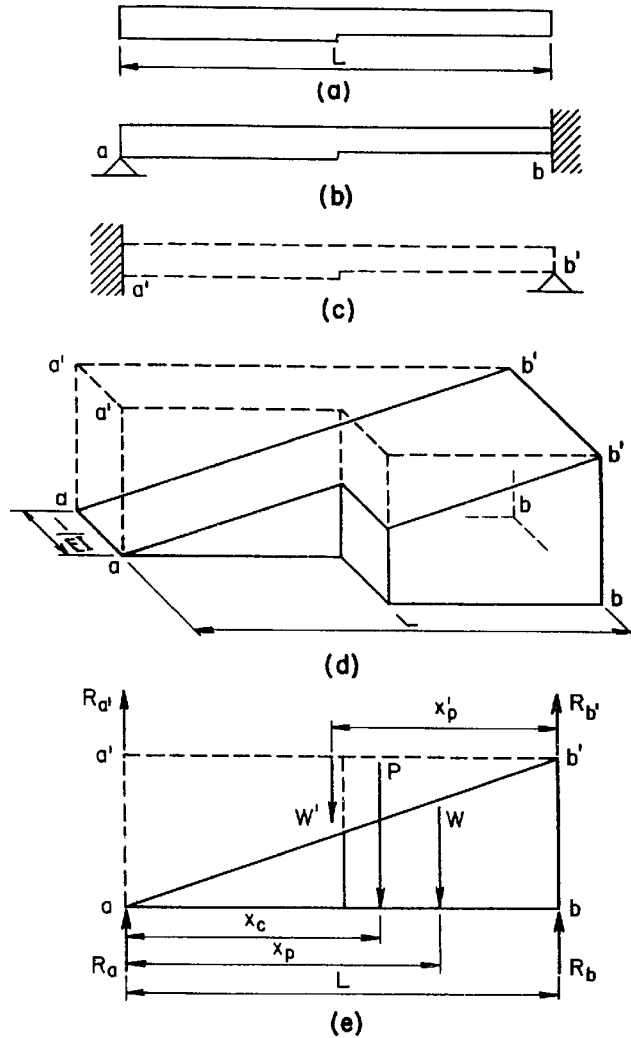


Fig. 7

desired to find the stiffness factors. Figs. 7b and 7c show the beam supported in a manner consistent with the definition of  $S_a$  and  $S_b$ , respectively.

Fig. 7d is an oblique view of a prismatic solid  $abb'a'$  whose base has a length equal to the span  $L$  of the beam and widths proportional to its  $l/EI$  values. The solid is cut diagonally along the plane  $aa - b'b'$ . The lower half of the cut solid is shown in continuous outline in continuous outline

while the upper half, volumetrically not equal to the lower, is dashed.

Let the lower half of the original solid be simply supported along edges  $aa$  and  $bb$ . The reactions are  $R_a$  and  $R_b$  and their sum is the weight  $W$ , Fig. 7e. Force  $W$  passes through the center of gravity of the half-solid and also

through the center of pressure in its base, located at a distance  $x_p$  to the right of  $\underline{a}$ .

Referring to Eq. 10, the stiffness factor at  $\underline{a}$  is

$$S_a = \frac{I}{A - \frac{Q_a^2}{J_a}}$$

Replacing  $Q_a/J_a$  by  $1/x_p$ ,

$$S_a = \frac{I}{A - \frac{Q_a}{x_p}} = \frac{I}{A - \frac{A x_c}{x_p}}$$

or

$$S_a = \frac{x_p}{A(x_p - x_c)} \quad \text{Eq. 13}$$

The centroidal distance  $x_c$  in Eq. 13 and Fig. 7e is found by the principle of moments:

$$(R_a + R_{a'})x_c = (R_b + R_{b'})(L - x_c)$$

$$x_c = \frac{(R_b + R_{b'})L}{P}$$

Substituting for  $x_p$  from Eq. 6 and simplifying, Eq. 13 becomes

$$S_a = \frac{R_b P}{A[R_b P - (R_b + R_{b'})W]} \quad \text{Eq. 14}$$

When  $P$  in the denominator is replaced by  $W + W'$ , the last equation becomes

$$S_a = \frac{R_b P}{A(R_b W' - R_{b'} W)} \quad \text{Eq. 15}$$

Similarly,

$$S_b = \frac{R_{a'} P}{A(R_{a'} W - R_a W')} \quad \text{Eq. 16}$$

It can be readily shown that the denominators in Eqs. 15 and 16 are equal. Therefore,

$$S_b = \frac{R_{a'}}{R_b} S_a \quad \text{Eq. 17}$$

The modified stiffness factor given by Eq. 12 is

$$S_a' = \frac{L^2}{J_b} = \frac{L^2}{\frac{J_b}{Q_b} Q_b} = \frac{L^2}{x_p' A(L - x_c)}$$

Substituting

$$L - x_c = \frac{(R_a + R_{a'}) L}{P}$$

the expression for  $S_a'$  becomes

$$S_a' = \frac{W' P}{R_{a'} (R_a + R_{a'}) A} \quad \text{Eq. 18}$$

If the beam has a constant moment of inertia,

$$W = W' = \frac{P}{2}, \quad R_{b'} = \frac{1}{3} W' = \frac{1}{3} \frac{P}{2}$$

$$R_b = \frac{2}{3} W = \frac{2}{3} \frac{P}{2}, \quad R_{a'} = R_b$$

so that the stiffness factors are

$$(\text{Eq. 15}) \quad S_a = \frac{\frac{2}{3} \frac{P}{2} P}{\frac{L}{EI} \left( \frac{2}{3} \frac{P}{2} \frac{P}{2} - \frac{1}{3} \frac{P}{2} \frac{P}{2} \right)} = \frac{4EI}{L}$$

$$(\text{Eq. 17}) \quad S_b = \frac{\frac{2}{3} \frac{P}{2}}{\frac{2}{3} \frac{P}{2}} S_a = S_a$$



Eqs. 15, 16, 17 and 18 express the stiffness factors in terms of four reactions  $R_a$ ,  $R_{a'}$ ,  $R_b$ ,  $R_{b'}$ , and area  $A$ . Referring to Eq. 7 it will be recalled that the carry-over factors are also functions of the four reactions. The determination of these reactions by weighing and the evaluation of carry-over and relative stiffness factors is illustrated in the following examples.

Example 1 - Deepened Beam. - The following data were obtained by weighing the reactions of the two half-solids shown in

Fig. 8b. The variation of  $1/EI$ -values is shown in Fig. 8c. All weights are expressed in grams.

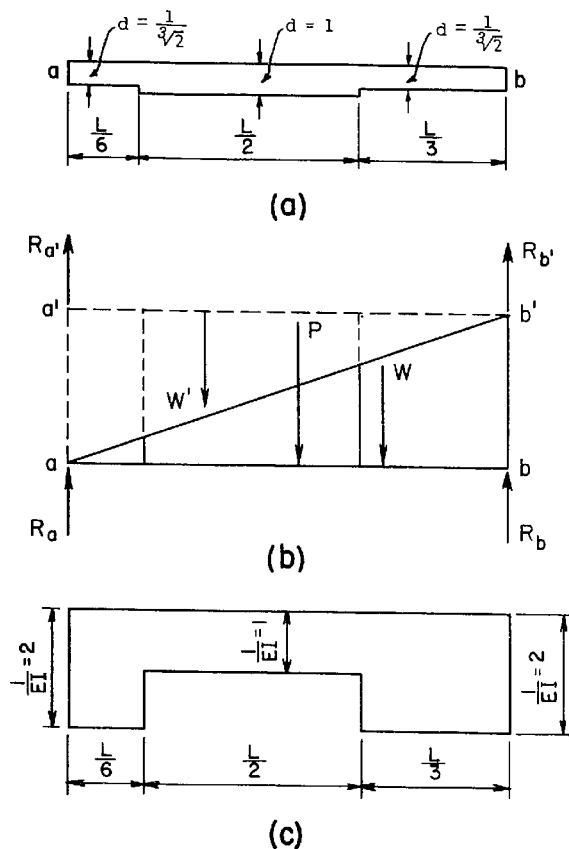


Fig. 8

$$R_a = 95 \quad R_{a'} = 221$$

$$R_b = 240 \quad R_{b'} = 97$$

$$W = 335 \quad W' = 318$$

$$P = 653$$

$$A = 2L - 1 \frac{L}{2} = \frac{3L}{2}$$

(a) Beam fixed at end  $\underline{b}$

(Eq. 7)

$$C_{ab} = \frac{R_a}{R_b} = \frac{95}{240} = 0.396$$

$$C_{ba} = \frac{R_{b'}}{R_{a'}} = \frac{97}{221} = 0.438$$

(Eq. 15)

$$\begin{aligned}
 S_a &= \frac{R_b P}{A(R_b W' - R_{b'} W)} \\
 &= \frac{(240)(653)}{\frac{3L}{2}[(240)(318) - (97)(335)]} = \frac{2.38}{L} \text{ (rel.)}
 \end{aligned}$$

(Eq. 17)

$$S_b = \frac{R_{a'}}{R_b} S_a = \frac{221}{240} \frac{2.38}{L} = \frac{2.19}{L} \text{ (rel.)}$$

(b) Beam simply supported at b

(Eq. 18)

$$\begin{aligned}
 S_a' &= \frac{W' P}{R_{a'}(R_a + R_{a'}) A} \\
 &= \frac{(318)(653)}{221(95 + 221) \frac{3L}{2}} = \frac{1.98}{L} \text{ (rel.)} \\
 S_b' &= \frac{W P}{R_b(R_{b'} + R_b) A} \\
 &= \frac{(335)(653)}{240(97 + 240) \frac{3L}{2}} = \frac{1.80}{L} \text{ (rel.)}
 \end{aligned}$$

The stiffness factors are relative inasmuch as relative  $1/EI$ -values were used in the calculations. For the purpose of distributing an unbalanced moment among the members framed into a joint relative stiffness factors may be used provided that the widths (that is, the  $1/EI$ -values) of the respective solids are laid off to the same scale. If it is impractical to use the same scale or if absolute stiffness factors are required, an adjustment is necessary.

In general, if the model represents the prototype to the lineal scale of 1 inch =  $m$ -inches of prototype, and the transverse  $I/EI$ -scale is 1 inch =  $n$ -  $1/lb\text{-in}^2$ , the absolute stiffness factor for the prototype is (Eq. 13)

$$S_a = \frac{x_p}{A(x_p - x_c)} \cdot \frac{m}{(mn)m}$$

$$= \frac{x_p}{A(x_p - x_c)} \cdot \frac{1}{mn} \quad \text{Eq. 19}$$

in which the base area  $A$  of the model is evaluated in square inches and  $S_a$  is expressed in  $lb\text{-in}$ .

Example 2 - Haunched Beam. - The reactions in Fig. 9 obtained

by weighing are:

$R_a = 88$	$R_{a'} = 233.5$
$R_b = 120.5$	$R_{b'} = 102.5$
$W = 208.5$	$W' = 336.0$

$$P = 544.5$$

From Fig. 9c,

$$A = 263.3 \text{ L}$$

(a) Beam fixed at end b

(Eq. 7)

$$C_{ab} = \frac{R_a}{R_b} = \frac{88}{120.5} = 0.72$$

$$C_{ba} = \frac{R_{b'}}{R_{a'}} = \frac{102.5}{233.5} = 0.44$$

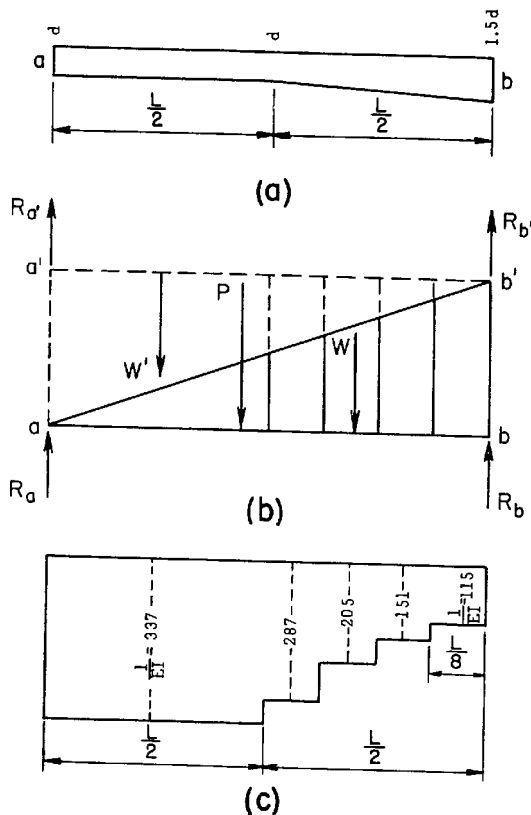


Fig. 9

(Eq. 15)

$$S_a = \frac{R_b P}{A(R_b W' - R_{b'} W)}$$

$$= \frac{(120.5)(544.5)}{A[(120.5)(336) - (102.5)(208.5)]} = \frac{3.43}{A}$$

$$S_a = \frac{3.43}{263.3L} = \frac{0.01302}{L} \text{ (rel.)}$$

(Eq. 17)

$$S_b = \frac{R_{a'}}{R_b} S_a = \frac{233.5}{120.5} \cdot \frac{0.01302}{L} = \frac{0.0252}{L} \text{ (rel.)}$$

(b) Beam simply supported at b

(Eq. 18)

$$S_a' = \frac{W' P}{R_{a'}(R_a + R_{a'}) A}$$

$$S_a' = \frac{(336)(544.5)}{233.5(88 + 233.5) 263.3L} = \frac{0.00925}{L} \text{ (rel.)}$$

$$S_b' = \frac{W P}{R_b(R_{b'} + R_b) A}$$

$$S_b' = \frac{(208.5)(544.5)}{120.5(102.5 + 120.5) 263.3L} = \frac{0.016}{L} \text{ (rel.)}$$

6. Making and Weighing the Model. - It is a very simple matter to make a model (that is, pressure solid, three-dimensional conjugate beam) capable of giving very good results. The models used in Examples 1 and 2 were made of red oak and eastern fir, respectively, although any kind of seasoned lumber that is reasonably free of defects is equally suitable. The wood should be uniformly dry to avoid a variation in its specific weight and to prevent warping when it is cut. Plaster of Paris, paraffin and other materials which can be molded or easily cut may also be used.

The composite specimen abb'a' in Example 1 was assembled by lightly gluing onto a prismatic block of seasoned red oak  $L = 12$  in. long, 3.9 in. deep and 0.9 in. thick two pieces of the same thickness and depth, and  $L/6 = 2$  in. and  $L/3 = 4$  in. long, respectively. Next, the composite block

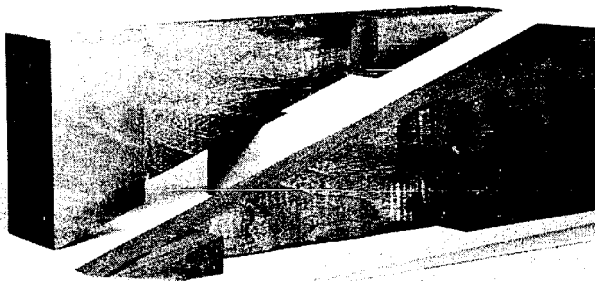


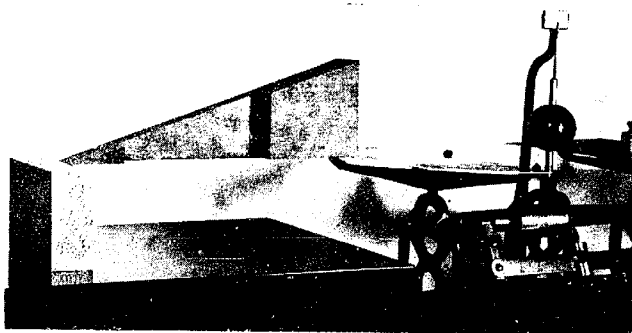
Fig. 10

abb'a' was cut diagonally from a to b' to form the two pressure solids shown in Fig. 10. When a power-driven saw is used and utmost precision is required, two parallel guide bars should be firmly clamped

to the work table to secure an exact diagonal cut. It should be noted that a deviation from the true diagonal cannot be readily corrected inasmuch as a correction of one of the two half-solids calls for a compensating change of the other.

From the point of view of accuracy the diagonal cut is most satisfactory when it bisects the right angle at the corner. This, however, requires deep or very short models. The first may necessitate the use of several layers of wood glued or cemented together, and unless the wood is well seasoned (kiln dried) the joints have a tendency to open up as the drying of the material progresses. Short models on the other hand are subject to inaccuracies in measurement and cutting and the effects of the glue, imperfect jointing, and internal defects of the material become more pronounced. The proportions of the beam models shown in this paper were found quite satisfactory.

One reaction was weighed at a time while the other support was provided by a block of wood of suitable height.



Example 1 - Weighing  $R_b$

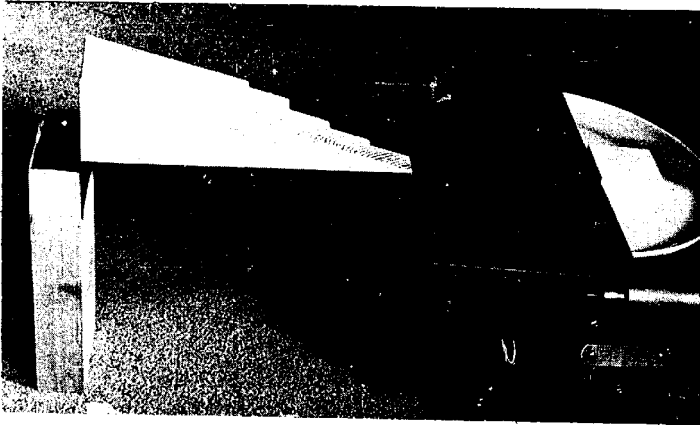
Fig. 11

A carpenter's level was used to check the horizontal alignment of the scale platform and the supporting block at the other end. It is evident from the nature of the data collected that the

entire experiment required only a few minutes of time.

In Example 2, the base of the model was laid out and cut in a stepwise fashion to represent the area  $A$  in a manner consistent with the summation process of numerical

analysis. It is customary in numerical methods of analysis



Example 2 - Weighing  $R_b$

Fig. 12

to subdivide the area bound by a continuous curve into several nearly trapezoidal elements which, for the purpose of determining the area and its first and second moments, are treated as rectangles.

If the moment of inertia of the beam varies continually the variation of the  $1/EI$ -values in the model should be likewise continuous. This was not done in Example 2 because its purpose was to ascertain the accuracy of the experimentally determined constants as compared with the results obtained by standard numerical methods. However, a second experiment was performed using a model whose base area was laid out to represent the continuous variation of the  $1/EI$ -values of the prototype. The carry-over and stiffness factors thus obtained are listed below and compared with those obtained in Example 2.

First Model - Stepwise  
Variation of  $1/EI$

$$C_{ab} = 0.72$$

$$C_{ba} = 0.44$$

$$S_a = 0.01302/L$$

$$S_b = 0.0252/L$$

Second Model - Continuous  
Variation of  $1/EI$

$$C_{ab} = 0.736$$

$$C_{ba} = 0.44$$

$$S_a = 0.01313/L$$

$$S_b = 0.0254/L$$

7. Verification of Experimental Data and Results. - Errors and inaccuracies in weighing the reactions are found by weighing the solids. If discrepancies appear between the weight of the solid and the sum of its reactions the weighing of reactions is repeated until a reasonably close agreement is obtained.

It should be noted that it is physically impossible to support the solid at the very ends of its span, which is especially true of its tapered end. Although the clear span is slightly shorter than the nominal span, the sum of the reactions determined by weighing is always equal to the weight of the solid which is constant. However, the bearing lengths and the clear span affect the computed value of  $x_p$ , and consequently the carry-over and stiffness factors. To appraise the effect of the bearing lengths the latter were varied within a reasonable range and the corresponding values of both factors were computed. It was found that for the purposes of actual analysis of indeterminate structures the differences were negligibly small.

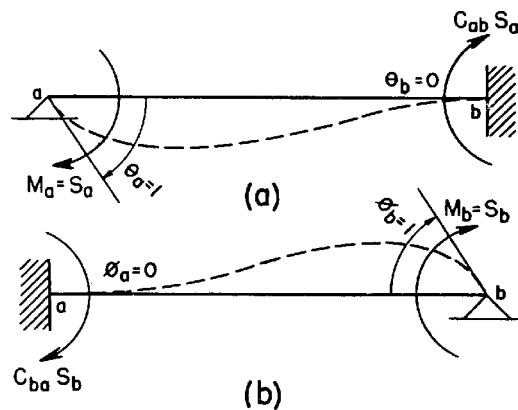
To insure extreme accuracy the solid may be supported with its one or both ends overhanging. This arrangement has the advantage that a straight line may be drawn at each support across the base. These lines mark the exact position of the supports and permit an accurate measurement of the clear span. The end-reactions for the solid are determined from the interior reactions by statics. To provide interior supports, razor blades, thumb tacks, map pins and the



like may be used. It should be pointed out that with the supports arranged in this manner the weighing of the reactions is more delicate inasmuch as the equilibrium of the balance is difficult to establish.

The condition that the sum of the reactions for either half-solid must equal its weight is useful in guarding against gross errors or inaccuracies in weighing. The final values of the four factors  $C_{ab}$ ,  $C_{ba}$ ,  $S_a$  and  $S_b$  may be checked in the following manner.

In Fig. 13a, the moment required to cause a unit rotation at a while end b is held fixed is  $M_a = S_a$ . The fixed



end moment at b is  $C_{ab} S_a$ .

Similarly, in Fig. 13b moment  $M_b = S_b$  causes a unit rotation

at b and fixed end moment

$C_{ba} S_b$  at a. Applying Maxwell-Mohr reciprocal theorem

(see reference on page 10) to

the equilibrated moment load

systems in Figs. (a) and (b) and to the rotations in Figs. (b) and (a),

$$S_a(\phi_a) + C_{ab} S_a(\phi_b) = C_{ba} S_b(\theta_a) + S_b(\theta_b)$$

Substituting for the rotations,

$$S_a(0) + C_{ab} S_a(1) = C_{ba} S_b(1) + S_b(0)$$

whence

$$\frac{C_{ab}}{C_{ba}} = \frac{S_b}{S_a} \quad \text{Eq. 20}$$

It follows that if any three of the four factors are known, the fourth may be obtained by means of Eq. 20.

Since the experimental method of determining the four factors is extremely simple it is best to evaluate each factor separately and to use Eq. 20 as a check. If a small discrepancy appears the individual values may be adjusted graphically, by the method of least squares, etc.

Substituting into Eq. 20 three of the experimentally found values from Example 1,

$$\frac{0.396}{0.438} = \frac{S_b}{\frac{2.38}{L}}$$

from which

$$S_b = \frac{2.145}{L}$$

This compares favorably with 2.19/L determined by experiment.

In Example 2,

$$\frac{0.72}{0.44} = \frac{S_b}{\frac{0.01302}{L}}$$

$$S_b = \frac{0.0213}{L}$$

whence

which differs from the experimental value of 0.0252/L. In

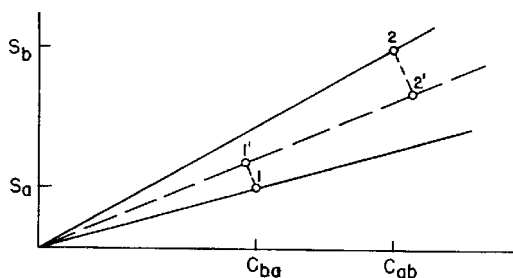


Fig. 14

Fig. 14 one method of adjustment is illustrated. Writing Eq. 20 in the form

$$\frac{S_a}{C_{ba}} = \frac{S_b}{C_{ab}}$$

the experimentally determined values of  $C_{ba}$  and  $C_{ab}$  are laid off as abscissae, and values of  $S_a$  and  $S_b$  are erected at their ends as ordinates. The slopes of the two lines connecting the origin with points 1 and 2 are the ratios  $S_a/C_{ba}$  and  $S_b/C_{ab}$ . Points 1 and 2 are projected into 1' and 2' on the dashed line which is the line of mean slope, and their coordinates represent the rectified values of the four factors.

The adjustment was carried out to a large scale (graph not shown) according to the principle just outlined and yielded the following values:

$$C_{ab} = 0.742$$

$$S_a = 0.01365/L$$

$$C_{ba} = 0.426$$

$$S_b = 0.02380/L$$

8. Fixed End Moments in Beams. - Concentrated Load. Fig.

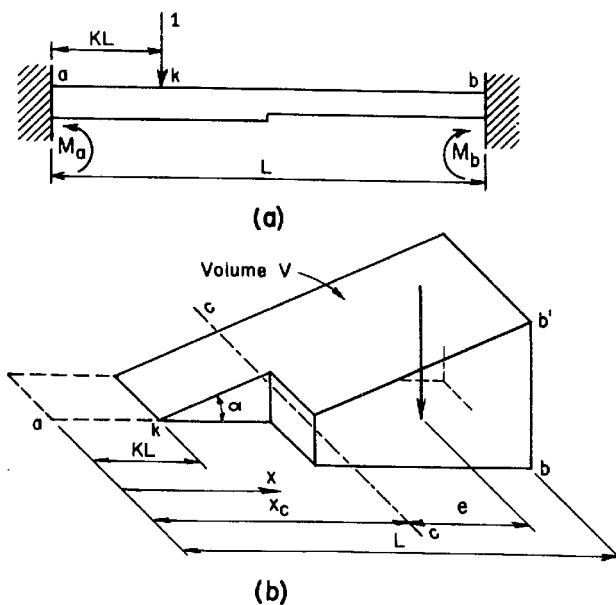


Fig. 15

15a represents a fixed-ended beam carrying a single unit load at point  $k$ . It is desired to find the fixed end moments  $M_a$  and  $M_b$ .

By the column analogy method of analysis<sup>(3)</sup> the fixed end moments are

<sup>3)</sup> "Continuous Frames of Reinforced Concrete" by H. Cross and N.D. Morgan; also "Theory of Modern Steel Structures" by L.E. Grinter, etc.

$$\left. \begin{aligned} M_a &= \frac{V}{A} - \frac{Ve x_c}{J_c} \\ M_b &= -(1)(L - KL) + \frac{V}{A} + \frac{Ve(L - x_c)}{J_c} \end{aligned} \right\} \text{Eq. 21}$$

in which

$$A = \int_0^L \frac{dx}{EI} = \text{area defined previously,}$$

$$V = \int_{KL}^L \frac{(1)(x - KL)}{EI} dx = \text{volume of the solid shown in Fig. 15b,}$$

$x_c$  = distance of the centroidal axis  $c - c$  of area  $A$  measured from  $\underline{a}$ ,

$e$  = eccentricity of the center of gravity (or center of pressure) of volume  $V$  referred to axis  $c - c$ ,

$J_c$  = second moment of area  $A$  about axis  $c - c$ .

From Eq. 5,

$$x_p = \frac{J_a}{Q_a} = \frac{J_a}{A x_c}$$

$$J_a = A x_c x_p$$

Applying the parallel-axis theorem of second moments,

$$J_a = J_c + A x_c^2,$$

substituting for  $J_a$  above,

$$J_c = A x_c (x_p - x_c)$$

Factoring  $V/A$  and substituting for  $J_c$  in the first of Eqs.

21, the fixed end moment at  $\underline{a}$  is

$$M_a = \frac{V}{A} \left[ 1 - \frac{e}{x_p - x_c} \right] \quad \text{Eq. 22}$$

Similarly,

$$M_b = -(1)(L - KL) + \frac{V}{A} \left[ 1 + \frac{e(L - x_c)}{x_c(x_p - x_c)} \right] \quad \text{Eq. 23}$$

Moments  $M_a$  and  $M_b$  given by Eqs. 22 and 23 can be evaluated if quantities  $V$ ,  $A$ ,  $e$ ,  $x_c$  and  $x_p$  are known.

Distances  $x_c$  and  $x_p$  were already encountered in the expressions for the stiffness and carry-over factors and can be expressed as functions of the reactions of the respective solids.

Quantities  $V$  and  $e$  may be determined experimentally by fashioning and weighing the solid shown in Fig. 15b. Its altitudes represent the moment of the unit load applied at  $\underline{k}$  so that again the solid may be conceived of as a "pressure solid." To avoid confusion with the pressure solid utilized in the determination of the carry-over and stiffness factors, the latter will be referred to as "the load solid."

The volume  $V$  of the load solid is best determined by dividing its weight  $W_1$  by the specific weight  $w$  of the material of which it is made. Specific weights of various kinds of wood are listed in engineering handbooks. However, the specific weight of the wood used in the experiment should be obtained more exactly by weighing a unit volume.

The moment of the unit load applied at  $\underline{k}$  at any distance  $x$  is  $M = (1)(x - KL)$ . Since the altitudes of the load solid in Fig. 15b represent the moments of the load, the slope of its upper surface is  $dM/dx = 1$ . If a load  $P$  acts at point  $\underline{k}$ , the slope should be  $(P)(1) = P$ .

It may be impractical to cut the solid at an angle corresponding to the load  $P$ . If the slope is arbitrarily made equal to  $\tan\alpha$ , the volume determined by weighing must be multiplied by the ratio  $P/\tan\alpha$  when substituted in Eqs. 22 and 23.

The distance  $e$  is the eccentricity of  $W_1$  referred to the centroidal axis  $c - c$ . It is determined by simply support-

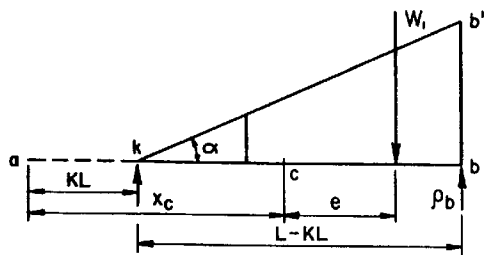


Fig. 16

ing the load solid along edges  $\underline{k}$  and  $\underline{b}$  and weighing the reaction  $\rho_b$  at  $\underline{b}$  (Fig. 16). Taking moments about  $\underline{k}$ ,

$$W_1(x_c + e - KL) = \rho_b(L - KL)$$

whence

$$e = \frac{\rho_b(L - KL) - W_1(x_c - KL)}{W_1} \quad \text{Eq. 24}$$

It is not advisable to support the load solid at  $\underline{c}$  and  $\underline{b}$  (part  $k - c$  overhanging). Although this arrangement permits a more direct evaluation of  $e$ , the necessity of a knife-edge support at  $\underline{c}$  makes the weighing of the reaction at  $\underline{b}$  more difficult on account of prolonged oscillations of the balance.

It will be noted that three solids are required for the experimental evaluation of the data entering in Eqs. 22 and 23. The first solid, needed to find  $x_c$ , must have a span equal or proportional to the span of the fixed-ended beam, a base whose widths correspond to its  $l/EI$ -values, and a

constant height. The second solid, called the "pressure solid," is required to evaluate  $x_p$  defined by Eq. 6. It is obtained from the first solid by cutting it diagonally along the plane  $a - b'$ . The third solid, referred to as the "load solid," is required for the evaluation of  $V$  and  $e$ . It is obtained from the second solid by cutting it along the plane  $k - b'$  or any other inclined plane passing through  $\underline{k}$ . It follows that a single solid of constant height, when properly cut, will suffice for an experimental evaluation of the data required for the determination of both carry-over and stiffness factors, and fixed end moments for a beam.

Although the relative value of area  $A$  may be obtained by direct measurement in the case of deepened beams, or by Simpson's rule, graphically, etc., in the case of haunched beams, it is generally preferable to compute it from the experimental data. Area  $A$  may be readily found by dividing the weight of the initial solid (prismatic solid of constant height) by its altitude  $\overline{bb'}$ , and the specific weight  $w$  of the material.

Example 3 - Deepened Beam. - Fig. 17a shows a deepened beam fixed at both ends. The carry-over and stiffness factors, and the fixed end moments caused by load  $P_k$  will be determined.

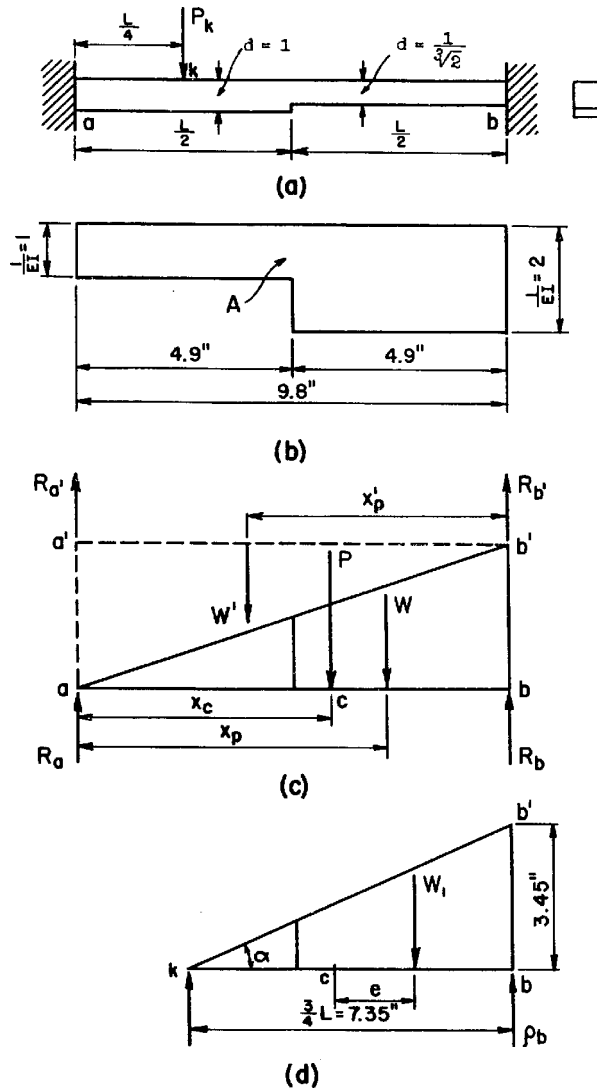


Fig. 17

(Fig. 17c)

$$x_c = \frac{(R_b + R'_b)L}{P} = \frac{(325 + 126.5)L}{768} = 0.588L$$

(Eq. 6)

$$x_p = \frac{R_b L}{W} = \frac{325L}{453} = 0.717L$$

$$x'_p = \frac{R'_b L}{W'} = \frac{126.5L}{315} = 0.398L$$

The following data were obtained by weighing. All weights are expressed in grams.

$$R_a = 128 \quad R'_a = 188.5$$

$$R_b = 325 \quad R'_b = 126.5$$

$$W = 453 \quad W' = 315$$

$$P = 768$$

$$\rho_b = 251 \quad W_1 = 361.5$$

Specimen of wood measuring 1.675" x 1.690" x 1.528" = 4.315 in<sup>3</sup> weighs 40.5.

$$w = 40.5/4.315 = 9.37/\text{in}^3$$



(Eq. 7)

$$C_{ab} = \frac{R_a}{R_b} = \frac{128}{325} = 0.394$$

$$C_{ba} = \frac{R_{b'}}{R_{a'}} = \frac{126.5}{188.5} = 0.671$$

(Eq. 13)

$$S_a = \frac{x_p}{A(x_p - x_c)} = \frac{0.717L}{\frac{3L}{2}(0.717L - 0.588L)} = \frac{3.71}{L} \text{ (rel.)}$$

$$S_b = \frac{x'_p}{A[x'_p - (L - x_c)]} = \frac{0.598L}{\frac{3L}{2}[0.598L - (L - 0.588L)]}$$

$$S_b = \frac{2.142}{L} \text{ (rel.)}$$

(Eq. 20)

$$\frac{C_{ab}}{C_{ba}} = \frac{S_b}{S_a}$$

$$\frac{C_{ab}}{0.671} = \frac{2.142}{3.71}$$

$$C_{ab} = 0.388 \text{ (vs. } 0.394) \checkmark \text{ check}$$

Volume of load solid:

$$V_\alpha = \frac{W_l}{w} = \frac{361.5}{9.37} = 38.5 \text{ in.}^3$$

Adjust V for load  $P_k$ :

$$V = V_\alpha \frac{P_k}{\tan \alpha} = 38.5 \frac{P_k}{\frac{3.45}{7.35}} = 82 P_k \text{ in.}^3$$

Area A (absolute):

$$A(bb') w = P$$

$$A(3.45)(9.37) = 768$$

$$A = 23.7 \text{ in.}^2 = \frac{23.7}{L} L = \frac{23.7}{9.8} L = 2.42 L$$

(Eq. 24)

$$\begin{aligned} e &= \frac{P_b(L - KL) - W_i(x_c - KL)}{W_i} \\ &= \frac{251(0.75L) - 361.5(0.588L - 0.25L)}{361.5} \end{aligned}$$

$$e = 0.1825L$$

(Eq. 22)

$$\begin{aligned} M_a &= \frac{V}{A} \left[ 1 - \frac{e}{x_p - x_c} \right] \\ M_a &= \frac{82 P_k}{23.7} \left[ 1 - \frac{0.1825L}{(0.717L - 0.588L)} \right] = -1.435 P_k \end{aligned}$$

In terms of any span L, the fixed end moment at a is

$$M_a = \frac{-1.435 P_k}{9.8} L = -0.1464 P_k L$$

(Eq. 23)

$$\begin{aligned} M_b &= -(P_k)(L - KL) + \frac{V}{A} \left[ 1 - \frac{e(L - x_c)}{x_c(x_p - x_c)} \right] \\ &= -(P_k)(7.35) + \frac{82 P_k}{23.7} \left[ 1 + \frac{0.1825L(L - 0.588L)}{0.588L(0.717L - 0.588L)} \right] \\ M_b &= -0.45 P_k = \frac{-0.45 P_k}{9.8} L = -0.046 P_k L \end{aligned}$$

9. Fixed End Moment. Beam Fixed at One End and Simply Supported at the Other. - The fixed end moment  $M'_b$  can be readily

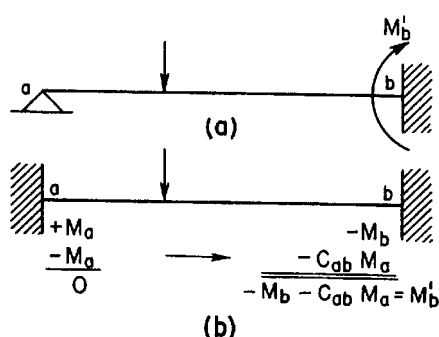


Fig. 18

over to joint b.

Assuming the beam in Example 3 to be simply supported at a and fixed at b, moment  $M'_b$  can be evaluated by substituting for  $M_b$ ,  $C_{ab}$ , and  $M_a$ :

$$M'_b = M_b + C_{ab} M_a = -0.046 P_k L + (0.394)(-0.1464 P_k L)$$

$$M'_b = -0.1036 P_k L$$

An alternate working formula may be derived without reference to moments  $M_a$  and  $M_b$ . In Fig. 19a, the beam is

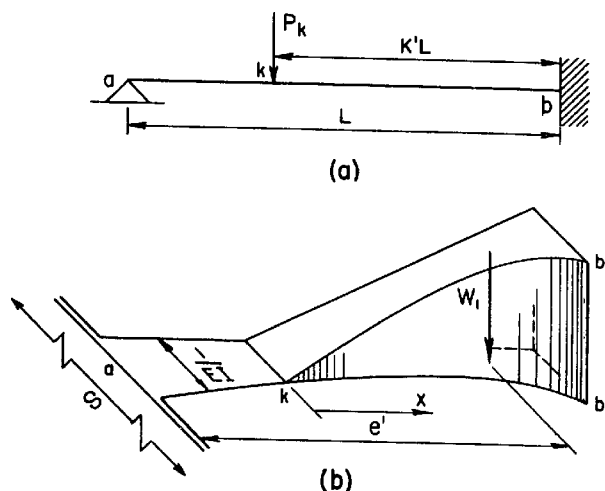


Fig. 19

simply supported at a and fixed at b. Since a simple support or hinge has zero stiffness (EI-value), in the column analogy method of analysis it adds an infinite area  $dx/EI$  to the column section at a. As a result the centroid of the

<sup>4)</sup> The fixed end moment is considered to be positive when the joint tends to rotate clockwise.

total area  $A$  shifts to  $\underline{a}$  and  $x_c$   $x'_c$  becomes zero.  
(Eqs. 21)

$$M'_a = \frac{V}{\infty} - \frac{Ve'(0)}{J_a} = 0$$

$$M'_b = -P_k K'L + \frac{V}{\infty} + \frac{Ve'L}{J_a}$$

But  $\frac{J_a}{Q_a} = x_p$  or  $J_a = Q_a x_p = A x_c x_p$

From Example 3,

$$e' = x_c + e = 0.588L + 0.1825L$$

$$e' = 0.7705L$$

Substituting in the second of Eqs. 21 for  $J_a$  and  $e'$  and using the values of  $A$ ,  $x_c$ ,  $x_p$ , and  $V$  determined in Example 3, the moment at  $\underline{b}$  is

$$\begin{aligned} M'_b &= -P_k (7.35) + \frac{82 P_k (0.7705L)}{(23.7)(0.588L)(0.717L)} \\ &= -7.35 P_k + 6.30 P_k \\ M'_b &= -1.05 P_k \end{aligned}$$

In terms of any span length  $L$  this becomes

$$M'_b = \frac{-1.05 P_k}{9.8} L = -0.107 P_k L$$

10. Fixed End Moments. - Uniformly Distributed Load. By the column analogy method, in Fig. 20 the fixed end moment at a due to a distributed load of unit intensity per unit of length is

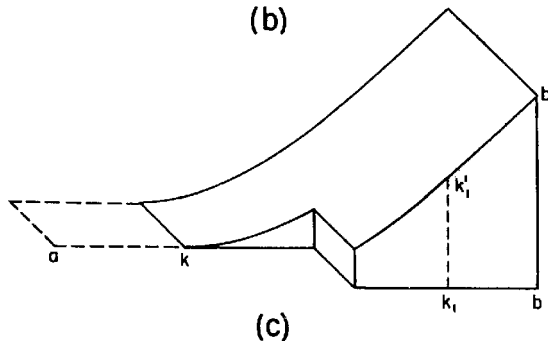
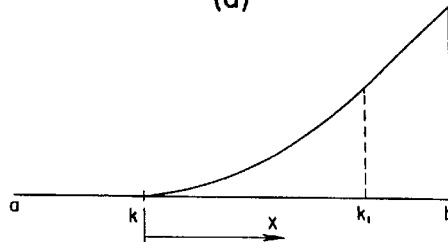
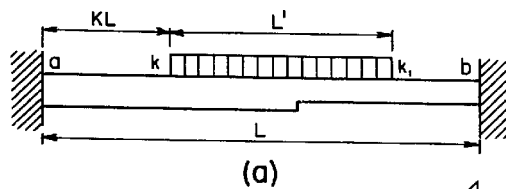
(Eq. 21)

$$M_a = \frac{V}{A} + \frac{Ve x_c}{J_c}$$

where

$$V = \int_k^{k_1} \frac{\frac{x^2}{2}}{EI} dx + \int_{k_1}^b \frac{L'(x - \frac{L'}{2})}{EI} dx \quad \text{Eq. 25}$$

is the volume of the load solid shown in Fig. 20c. From



k to k<sub>1</sub> the altitudes of the solid vary as the second power of x. From k<sub>1</sub> to b the variation is linear. Except for the parabolic variation of altitude between k and k<sub>1</sub>, the principles of making and weighing the load solid developed in articles 8 and 9 remain valid.

The first of the two definite integrals in Eq. 25 may be written in the equivalent form

$$\int_k^{k_1} \frac{x}{2EI} x dx$$

Fig. 20

which may be interpreted as the volume of a solid whose base has widths equal to the  $x/2EI$ -values and whose altitudes vary linearly with  $x$ . If the  $1/EI$ -values for the beam vary continuously (for example, in a beam with a curved intrados), the equivalent form of the first integral suggests that only one curved cut is necessary in fashioning the load solid, provided that the  $x/2EI$ -values are laid off in the  $\overline{kk}_1$  portion of its span. If this alternate solid is used, the determination of the carry-over and stiffness factors as well as of quantities  $A$ ,  $x_c$  and  $J_c$  in Eq. 21 involves a separate solid inasmuch as the latter must have widths proportional to the  $1/EI$ -values throughout its entire length. It follows that unless these quantities are known from a previous analysis the alternate load solid does not simplify the overall cutting operations.

11. Influence Lines for Fixed End Moments. - Influence lines for fixed end moments may be obtained by applying the procedure outlined in articles 8 and 9 to a series of load points  $\underline{k}$ . Starting from one end, a new load solid is cut off from the preceding one, its weight  $W_1$  and reaction  $\rho_b$  are determined, and fixed end moments are evaluated. This is repeated for a sufficient number of  $KL$ -values. An alternate method based on the properties of the neutral point is outlined and illustrated for an arch in Example 7 in Part III of this paper.

12. Moments Caused by Impressed Distortions. - The foundations of a structure may settle, spread, or rotate. Furthermore, members framed into a joint may shorten or lengthen as a result of direct stress or temperature change, thereby causing the joint to translate. These and similar distortions induce moments in the structure in addition to those caused by actual loads. The column analogy method is the most expedient method for analyzing the effects of such distortions.

(a) Transverse Displacement. Joint Rotation Prevented. - The effect of a relative transverse displacement  $\Delta$  of ends a and

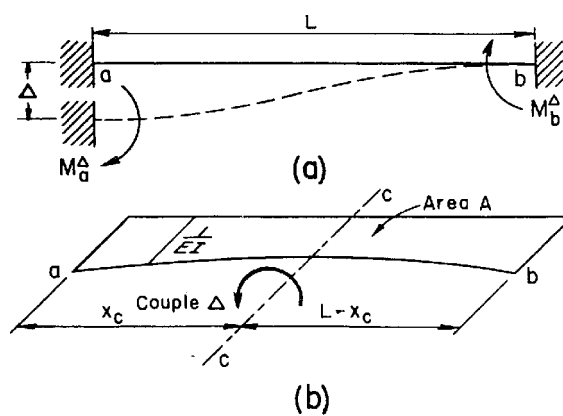


Fig. 21

b of the restrained member in Fig. 21a corresponds in the column analogy method to a couple numerically equal to  $\Delta$ , acting about the transverse centroidal axis  $c - c$  of the column cross section, shown in Fig. 21b. The moments induced in the member correspond to the stresses in the column, that is,

$$M_a^{\Delta} = \frac{\Delta}{J_c} x_c \quad \text{Eq. 26}$$

Using the relationships developed earlier in this paper, the expression for the moment  $M_a^{\Delta}$  may be written in the form

$$M_a^\Delta = \frac{\Delta}{J_a - A x_c^2} x_c = \frac{\Delta}{Q_a \left( \frac{J_a}{Q_a} - x_c \right)} x_c$$

$$M_a^\Delta = \frac{\Delta x_c}{Q_a (x_p - x_c)} = \frac{\Delta}{A (x_p - x_c)} \quad \text{Eq. 27}$$

In terms of the stiffness factor given by Eq. 13 the last equation becomes

$$M_a^\Delta = \frac{\Delta}{x_p} S_a \quad \text{Eq. 28}$$

Similarly, the moment induced at b is

$$M_b^\Delta = - \frac{\Delta}{J_c} (L - x_c) = - \frac{\Delta (L - x_c)}{A x_c (x_p - x_c)} = - \frac{\Delta (L - x_c)}{x_c x_p} S_a$$

$$\text{or} \quad M_b^\Delta = - \frac{L - x_c}{x_c} M_a^\Delta \quad \text{Eq. 29}$$

If the member is symmetrical about the *c - c* axis, the centroidal distance  $x_c$  is  $L/2$  and Eq. 29 yields

$$M_b^\Delta = - M_a^\Delta$$

The signs of moments  $M_a$  and  $M_b$  depend on the sense of the impressed displacement and the sign convention used<sup>(5)</sup>. Since they can be readily determined by sketching the distorted member a rigorous sign convention is not essential.

If a relative transverse displacement  $\Delta$  occurs between

---

<sup>(5)</sup> In this paper a downward displacement is considered negative and corresponds to a negative couple (beam sign convention) acting on the column section. A compressive stress caused by the couple is positive and is interpreted as a positive moment (beam sign convention) acting on the member.



two ends of which one is fixed and the other simply supported, the fixed end moment may be obtained by following the procedure of article 9. Thus, when a is the simple support, the moment at b is

$$M_b'^{\Delta} = -M_b^{\Delta} + C_{ab} M_a^{\Delta} = -\frac{L - x_c}{x_c} M_a^{\Delta} + C_{ab} M_a^{\Delta}$$

Substituting from Eqs. 27, 4, 6 and reducing, the last equation becomes

$$M_b'^{\Delta} = -\frac{\Delta}{Ax_c x_p} L \quad \text{Eq. 30}$$

(b) Joint Rotation. By definition, if moment  $S_a$  is applied at joint or abutment a, the far end remaining fixed, the rotation at a is  $\theta=1$ . The moment corresponding to any rotation  $\theta_a$  is

$$M_a^{\theta} = \theta_a S_a \quad \text{Eq. 31}$$

and

$$M_b^{\theta} = C_{ab} M_a^{\theta} = C_{ab} \theta_a S_a \quad \text{Eq. 32}$$

13. Shear Stiffness and Flexibility. - The shear stiffness  $S_s$  of a restrained flexural member ab is defined as the shear at the end of the member required to cause a unit relative transverse displacement of a and b. The flexibility  $F_s$  is the reciprocal of shear stiffness, i.e., the relative transverse displacement produced by a unit shearing force. The knowledge of these two factors is prerequisite in the

analysis of sidesway of unsymmetrical and complex frames by the moment distribution method. The derivation follows directly from article 12, paragraph (a).

The shear at a in Fig. 21a is

$$S = \frac{M_a^\Delta + M_b^\Delta}{L}$$

Substituting for  $M_a^\Delta$  and  $M_b^\Delta$  from Eqs. 27 and 28, the last equation becomes

$$S = \frac{\frac{\Delta}{x_p} S_a + \frac{L - x_c}{x_c} \frac{\Delta}{x_p} S_a}{L}$$

which reduces to

$$S = \frac{\Delta}{x_c x_p} S_a \quad \text{Eq. 33}$$

The shear stiffness corresponds to  $\Delta = 1$ . Therefore,

$$S_s = \frac{S_a}{x_c x_p} \quad \text{Eq. 34}$$

Combining Eqs. 28 and 26,

$$M_a^\Delta = \frac{l}{x_p} S_a = \frac{l}{J_c} x_c$$

and substituting for  $S_a/x_p$  in Eq. 34,

$$S_s = \frac{x_c}{x_c J_c} = \frac{l}{J_c} \quad \text{Eq. 35}$$

and

$$F_s = \frac{l}{S_s} = J_c \quad \text{Eq. 36}$$

14. Correlation between Model and Prototype. - The stiffness factor  $S_a$  in Eqs. 28, 31, etc., is a function of model area  $A$  (see Eq. 13). Since absolute values of fixed end moments caused by known or assumed distortions are generally required, the absolute stiffness factor or prototype area  $A = \int \frac{dx}{EI}$  must be introduced in the respective expressions.

The absolute stiffness factor for the prototype is expressed by Eq. 19 on page 19. Using the  $m$ - and  $n$ -scales defined on page 19 the prototype moments are (Eq. 27)

$$M_a^\Delta = \frac{\Delta}{A(x_p - x_c)} \cdot \frac{1}{(mn)m} \quad \text{Eq. 37}$$

When  $\Delta$ ,  $x_p$  and  $x_c$  are expressed in inches,  $A$  in square inches,  $M_a^\Delta$  is expressed in lb-in.

(Eq. 28)

$$M_a^\Delta = \frac{\Delta}{x_p} (S_a)_{\text{model}} \cdot \frac{1}{m} \cdot \frac{1}{mn} \quad \text{Eq. 38}$$

When  $\Delta$  and  $x_p$  are expressed in inches,  $(S_a)_{\text{model}}$  in  $1/\text{in}^2$ ,  $M_a^\Delta$  is expressed in lb-in.

(Eq. 31)

$$M_a^\theta = \theta_a (S_a)_{\text{model}} \cdot \frac{1}{mn} \quad \text{Eq. 39}$$

When  $\theta_a$  is expressed in radians and  $(S_a)_{\text{model}}$  in  $1/\text{in}^2$ ,  $M_a^\theta$  is expressed in lb-in.

Relative values of shear stiffness and flexibility given by Eqs. 35 and 36 can be used for the purpose of distributing shears to the members of a structure analyzed by

the moment distribution method. No scale adjustment is therefore necessary provided that the solids used to evaluate shear stiffnesses of the component members are laid out to the same scales. If this is not feasible an adjustment of scales is necessary, or absolute shear stiffnesses must be found.

The absolute shear stiffness is

$$(Eq. 34) \quad S_s = \frac{(S_a)_{model}}{x_c \times x_p} \cdot \frac{\frac{1}{mn}}{m^2} = \frac{(S_a)_{model}}{x_c \times x_p} \cdot \frac{1}{m^3 n} \quad Eq. 40$$

When  $(S_a)_{model}$  is expressed in  $1/in^2$ ,  $x_c$  and  $x_p$  are in inches,  $S_s$  is expressed in lb/in.

$$(Eq. 35) \quad S_s = \frac{1}{(J_c)_{model}} \cdot \frac{1}{(mn)m^2} = \frac{1}{(J_c)_{model}} \cdot \frac{1}{m^3 n} \quad Eq. 41$$

When  $(J_c)_{model}$  is expressed in  $in^4$ ,  $S_s$  is expressed in lb/in.

Example 4 - Deepened Beam. - Assuming that the model in Example 3 represents the prototype to the lineal scale of 1 in. = 24.5 in., the cross section of the prototype is 8 in. deep and 6 in. wide at a, E is 2,000,000 psi., determine for the prototype:

- (a) absolute stiffness factors
- (b) fixed end moments caused by a settlement  $\Delta = 0.5$  in. at a
- (c) fixed end moments caused by a clockwise rotation of  $0.2^\circ$  at a
- (d) absolute shear stiffness

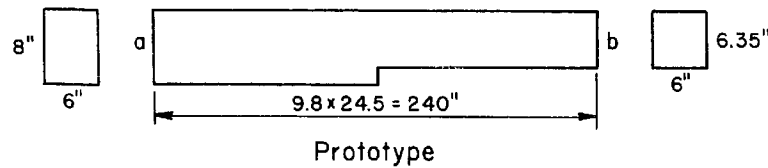
Data

Fig. 22

$$(EI_a)_{\text{prot.}} = 2,000,000 \times \frac{1}{12} (6 \times 8^3) = 5.12 \times 10^8 \text{ lb-in.}^2$$

$$\frac{1}{(EI_a)_{\text{mod.}}} = 1.613 \text{ in. (by measurement of model in Ex.3)}$$

$$\text{Scale } n = \frac{1}{1.613 \times 5.12 \times 10^8}$$

$$\text{Scale } m = 24.5$$

$$\text{Area } A_{\text{mod.}} = 23.7 \text{ in.}^2$$

$$x_p = 9.8 \times 0.717 \text{ in.}$$

$$x_c = 9.8 \times 0.588 \text{ in.}$$

} from Example 3

(a)

(Eq. 19)

$$S_a = \frac{x_p}{A(x_p - x_c)} \cdot \frac{1}{mn}$$

$$= \frac{9.8 \times 0.717}{23.7 \times 9.8 (0.717 - 0.588)} \cdot \frac{1.613 \times 5.12 \times 10^8}{24.5}$$

$$S_a = 7,900,000 \text{ lb-in.} = 658,000 \text{ lb-ft.}$$

(Eq. 20)

$$S_b = \frac{C_{ab}}{C_{ba}} S_a$$

$$C_{ab} = 0.394 \text{ and } C_{ba} = 0.671 \text{ from Example 3}$$

$$S_b = \frac{0.394}{0.671} \times 658,000 = 386,000 \text{ lb-ft.}$$

(b)

(Eq. 37)

$$M_a^A = \frac{\Delta}{A(x_p - x_c)} \cdot \frac{I}{m^2 n}$$

$$= \frac{0.5}{23.7 \times 9.8(0.717 - 0.588)} \cdot \frac{1.613 \times 5.12 \times 10^8}{24.5^2}$$

$$M_a^A = 22,900 \text{ lb-in.} = 1,910 \text{ lb-ft.}$$

(Alternate Eq. 38)

$$M_a^A = \frac{\Delta}{x_p} (S_a)_{mod.} \cdot \frac{I}{m^2 n}$$

$$= \frac{0.5}{9.8 \times 0.717} \cdot \frac{3.71}{9.8 \times 1.613} \cdot \frac{1.613 \times 5.12 \times 10^8}{24.5^2}$$

$$M_a^A = 22,900 \text{ lb-in.}$$

(Eq. 29)

$$M_b^A = - \frac{L - x_c}{x_c} M_a^A$$

$$M_b^A = - \frac{L - 0.588L}{0.588L} \times 1,910 = 1,340 \text{ lb-ft.}$$

(c) Rotation of  $0.2^\circ = 0.00349 \text{ rad.}$

(Eq. 31)

$$M_a^\theta = \theta_a S_a = 0.00349 \times 658,000$$

$$M_a^\theta = 2,300 \text{ lb-ft.} \downarrow$$

(Alternate Eq. 39)

$$M_a^\theta = \theta_a (S_a)_{\text{mod.}} \cdot \frac{I}{mn}$$

$$M_a^\theta = 0.00349 \cdot \frac{3.71}{9.8 \times 1.613} \cdot \frac{1.613 \times 5.12 \times 10^8}{24.5}$$

$$M_a^\theta = 27,600 \text{ lb-in.} = 2,300 \text{ lb-ft.} \downarrow$$

(Eq. 32)

$$M_b^\theta = C_{ab} M_a = 0.394 \times 2,300 = 905 \text{ lb-ft.} \downarrow$$

(d)

(Eq. 40)

$$S_s = \frac{(S_a)_{\text{mod.}}}{x_c \times p} \cdot \frac{I}{m^3 n}$$

$$S_s = \frac{\frac{3.71}{9.8 \times 1.613}}{9.8^2 (0.588 \times 0.717)} \cdot \frac{1.613 \times 5.12 \times 10^8}{24.5^3}$$

$$S_s = 324 \text{ lb/in.}$$

(Alternate solution)

$$S_s = \frac{I}{0.5''} \cdot \frac{M_a^A + M_b^A}{L} = 2 \times \frac{1,910 + 1,340}{20} = 325 \text{ lb/in.}$$

15. Accuracy of the Experimental Method. - Examples 1, 2 and 3 are solved analytically in the Appendix. The theoretical results are entered in Table I on page 49 and compared with those obtained experimentally. To provide a positive check, Examples 1 and 2 are solved in the Appendix by using the working equations of the experimental method, and by the column analogy method. Where slight discrepancies appear in the theoretical results (all numerical work was performed by slide rule), the value which deviates more from its experimental counterpart is entered in the Table.

An inspection of the results reveals very close agreement between the experimental and theoretical carry-over and stiffness factors. The average error in the six carry-over factors is 2.3% and in the six stiffness factors the average error is 3.8%.

The relatively large error (8.6%) in  $S_b$ , Example 2, was adjusted by means of Eq. 20 and graphics. The adjusted values and new per cent errors are as follows:

Adjusted values:	Theoret. values:	Adjusted % error:	Unadjusted % error:
$C_{ab} = 0.742$	0.731	+1.5	-1.5
$C_{ba} = 0.426$	0.422	0.9	4.3
$S_a = 0.01365$ rel.	0.0134	+1.9	-3.0
$S_b = 0.02380$ rel.	0.0232	2.6	8.6

A comparison of the adjusted and unadjusted per cent errors shows that Eq. 20 provides a substantial improvement of the experimental results.





The fixed end moments at a in Example 3 agree within 2.1% although at b the experimental and theoretical moments differ by 27.8%. This large percentual discrepancy must be interpreted in terms of relative errors.

Any small-scale experimental model study involves a more or less fixed amount of error inherent to the accuracy and sensitivity of equipment and gages used, the degree of fulfilment of geometric and other similarity between prototype and model, etc. In two experimental results of different magnitude the influence of this amount of error will be more pronounced in the smaller of the two. It follows that errors in model studies must be appraised on a basis other than percentual deviation from theoretical values.

A practical and reasonable basis of comparison is the per cent error in the largest of the quantities investigated in a given experiment. In Example 3, the maximum moment occurs at the left support and its theoretical relative value is 1495. The difference between the latter and the experimental relative value of 1464 is 31, or 2.07%. Similarly, the difference between the two values of moment at b is 460 - 360, or 100. If the former difference of 31 and 2.07% error are considered as a comparative deviation index for the experiment on hand, a difference of 100 is not serious.

For the purposes of moment distribution and structural design an error of 27.8% in a comparatively small moment would be of little consequence.

A good agreement was found to exist between the experimental and theoretical results in Example 4. Their summary and per cent error are given in Table II.

TABLE II

Item	Impressed Distortion	Experimental	Theoretical	% Error
$S_a$	$\theta_a = 1$	658,000	647,000	1.7(*)
$S_b$	$\theta_b = 1$	386,000	388,000	0.5
$M_a^\theta$	$\theta_a = 0.2^\circ$	2,300	2,260	1.8(*)
$M_b^\theta$	$\theta_a = 0.2^\circ$	905	904	0.1
$M_a^\Delta$	$\Delta = 0.5''$	1,910	1,880	1.6
$M_b^\Delta$	$\Delta = 0.5''$	1,340	1,344	0.3
$S_s$	$\Delta = 1.0''$	324	322	0.6

(\*) All computations by slide rule.

### III - SYMMETRICAL ARCHES

1. General. - It was assumed in the foregoing derivations that the longitudinal axis of the member was straight. This assumption is valid only in a limited number of cases, namely, when the beam has a constant moment of inertia, or when its cross sections everywhere are symmetrical about the neutral axis. Fixed-ended beams which are deepened, stepped or haunched on one side of the neutral surface, and beams with knees, curved intrados, etc., are unsymmetrical and produce some lateral thrust against the supporting walls or columns into which they are framed. As long as this thrust can be neglected, such members may be analyzed without an appreciable error as if they were true straight-axis members.

In the experimental method of analysis developed in this paper, the assumption that the longitudinal axis of the member is straight is equivalent to disregarding the properties of the pressure and load solids with regard to their longitudinal axes. In the foregoing examples the  $1/EI$ -values were laid off to one side of the long dimension of the base, keeping the other side straight. This layout simplifies the preparation of the solids and is permissible whether or not the beam is symmetrical about its neutral surface, inasmuch as the lateral positions of the centroid  $\bar{c}$  and center of pressure,  $\bar{p}$ , have no effect upon the numerical values of the reactions determined by weighing.



Fig. 23c represents the analogous column section subjected to load  $\theta_a$ , arbitrarily chosen as unity.

The column stress (arch moment) at  $\underline{a}$  caused by load  $\theta_a$  is

$$M_a = \frac{I}{A} + \frac{(I) x_c^2}{J_{y_o}} + \frac{(I) y_c^2}{J_{x_o}} \quad \text{Eq. 42}$$

in which  $x_c$  and  $y_c$  are the coordinates of point  $\underline{a}$  referred to the neutral-point axes, and  $J_{x_o}$  and  $J_{y_o}$  are the second moments of area  $A$  about axes  $x_o - x_o$  and  $y_o - y_o$ , respectively. Applying the parallel-axis theorem, the second moments may be expressed in the form

$$J_{y_o} = J - A x_c^2 = J - Q x_c$$

$$J_{x_o} = j - A y_c^2 = j - q y_c$$

in which  $J$  and  $Q$  are the second and first moments of area  $A$  about the  $y$ -axis, and  $j$  and  $q$  are the same moments about the  $x$ -axis, shown in Fig. 23b. Substituting for  $J_{y_o}$  and  $J_{x_o}$  in Eq. 42, reducing to a common denominator and rearranging, the equation becomes

$$M_a = \frac{1 - \frac{Q}{A} \frac{Q}{J} \frac{q}{A} \frac{q}{j}}{(1 - \frac{Q}{A} \frac{Q}{J})(1 - \frac{q}{A} \frac{q}{j})A} \quad \text{Eq. 43}$$

Next assume the column cross section to be subjected to two separate hydrostatic pressures, one varying linearly with  $x$  from zero intensity at  $\underline{a}$  to a maximum intensity at  $\underline{b}$ , and the other varying linearly with  $y$  from zero intensity at  $\underline{a}$  and  $\underline{b}$  to a maximum intensity at  $\underline{d}$ . The distances of the two centers of pressure referred to axes  $y$  and  $x$

are the ratios  $J/Q$  and  $j/q$ , respectively. Since ratios  $Q/A$  and  $q/A$  are equal to  $x_c$  and  $y_c$  by definition of the neutral-point, Eq. 43 may be written in the form

$$M_a = \frac{1 - \frac{x_c}{x_p} \frac{y_c}{y_p}}{\left(1 - \frac{x_c}{x_p}\right)\left(1 - \frac{y_c}{y_p}\right) A}$$

which reduces to

$$M_a = \frac{x_p y_p - x_c y_c}{(x_p y_p - x_c y_p - x_p y_c + x_c y_c) A} \quad \text{Eq. 44}$$

Similarly, the moment at b is

$$M_b = \frac{1}{A} - \frac{(1) x_c^2}{J_{y_o}} + \frac{(1) y_c^2}{J_{x_o}}$$

Using the same notation as before and simplifying, the last equation becomes

$$M_b = \frac{x_p y_p - 2 x_c y_p + x_c y_c}{(x_p y_p - x_c y_p - x_p y_c + x_c y_c) A} \quad \text{Eq. 45}$$

By definition, the carry-over factor is

$$C_{ab} = - \frac{M_b}{M_a} = \frac{x_p y_p - x_c y_p + x_c y_c}{x_c y_c - x_p y_p} \quad \text{Eq. 46}$$

By symmetry,

$$C_{ab} = C_{ba} \quad \text{Eq. 47}$$

Eq. 46 may be verified in the following manner. Let the rise of the arch be gradually decreased so that in the limit it becomes a straight beam as  $y_c$  approaches zero.

Then

$$\lim_{y_c \rightarrow 0} C_{ab} = \frac{x_P y_P - L y_P}{-x_P y_P} = -1 + \frac{L}{x_P}$$

or

$$C_{ab} = \frac{Q}{J} L - 1$$

which agrees with Eq. 7.

Sign Convention. - Unlike the case of straight members, the carry-over factor for arches, regardless of the sign convention used, may be either positive or negative, depending on the geometry of the arch. It is therefore important to interpret correctly the sign of the carry-over factor as determined experimentally or analytically in this paper.

In the column analogy relationships used herein, moments  $M_a$  and  $M_b$  are external moments and their signs agree with the ordinary beam sign convention, that is, a positive bending moment causes tension on the intrados side of the member. Thus a clockwise external moment at the left support and a counterclockwise external moment at the right support are positive.

In the moment distribution method of analysis the sign convention generally used for the carry-over factor is such that if a clockwise moment applied at one end of the member induces a clockwise fixed-end moment at the other, the ratio of the two moments is positive. It follows that if this sign convention is used, the sign of the ratio  $M_b/M_a$  determined by the column analogy method must be reversed (see the negative sign in Eq. 46).



3. Stiffness Factor. - The stiffness factor at a is the moment required at a to rotate that end through a unit angle while end b is held fixed. Since a unit rotation (unit load on the analogous column section) was used in the preceding derivation, the moment  $M_a$  expressed by Eqs. 42, 43 and 44 is the stiffness factor at a. Therefore, (Eq. 44)

$$S_a = M_a = \frac{x_p y_p - x_c y_c}{(x_p y_p - x_c y_p - x_p y_c + x_c y_c) A} \quad \text{Eq. 48}$$

By symmetry

$$S_b = S_a \quad \text{Eq. 49}$$

When the arch approaches a straight beam,  $y_c$  approaches zero so that in the limit Eq. 48 becomes

$$S_a = \frac{x_p y_p}{(x_p y_p - x_c y_p) A} = \frac{x_p}{(x_p - x_c) A}$$

which agrees with Eq. 13.

An alternate set of working formulae giving the stiffness and carry-over factors is derived in the following manner. Fig. 24 represents the cross section of the analogous column. A unit angle change induced at end a of the arch corresponds to a unit load applied at point a of the column section. The unit stress at any point  $(x_o, y_o)$  caused by the load is

$$f = \frac{1}{A} + \frac{(1) x_c}{J_{y_o}} x_o + \frac{(1) y_c}{J_{x_o}} y_o \quad \text{Eq. 50}$$

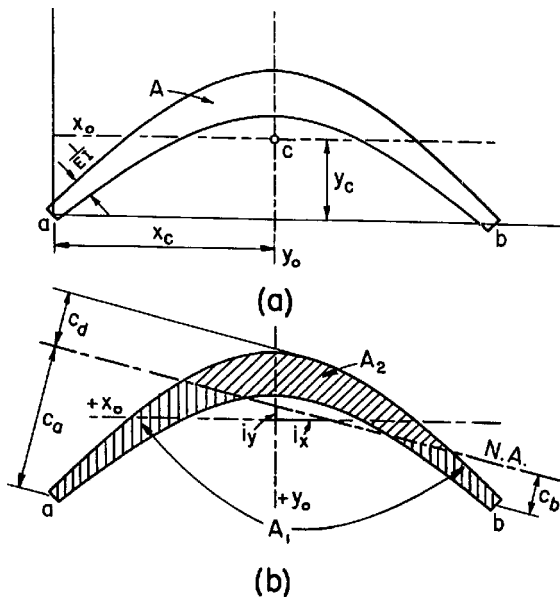


Fig. 24

The equation of the neutral axis N.A. shown in Fig. 24b is obtained from Eq. 50 by letting stress  $f$  equal zero:

$$0 = \frac{1}{A} + \frac{x_c}{J_{y_0}} x_0 + \frac{y_c}{J_{x_0}} y_0$$

Eq. 51

The  $x$ -intercept,  $i_x$ , of the neutral axis is obtained from Eq. 51 by letting  $y_0$

equal zero:

$$i_x = x_0 = - \frac{J_{y_0}}{A x_c} = - \frac{J_a - A x_c^2}{A x_c} = x_c - x_p \quad \text{Eq. 52}$$

Similarly, when  $x_0$  is zero,

$$i_y = y_0 = - \frac{J_{x_0}}{A y_c} = - \frac{J_{a-b} - A y_c^2}{A y_c} = y_c - y_p \quad \text{Eq. 53}$$

The unit stress varies linearly with the distance  $z$  from the neutral axis, that is

$$f = k z \quad \text{Eq. (a)}$$

in which  $k$  is a constant.

The resultant of the stresses is the load, that is,

$$I = k \int_0^{c_a} z dA - k \int_0^{c_d} z dA$$

or

$$I = k Q_1 - k Q_2 = k Q_{N.A.}$$

whence

$$k = \frac{I}{Q_{N.A.}} \quad \text{Eq. (b)}$$

in which  $Q_1$  and  $Q_2$  are the first moments of areas  $A_1$  and  $A_2$  on either side of the neutral axis N.A. taken about N.A., and  $Q_{N.A.}$  is the first moment of the whole area  $A = A_1 + A_2$  about N.A.

Since the moment of the unit load about N.A. equals the sum of the moments of the stresses about N.A.,

$$(1) C_a = k \int_0^{c_a} z^2 dA + k \int_0^{c_d} z^2 dA$$

or

$$C_a = k J_1 + k J_2 = k J_{N.A.} \quad \text{Eq. (c)}$$

in which  $J_1$  and  $J_2$  are the second moments of  $A_1$  and  $A_2$ , respectively, about N.A., and  $J_{N.A.}$  is the second moment of the whole area about N.A.

Combining Eqs. (b) and (c),

$$C_a = \frac{J_{N.A.}}{Q_{N.A.}} \quad \text{Eq. (d)}$$

The stress at point a of the column section corresponds to the stiffness factor for the arch, that is,

$$f_a = M_a = S_a = \frac{[(1) C_a] C_a}{J_{N.A.}} \quad \text{Eq. (e)}$$

Replacing  $c_a$  outside the brackets in Eq. (e) by its equivalent given by Eq. (d),

$$S_a = \frac{C_a}{Q_{N.A.}} \quad \text{Eq. (f)}$$

But

$$Q_{N.A.} = A \bar{z} \quad \text{Eq. (g)}$$

where  $\bar{z}$  is the distance of N.A. from the centroid  $\underline{c}$  of area  $A$ , shown in Fig. 25.

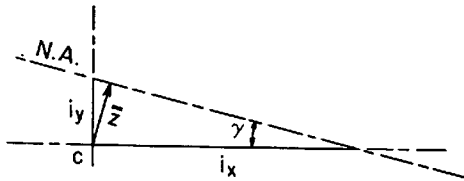


Fig. 25

But

$$\bar{z} = i_x \sin \gamma = i_x \frac{i_y}{\sqrt{i_x^2 + i_y^2}} \quad \text{Eq. (h)}$$

Combining Eqs. (f), (g), and (h),

$$S_a = \frac{c_a \sqrt{i_x^2 + i_y^2}}{A i_x i_y} \quad \text{Eq. 54}$$

The stress at point  $\underline{b}$  of the column section corresponds to moment  $M_b$  required to hold end  $\underline{b}$  of the arch fixed while end  $\underline{a}$  is rotated through a unit angle. Therefore

$$f_b = M_b = \frac{[(1) c_a] c_b}{J_{N.A.}} = \frac{c_b}{Q_{N.A.}}$$

By definition, the carry-over factor from  $\underline{a}$  to  $\underline{b}$  is

$$C_{ab} = -\frac{M_b}{M_a} = -\frac{\frac{c_b}{Q_{N.A.}}}{\frac{c_a}{Q_{N.A.}}} = -\frac{c_b}{c_a} \quad \text{Eq. 55}$$

By symmetry,

$$\left. \begin{aligned} S_a &= S_b \\ C_{ab} &= C_{ba} \end{aligned} \right\} \quad \text{Eq. 56}$$

Quantities  $i_x$  and  $i_y$  in Eq. 54 are defined by Eqs. 52 and 53 and are determined experimentally by weighing the respective solids and their reactions. Quantities  $c_b$  and  $c_a$  in Eq. 55 are best determined graphically (see Example 5).

4. Experimental Determination of Carry-Over and Stiffness Factors. - The experimental determination of  $C_{ab}$  and  $S_a$  given by Eqs. 46 and 48 or Eqs. 55 and 54 is based on the evaluation of quantities  $A$ ,  $x_p$ ,  $y_c$ , and  $y_p$ . These are found experimentally in very much the same manner as was done in the case of beams. However, two "pressure solids" are required; namely, one solid for the evaluation of  $x_p$  and the other for  $y_c$  and  $y_p$ . A single wooden blank may be used to make both.

Pieces of 2 x 4 in. nominal size or larger seasoned lumber may be used to make the block from which the initial blank is cut. Several pieces may be glued together as is



shown in Fig. 26, the number of strips depending on the size of the blank required.

The arch rib is drawn to scale on the upper side of the composite block and the  $1/EI$ -

Fig. 26 values are laid off transversely, one-half on each side of the rib. The blank is then cut from the block with the aid of a narrow blade.

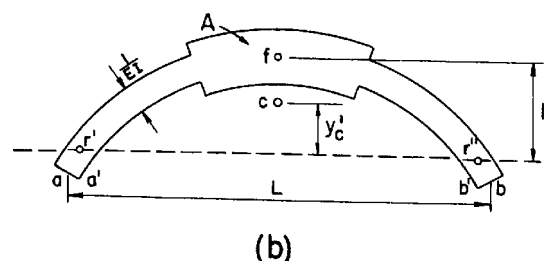
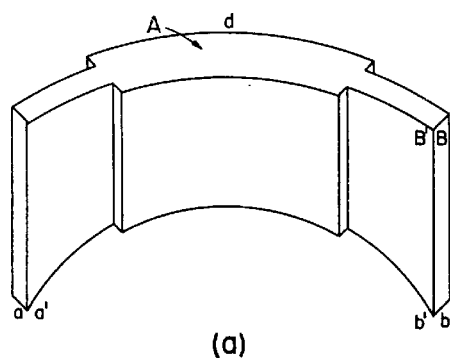
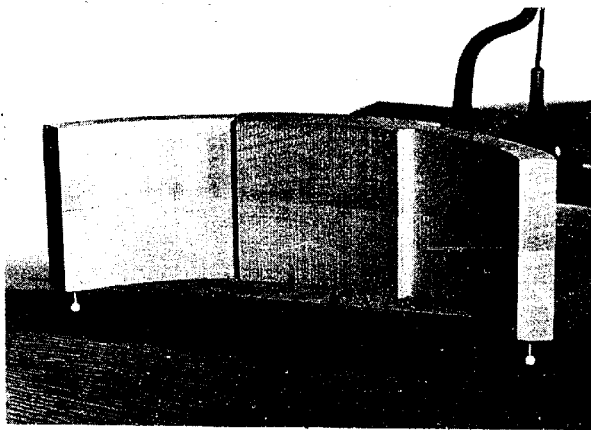


Fig. 27

Fig. 27a is a pictorial view of the initial blank representing a deepened circular arch (see Example 5). Fig. 27b shows the top view of the blank and the notation used in the outline of the experimental procedure in determining the carry-over and stiffness factors.

To evaluate quantities  $A$ ,  $y_c$ ,  $y_p$  and  $x_p$ , the following procedure is recommended.

(a) Determine area  $A$ . Area  $A$  is determined by weighing the initial blank shown in Fig. 27a and dividing the weight by its altitude and the specific weight of the wood (see Example 3 - Deepened Beam);



Weighing  $R_f$

Fig. 28

(b) Determine  $y_c$ . The blank is supported at the crown point  $\underline{f}$  (Fig. 27b, black pin in Fig. 28), resting on the scale platform and at points  $\underline{r'}$  and  $\underline{r''}$  (white pins in the foreground).

The white pins rest on a block of appropriate height

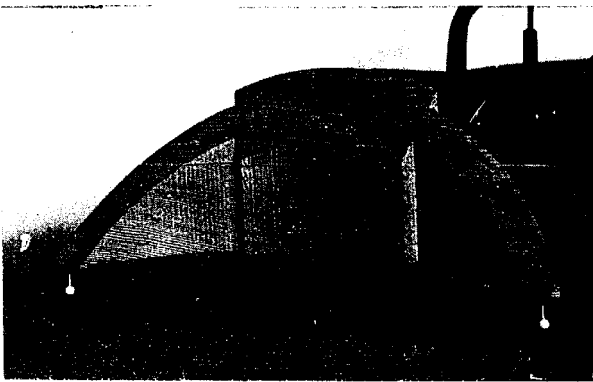
so that supports  $\underline{f}$ ,  $\underline{r'}$  and  $\underline{r''}$  are in the same horizontal plane, checked by means of a carpenter's level. Pins  $\underline{r'}$  and  $\underline{r''}$  are set back from the front corners of the blank to preclude the splitting of the wood.

The crown-point reaction  $R_f$  is determined by weighing. Taking moments about axis  $\underline{r' - r''}$ ,

$$P y_c' = R_f h$$

$$y_c' = \frac{R_f h}{P}$$

in which  $P$  is the weight of the blank and  $y_c'$  is the distance of centroid  $\underline{c}$  (neutral-point) of area  $A$ , measured from axis  $r' - r''$ .



Weighing  $R_f'$

Fig. 29

supported by a block of suitable height. As before, supports  $\underline{f}$ ,  $\underline{r}'$  and  $\underline{r}''$  must lie in the same horizontal plane.

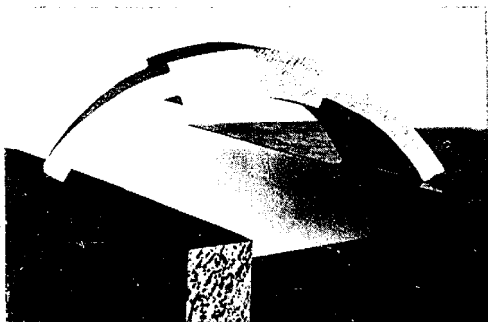
The crown-point reaction  $R_f'$  is determined by weighing. Taking moments about axis  $r' - r''$ ,

$$W' y_p' = R_f' h$$

$$y_p' = \frac{R_f' h}{W'}$$

in which  $W'$  is the weight of the pressure solid  $a - b - d$ , and  $y_p'$  is the distance of the center of pressure referred to axis  $r' - r''$ .

(c) Determine  $y_p$ . Cut blank diagonally through points  $\underline{d}$ ,  $\underline{a}$  and  $\underline{b}$  (Fig. 27a and Fig. 29). Support the part  $a - b - d$  of the blank on a pin at  $\underline{f}$  (black pin in Fig. 29) resting on the scale platform, and on pins at  $\underline{a}$  and  $\underline{b}$  (white pins),



Weighing  $R_{b'B'}$

Fig. 30

(d) Determine  $x_p$ . The two half-solids severed by cutting in step (c) are glued together so that the initial blank shown in Fig. 28 is restored. Next the blank is cut diagonally through points  $\underline{a}$  and  $\underline{B}$  (see Fig. 27a).

Support the severed solid  $a - b - B$  in a semi-inverted position along edge  $b' - B'$  resting on the scale platform, and at point  $\underline{a'}$  supported by a suitable block as is shown in Fig. 30. Points  $\underline{a'}$ ,  $\underline{b'}$  and  $\underline{B'}$  must be in the same horizontal plane. Since the supporting edge and point  $\underline{a'}$  clearly define the span, pins are not necessary at the supports.

The total reaction  $R_{b'B'}$  along edge  $b' - B'$  is determined by weighing. Taking moments about an axis through support  $\underline{a'}$  and parallel to edge  $b' - B'$ ,

$$W'' x_p' = R_{b'B'} L'$$

$$x_p' = \frac{R_{b'B'} L'}{W''}$$

in which  $W''$  is the weight of the pressure solid  $a' - b' - B'$  and  $L'$  is the clear span between the supports as shown in Fig. 30. The distance  $y_p'$  locates the center of pressure for the solid with reference to point  $\underline{a'}$ .

For symmetrical arches considered in this paper the



neutral-point c is located on the vertical axis of symmetry of the arch.

The use of map pins or thumb tacks in steps (b) and (c) is necessary in order to eliminate the indefiniteness of moment arms of the reactions involved. Ordinary map pins and thumb tacks weigh less than one gram each. When extreme accuracy is desired the weight of the pins should be subtracted from the reaction caused by the weight of the solid and the pin or pins resting on the scale platform.

5. Equivalent Arch Models. - It is possible to make and experimentally analyze equivalent arch models having a straight rib and resembling the beam models investigated earlier in this paper. This alternative eliminates the need for three-point supports and the inherently delicate weighing of reactions and simplifies to some extent the cutting of the models. The relationship between the arch and its equivalent straight-axis component solids is derived in the following paragraphs.

It was shown in articles 2 and 3 that the carry-over and stiffness factors are functions of the elastic area  $\int \frac{ds}{EI}$ , its first and second moments  $Q$  and  $J$ , and the span  $L$  of the arch. Fig. 31 represents a curved segment  $A$  of the elastic area confined between lines 1,1 and 2,2 and a segment  $A'$  bound by lines 1',1' and 2',2' and the  $x$ -axis.

The first and second moments of  $A$  about the  $y$ -axis are

$$\left. \begin{aligned} Q_y &= \int x dA \\ J_y &= \int x^2 dA \end{aligned} \right\} \text{Eqs. 57}$$

and the moments of  $A'$  about the same axis are

$$\left. \begin{aligned} Q_y' &= \int x dA' \\ J_y' &= \int x^2 dA' \end{aligned} \right\} \text{Eqs. 58}$$

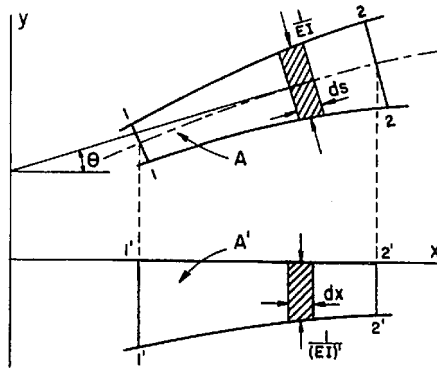


Fig. 31

A comparison of Eqs. 57 and 58 shows that if areas  $A$  and  $A'$  are to have the same moments about the  $y$ -axis, the elemental areas  $dA$  and  $dA'$  must be equal; that is,

$$dA = \frac{ds}{EI} = dA' = \frac{dx}{(EI)'} = \frac{ds \cos \theta}{(EI)'}$$

or

$$\frac{1}{(EI)'} = \frac{1}{EI \cos \theta} \quad \text{Eq. 59}$$

Consequently if the  $1/EI$ -values along the arch rib are divided by the cosines of the angle which the tangents to the arch rib make with the  $x$ -axis, the resulting values laid off normal to and along the  $x$ -axis yield an area which for the purposes of the first and second moments about the  $y$ - or any parallel axis is equivalent to area  $A$ . Whether or not the  $1/EI$ -values for the arch are constant, the equivalent  $1/(EI)'$ -values along the  $x$ -axis vary.

The adjusted values may be laid off to one side of the x-axis so that a single curved cut is required in the preparation of the blank. To determine  $x_c$  and  $x_p$  the respective solids are supported exactly in the same manner as in the case of beams investigated in Part II.

The same principle applies in the rectification of the arch in the y-direction, except that the  $1/EI$ -values are divided by  $\sin \theta$ .

At the crown of a circular, parabolic or similar symmetrical arch the slope of the tangent to the rib is zero so that  $1/EI \sin 0^\circ$  is infinite. Experience has shown that if the width of the equivalent blank in the neighborhood of the crown-point is made reasonably large, the resulting errors in the values of  $y_c$  and  $y_p$  are of the order of a few per cent.

When utmost accuracy is desired the effect of the infinite  $1/(EI)'$ -value at the crown-point can be compensated for by evaluating numerically a small element  $\Delta A$  of the arch elastic area adjoining the crown. If the length of this element is  $\Delta s$  and  $1/(EI)'$  is finite at the beginning of the interval  $\Delta s$ , the finite increment  $\Delta[1/(EI)']$  is obtained as follows:

$$\Delta A = \frac{1}{(EI)_{\text{crown}}} \Delta S = \Delta A' = \Delta \left[ \frac{1}{(EI)'} \right] \Delta y$$

whence

$$\Delta \left[ \frac{1}{(EI)'} \right] = \frac{\Delta A}{\Delta y}$$

in which  $\Delta y$  is the y-projection of  $\Delta s$ . The compensation is effected by adding to the  $1/(EI)'$  diagram immediately below the crown point a rectangle  $\Delta A/\Delta y$  long and  $\Delta y$  deep.

A semi-graphical method of adjusting the  $1/EI$ -values for a circular arch is shown in Fig. 32 in which the transformation of the elastic area with respect to the y-axis is illustrated for point 5 of the arch rib.

(Eq. 59)

$$\frac{1}{(EI)'} = \frac{1}{EI \cos \theta}$$

From Fig. 32,

$$\cos \theta_5 = \sin \varphi_5 = \frac{1}{\csc \varphi_5} = \frac{1}{O5'}$$

Thus distances  $\overline{O5'}$ ,  $\overline{O4'}$ ,  $\overline{O3'}$ , etc., represent to some scale the factors  $1/\cos \theta$  by which the  $1/EI$ -values of the arch must be multiplied to yield the equivalent area  $A'$ . The length  $\overline{O5'}$  is scaled off, multiplied by  $1/(EI)_5$ , and the product is plotted as  $\overline{m_5 n_5}$ . The construction is repeated for a sufficient number of points. The transformed area is the cross-hatched area below the x-axis.

The transformation of the area with respect to the x-axis is carried out in a similar manner. At point 4 of the arch,

$$\sin \theta_4 = \cos \varphi_4 = \frac{1}{\sec \varphi_4} = \frac{1}{O4''}$$

The length  $\overline{O4''}$  is scaled off, multiplied by  $1/(EI)_4$ , and the product is plotted as  $\overline{M_4 N_4}$ . By repeating this for several points the cross-hatched area above the x-axis is obtained.

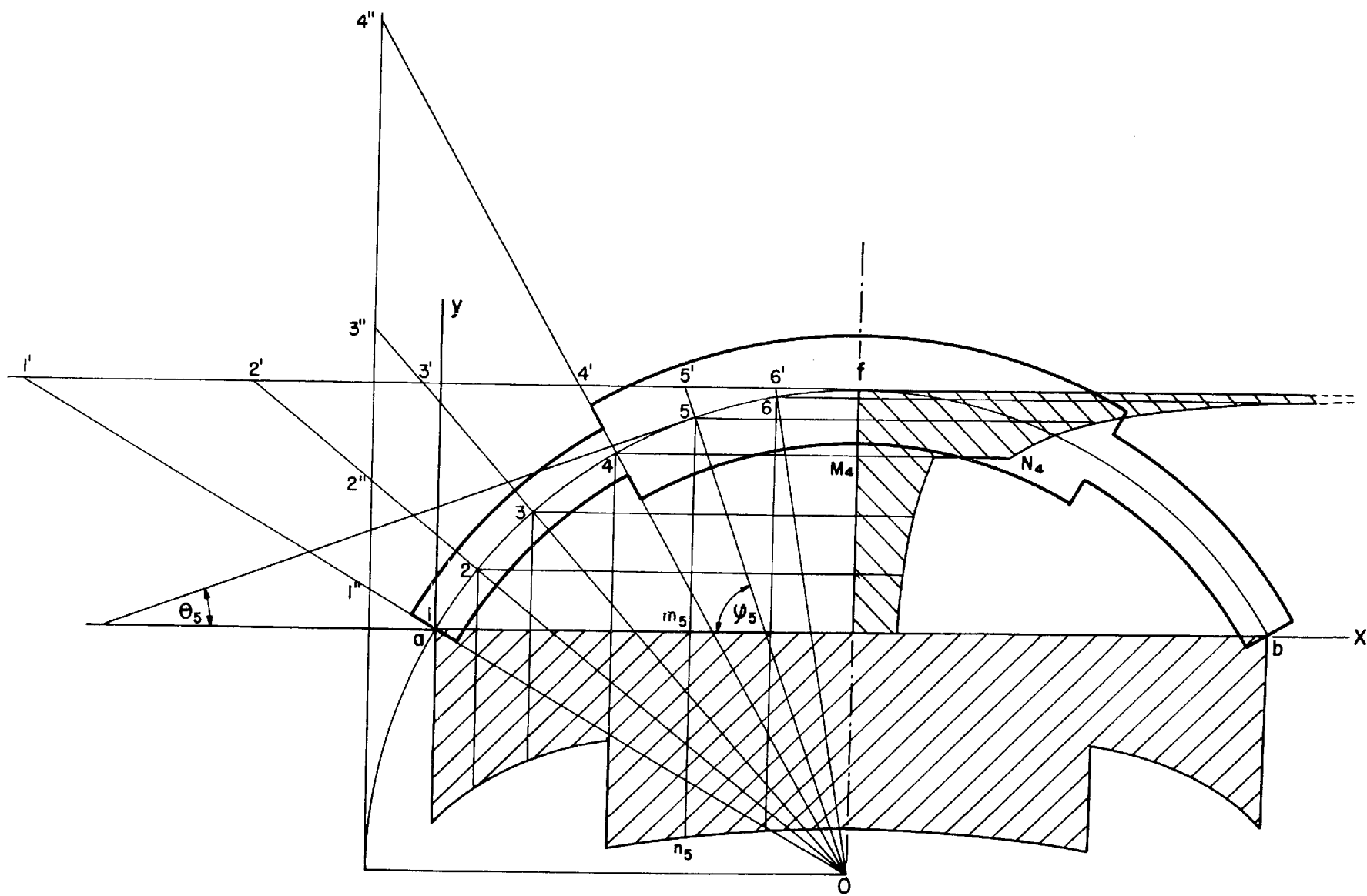


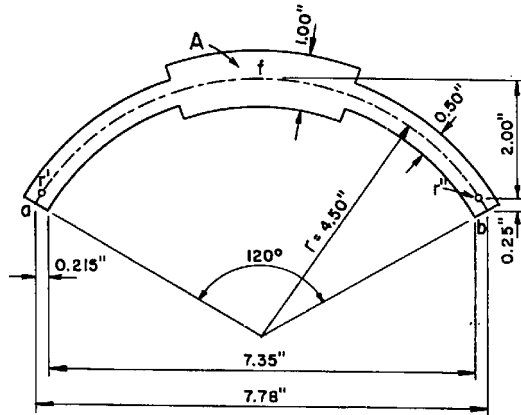
Fig. 32

If a point is inaccessible (such as points 5", 6") the cosine values are scaled off and their reciprocals are used. The scale is obtained by correlating the secant and cosine readings for an accessible point.

For the experimental purposes outlined in this paper the scales of the equivalent areas need not be the same. Also it suffices to transform only one-half the area with respect to the x-axis, inasmuch as  $y_o$  and  $y_p$  for half-area solids are the same as if the total area were used.

For a non-circular arch angles  $\theta$  can be computed by the methods of calculus, or tangents may be drawn at a series of points and the respective trigonometric functions scaled off.

Example 5 - Deepened 120° Circular Arch. - Determination of Carry-Over and Stiffness Factors.



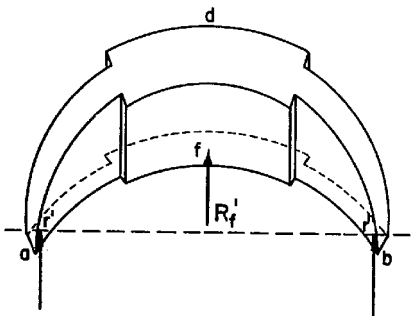
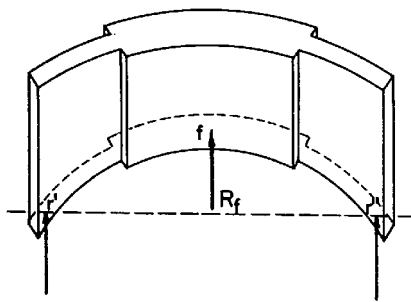
Experimental Data and Determination of  $y_c$ ,  $y_p$  and  $x_p$ .

$$P = 149, \quad R_f = 106$$

$$149y_c' = (106)(2")$$

$$y_c' = 1.423"$$

$$y_c = 1.423 + 0.25 = 1.673"$$

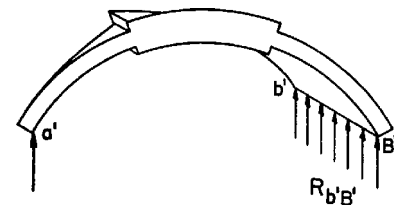


$$W' = 90, \quad R_f' = 77$$

$$90 y_p' = (77)(2")$$

$$y_p' = 1.710"$$

$$y_p = 1.710 + 0.25 = 1.960"$$



$$W'' = 91.5, \quad R_{b'B'} = 60.5$$

$$91.5 x_p' = (60.5)(7.35")$$

$$x_p' = 4.86"$$

$$x_p = 4.86 + 0.215 = 5.075"$$

Fig. 33

(1) Solution by Eqs. 46 and 48.

$$C_{ab} = \frac{x_P y_P - L y_P + x_c y_c}{x_c y_c - x_P y_P}$$

$$C_{ab} = \frac{(5.075)(1.960) - (7.78)(1.960) + (3.89)(1.673)}{(3.89)(1.673) - (5.075)(1.960)}$$

$$C_{ab} = -0.356$$

$$S_a = \frac{x_P y_P - x_c y_c}{(x_P y_P - x_c y_P - x_P y_c + x_c y_c) A}$$

$$S_a = \frac{(5.075)(1.960) - (3.89)(1.673)}{[(5.075)(1.960) - (3.89)(1.960) - (5.075)(1.673) + (3.89)(1.673)] A}$$

$$S_a = \frac{10.15}{A}$$

(2) Solution by Eqs. 55 and 54, supplemented by graphics.

$$(\text{Eq. 52}) \quad i_x = x_c - x_P = 3.89 - 5.075 = -1.185$$

$$(\text{Eq. 53}) \quad i_y = y_c - y_P = 1.673 - 1.960 = -0.287$$

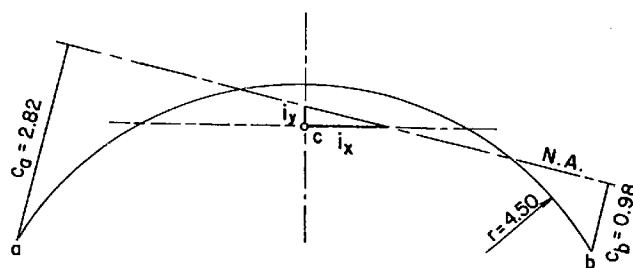


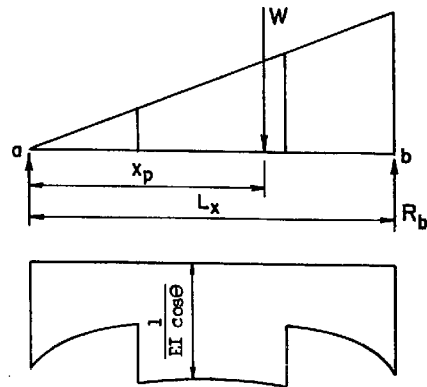
Fig. 34

$$(\text{Eq. 55}) \quad C_{ab} = -\frac{c_b}{c_a} = -\frac{0.98}{2.82} = -0.348$$

$$(\text{Eq. 54}) \quad S_a = \frac{c_a \sqrt{i_x^2 + i_y^2}}{A i_x i_y} = \frac{2.82 \sqrt{(-1.185)^2 + (-0.287)^2}}{A (-1.185)(-0.287)} = \frac{10.10}{A}$$



## (3) Solution Based on Alternate Models.



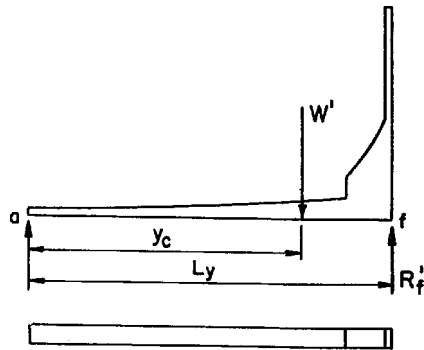
Experimental Data and Evaluation.

$$W = 254$$

$$R_b = 164$$

$$W x_p = R_b L_x$$

$$x_p = \frac{164 L_x}{254} = 0.645 L_x$$

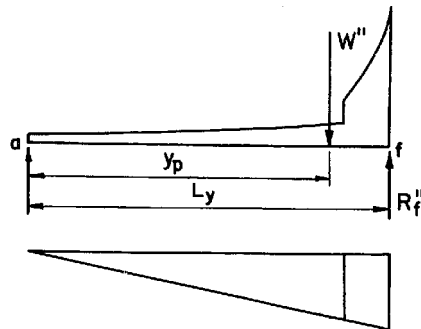


$$W' = 89.5$$

$$R_f' = 65.5$$

$$W' y_c = R_f' L_y$$

$$y_c = \frac{65.5 L_y}{89.5} = 0.731 L_y$$



$$W'' = 87$$

$$R_f'' = 72.5$$

$$W'' y_p = R_f'' L_y$$

$$y_p = \frac{72.5 L_y}{87} = 0.833 L_y$$

Fig. 35

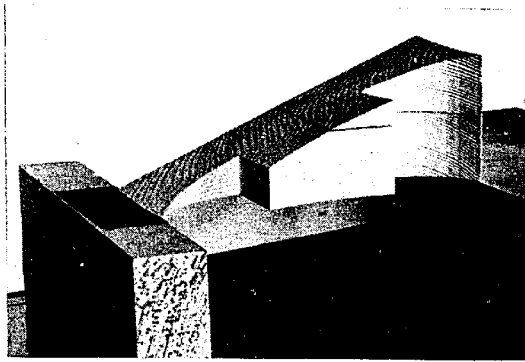
(Eqs. 46 and 48)

$$C_{ab} = \frac{L_x L_y [(0.645)(0.833) - 0.833 + (0.5)(0.731)]}{L_x L_y [(0.5)(0.731) - (0.645)(0.833)]} = -0.406$$

$$S_a = \frac{L_x L_y [(0.645)(0.833) - (0.5)(0.731)]}{L_x L_y [(0.645)(0.833) - (0.5)(0.833) - (0.645)(0.731) + (0.5)(0.731)] A}$$

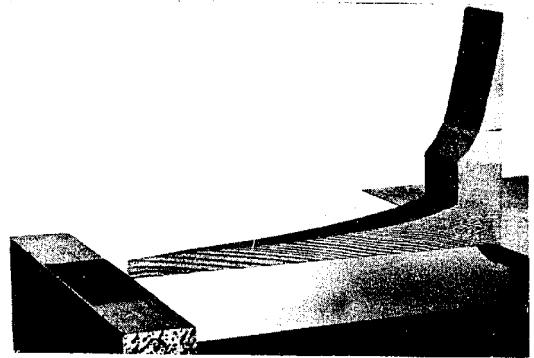
$$S_a = \frac{11.61}{A}$$

The alternate models were laid out with the help of the graphic transformation illustrated in Fig. 32<sup>(6)</sup>. Two separate models were made to determine  $y_c$  and  $y_p$ . The  $y_c$ -model included a corrective rectangle corresponding to the 10-degree element adjoining the crown of the arch. The  $y_p$ -model was cut off abruptly near the crown without correction. The actual weighing of reactions  $R_b$  and  $R_f''$  is shown in Figs. 36 and 37.



Weighing  $R_b$

Fig. 36



Weighing  $R_f''$

Fig. 37

6. Modified Stiffness Factor. - The modified stiffness factor  $S'_a$  is the moment which must be applied at end a of the arch to rotate that end through a unit angle while the other end is hinged.

Fig. 38 represents the cross section of the analogous column. The hinge at end b of the arch corresponds to an infinite point-area at b of the column section so that the neutral-point c shifts to b and axes  $x_0$  and  $y_0$  are as shown.

<sup>(6)</sup> Fig. 32 illustrates the area-transformations of an arch similar to that in Example 5.

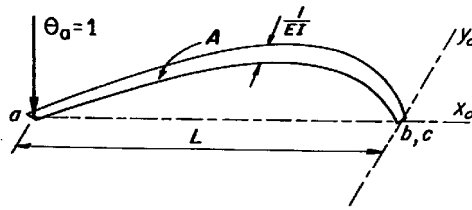


Fig. 38

A unit rotation  $\theta_a$  at support a of the arch corresponds to a unit load at point a of the column section. Since neither the  $x_0$ - nor the  $y_0$ -axis is

an axis of symmetry, the general form of column analogy equation<sup>(7)</sup> must be used,

$$M = f = \frac{\theta_a}{A} \pm \frac{M_{y_0} J_{x_0} - M_{x_0} J_{x_0 y_0}}{J_{x_0} J_{y_0} - J_{x_0 y_0}^2} x_0 \pm \frac{M_{x_0} J_{y_0} - M_{y_0} J_{x_0 y_0}}{J_{x_0} J_{y_0} - J_{x_0 y_0}^2} y_0 \quad \text{Eq. 60}$$

in which  $M$  is the bending moment at any point  $(x_0, y_0)$  of the arch,  $f$  the equivalent column unit stress,  $M_{y_0}$  and  $M_{x_0}$  are the moments of the angle load  $\theta_a$  about axes  $y_0$  and  $x_0$ , respectively,  $J_{x_0 y_0}$  is the product of inertia of area  $A$  about axes  $x_0$  and  $y_0$ , and  $J_{x_0}$  and  $J_{y_0}$  are the second moments of  $A$  about the same axes.

The moment at a corresponding to  $\theta_a = 1$  is

$$S'_a = \frac{1}{\infty} + \frac{(1) L J_{x_0} - (0) J_{x_0 y_0}}{J_{x_0} J_{y_0} - J_{x_0 y_0}^2} L + 0$$

or

$$S'_a = \frac{L^2}{J_{y_0} - \frac{J_{x_0 y_0}^2}{J_{x_0}}} \quad \text{Eq. 61}$$

For a flat arch the ratio  $J_{x_0 y_0}^2 / J_{x_0}$  is small and approaches zero as the arch approaches a straight beam.

Therefore in the limit Eq. 61 becomes

$$S'_a = \frac{L^2}{J_{y_0}}$$

which is in agreement with Eq. 12.

<sup>(7)</sup> See "Theory of Modern Steel Structures" by L.E. Grinter, page 231.

Example 6 - Elliptical Arch of Constant Moment of Inertia. -  
 Determination of (a) Carry-Over and Stiffness Factors and  
 (b) Modified Stiffness Factor.

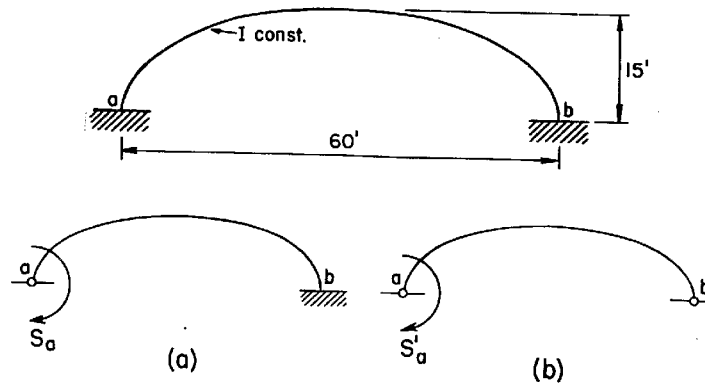


Fig. 39

For experimental data and evaluation see Example 7.

(a)	(b)
$x_o = 30.00$ ft.	$J_{x_o} = J_{a-b} = J_x = 9,400$
$x_p = 42.45$ ft.	$J_{y_o} = J_b = J_y = 92,500$
$y_o = 10.55$ ft.	$J_{x_o y_o} = J_{xy} = 23,050$
$y_p = 12.21$ ft.	$A = 72.75$
$A = 72.75$ (rel.)	

(rel.)

(a)

(Eq. 46)

$$C_{ab} = \frac{(42.45)(12.21) - (60)(12.21) + (30)(10.55)}{(30)(10.55) - (42.45)(12.21)}$$

$$C_{ab} = -0.507$$

(Eq. 48)

$$S_o = \frac{(42.45)(12.21) - (30)(10.55)}{[(42.45)(12.21) - (30)(12.21) - (42.45)(10.55) + (30)(10.55)] 72.75}$$

$$S_a = 0.134(rel.) = \frac{0.134}{A} \cdot 72.75 = \frac{9.77}{A} (rel.)$$

(b)

(Eq. 61)

$$S'_a = \frac{(60)^2}{92,500 - \frac{(23,050)^2}{9,400}} = 0.1001(rel.)$$

$$S'_a = \frac{0.1001}{A} \cdot 72.75 = \frac{7.30}{A} (rel.)$$

7. Accuracy of the Experimental Method. - The experimental results obtained in Examples 5 and 6 are listed in Table III and compared with theoretical values computed in Appendix.

TABLE III

Example	Carry-Over Factor				Stiffness Factor		
	Experimental	Theor.	% Error		Exper.	Theor.	% Error
5 - Deepened 120° Circular Arch	Solution (1) -0.356	-0.411	13.4		10.15	11.36	10.6
	Solution (2) -0.348		15.3		10.10		11.1
	Solution (3) -0.406		1.2		11.61		2.2
6 - Elliptical Arch	(a) -0.507	-0.517	1.9		9.77	9.87	1.0
	(b)				7.30	7.21	1.2

In Example 5 the carry-over and stiffness factors obtained by solutions (1) and (2) are in error by more than 10 per cent. On the other hand, solution (3) of Example 5, and results in Example 6 have errors of 1 or 2 per cent only.

The principal source of the large per cent error in

solutions (1) and (2) can be traced to the relative geometric and  $1/EI$  scales of the model. The radius of the models used in solutions (1) and (2) was 4.50 in., and the larger of the two  $1/EI$ -values was laid off as 1.00 in. In Example 6, the models were 16 and 20 in. long, and the  $1/EI$  width was 0.728 in.

The limitations of the concept of the elastic area  $A$  as used in the neutral-point and column analogy methods are frequently overlooked. Failure to interpret the concept correctly may lead to serious errors in solving certain types of problems by either of the two methods. The  $1/EI$ -values of a member are associated with the individual points along its axis. In the column analogy method these values are laid off transversely with regard to the axis of the member to form the cross section of a hypothetical column. This artifice simplifies the sign convention and the interpretation of the working equations. Furthermore a fairly complex problem of statically indeterminate analysis is reduced to a simple one of resistance of materials. However, the device does not permit the treatment of the fictitious cross section as a bona-fide area, particularly when its second moments are concerned.

The working equations of the experimental method were developed from the conjugate beam or column analogy methods in which  $A = \int \frac{ds}{EI}$ , expressed in  $(\text{lb-ft.})^{-1}$ , is uni-dimensional, and from hydrostatics where the immersed area is a true

geometric area expressed in  $\text{ft.}^2$ . For this reason the second moment of area  $A$  about the axis which is perpendicular to the  $l/EI$ -values is zero (sometimes in technical literature incorrectly called "negligibly small"). Applying this important principle to the experimental analysis of curved members, it follows that the scale of the  $l/EI$ -values must be made sufficiently small to approximate the uni-dimensional character of the latter. In Example 5 the model satisfying this condition would be one made of thin sheet metal and possessing a double thickness within the middle third of the rib. The models would be cut and their reactions weighed in exactly the same manner as was done in Example 5. In Example 6, the ration of the  $l/EI$  width and the lineal dimensions of the model was more favorable, explaining the very close agreement between model and analytic results.

Significantly, for straight-axis members the scale of the  $l/EI$ -values is immaterial inasmuch as the position of both the centroid and center of pressure is unaffected in the longitudinal direction. This explains why solution (3) in Example 5 yielded very good results.

For flat arches approaching straight-axis members the effect of the  $l/EI$ -scale choice diminishes so that a much closer agreement between experimental and theoretical values is to be expected.

8. Fixed End Moments. - Fig. 40a shows a symmetrical arch

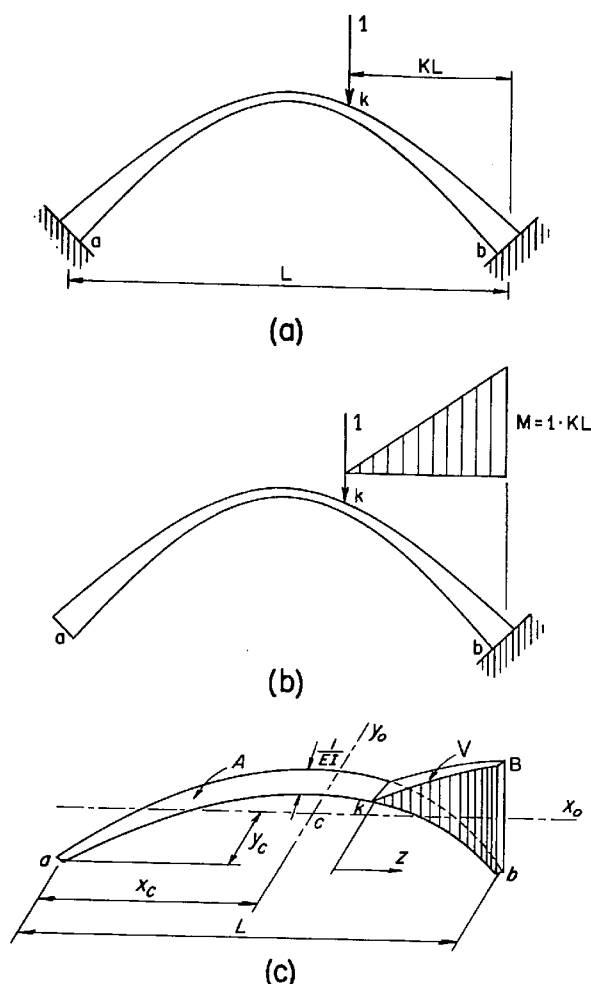


Fig. 40

fixed at both ends carrying a unit load at point  $\underline{k}$ . To find the fixed end moments by the column analogy method the arch is cut back to a statically determinate condition. Fig. 40b shows the determinate cantilever arch and its bending moment diagram.

Fig. 40c represents the analogous column section and the  $M/EI$ -load acting upon it. The bending moment at  $\underline{a}$  of the arch is equivalent to the unit stress at  $\underline{a}$  of the column section and is

$$M_a = f_a = \frac{V}{A} - \frac{M_{y_0}}{J_{y_0}} x_c + \frac{M_{x_0}}{J_{x_0}} y_c \quad \text{Eq. 62}$$

in which  $V = \int \frac{M}{EI} ds$ , the total load on the column section, may be visualized as the volume of the load solid in Fig. 40c, and  $M_{y_0}$  and  $M_{x_0}$  its statical moments about the neutral axes  $y_0$  and  $x_0$ , respectively; that is,

$$M_{y_0} = V e_{x_0} \quad \text{and} \quad M_{x_0} = V e_{y_0}$$



where  $e_{x_0}$  and  $e_{y_0}$  are the coordinates of the center of gravity of  $V$  referred to axes  $y_0$  and  $x_0$ . Substituting the last two expressions together with the relationships given by Eqs. 52 and 53 into Eq. 62 and factoring  $V/A$ , the equation becomes

$$M_a = \frac{V}{A} \left[ 1 - \frac{e_{x_0}}{x_p - x_c} + \frac{e_{y_0}}{y_p - y_c} \right] \quad \text{Eq. 63}$$

The experimental determination of quantities  $x_p$ ,  $x_c$  and  $y_p$ ,  $y_c$  was established in conjunction with carry-over and stiffness factors. Quantities  $V$  and  $A$  are found in exactly the same manner as in the case of straight-axis members. Coordinates  $e_{x_0}$  and  $e_{y_0}$  may be found experimentally by appropriately supporting the load solid, weighing its reactions, and the use of statics. It should be noted that the base area  $A$  of the solid is the part of the area of the column section extending from load point k to abutment b. Its altitudes  $M$ , erected along the curved centroidal axis of the base area, are  $M = (l).(z)$  in which  $z$  is the abscissa of  $M$  referred to k. It follows that the sloping upper surface of the elastic solid is a plane surface so that the cutting operation is a relatively simple one.

The experimental method was applied to the solution of circular, parabolic and elliptical arches of variable and constant moments of inertia. It was found that for small size models such as can be made inexpensively and with a minimum of equipment, the method was not generally satisfactory.

The determination of eccentricities  $e_{x_0}$  and  $e_{y_0}$  by weighing was tedious inasmuch as the equilibrium of the balance was difficult to establish. Considering these and other difficulties, the amount of work involved, the questionable accuracy of results obtained (with small models errors of 15% were found to exist), etc., the method is not recommended. An alternate approach to the problem on hand is outlined and illustrated in the following article.

9. Influence Lines for Thrust, Shear and Fixed End Moment. - Influence lines for the redundants of an arch or beam may be constructed by utilizing the experimentally determined properties of the elastic area  $A = \int \frac{ds}{EI}$  in conjunction with the properties of the neutral-point and the conjugate beam.

It follows from the derivation of the neutral-point properties that a vertical force applied at that point causes a purely vertical displacement of the neutral-point. In general if a redundant ( $V_0$ ,  $H_0$ ,  $M_0$ ) is allowed to induce a movement at the neutral-point, the latter undergoes a distortion (translation, or rotation) in the nature of that redundant only.<sup>(8)</sup>

According to the Müller-Breslau principle, if a single reaction component (force or moment) is allowed to induce a unit movement in the nature of the component reaction, the deflected structure is the influence line for that component reaction. The neutral-point forces and moment required to

---

<sup>(8)</sup> See "Theory of Modern Steel Structures" by L.E. Grinter, page 211.

induce unit movements of the neutral-point may be computed by the method of virtual work and the deflection ordinates of the structure may be found by the conjugate beam method.

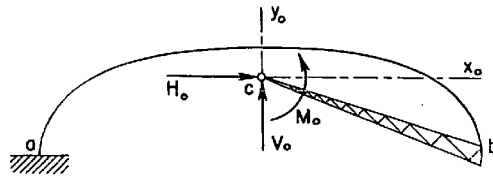


Fig. 41

In Fig. 41, the displacements and rotation caused by each of the three loads acting singly at the neutral-point are

$$\left. \begin{aligned} \Delta_{y_o}^{V_o=1} &= \int \frac{(l \cdot x_o)^2 ds}{EI} = J_{y_o} \\ \Delta_{x_o}^{H_o=1} &= \int \frac{(l \cdot y_o)^2 ds}{EI} = J_{x_o} \\ \Theta^{M_o=1} &= \int \frac{(l)^2 ds}{EI} = A \end{aligned} \right\} \text{Eqs. 64}$$

and the forces and moment required to cause unit displacements and rotation, respectively, are

$$\left. \begin{aligned} V_o &= \frac{1}{J_{y_o}} \\ H_o &= \frac{1}{J_{x_o}} \\ M_o &= \frac{1}{A} \end{aligned} \right\} \text{Eqs. 65}$$

The deflection ordinates of the arch correspond to the bending moments in the conjugate arch caused by each of the three loads given by Eqs. 65 and such other loads as are

required by the slope and deflection characteristics at the cantilever end b of the arch. In each case the conjugate arch may be replaced by a straight beam whose end conditions at a and b satisfy the slope and deflection conditions brought about at the corresponding ends of the arch by the neutral-point load. The neutral-point loads, conveniently taken as unity, and the corresponding conjugate beams are shown in Figs. 43, 44 and 45. The distributed moment loads on the conjugate beams are replaced by concentrated loads acting at the mid-points of a series of arch elements shown in Fig. 42.

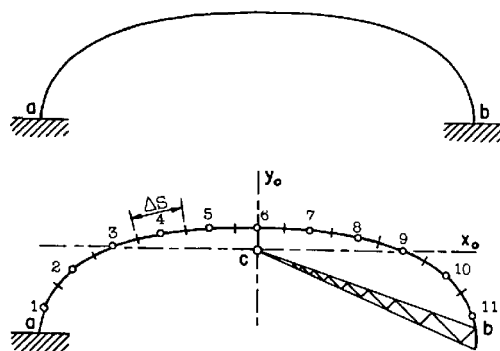


Fig. 42

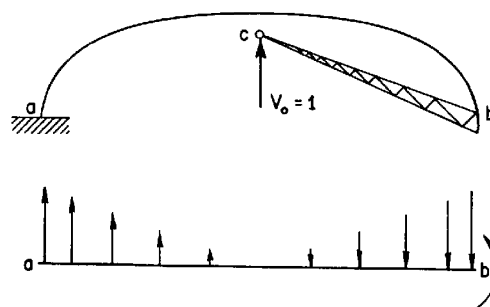


Fig. 43

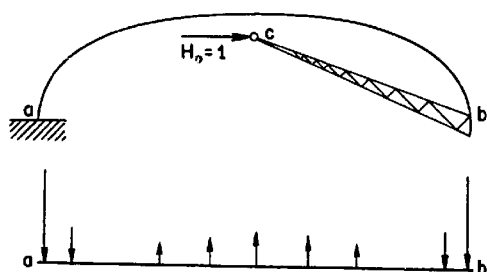


Fig. 44

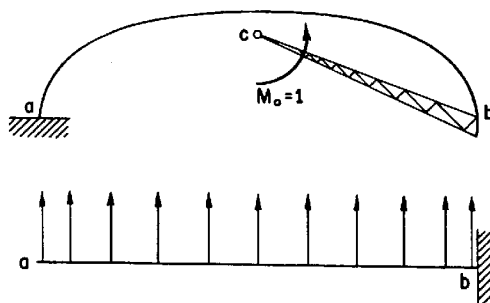


Fig. 45

The subdivision of the arch rib into equal elements  $\Delta s$  is usually done by trial with a pair of dividers. The centers

of the elements are then located and their coordinates  $x_0$  and  $y_0$  scaled. If  $EI$  is constant, the values of  $ds/EI$  may be taken as unity in all computations. The cantilever arch deflections corresponding to unit displacements induced at the neutral-point are obtained from deflections corresponding to unit loads by proportion (see Eqs. 65 and 64).

Example 7 - Influence Lines for Reactions. - The principle outlined in article 9 will be applied to the solution of the elliptical arch of constant moment of inertia<sup>(9)</sup> shown in Fig. 46.

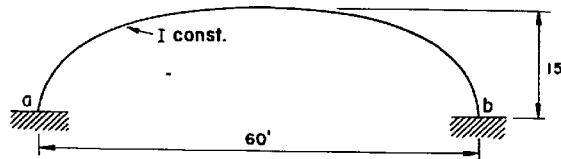


Fig. 46

(1) Determine area  $A = \int \frac{ds}{EI}$ .

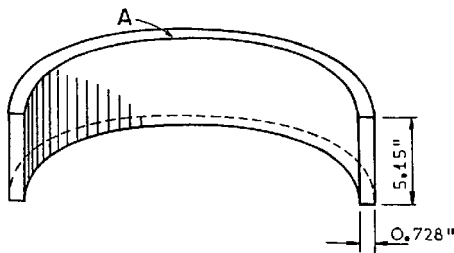


Fig. 47

Specific weight  $w$  of wood. -  
Prismatic specimen 12.51 in.<sup>3</sup>  
weighs 135 gr.; therefore

$$w = \frac{135}{12.51} = 10.79$$

The blank shown in Fig. 47  
weighs 980 gr. so that its

volume is

$$V = \frac{980}{10.79} = 91.0$$

<sup>(9)</sup> See "Statically Indeterminate Structures" by L.C. Maugh, Examples 43, 44, 45 and 46, pages 220 to 228.

$$A = \frac{91.0}{5.15} = 17.69 \text{ in.}^2$$

$$\text{Area per unit width (1/EI = 1 in.)} = \int ds = \frac{17.69}{0.728} = 24.25 \text{ in.}$$

The geometric scale of the model is 1 in. = 3 ft. For prototype, the rib length is

$$\int ds = (24.25)(3) = 72.75 \text{ ft.}$$

(2) Locate centroid of A. Geometric scale 1 in. = 3.75 ft.

$$P = 507 \quad R_f = 357$$

$$507 y_c = (357)(4.00)$$

$$y_c = 2.81 \text{ in.}$$

For prototype,

$$y_c = (2.81)(3.75) = 10.55 \text{ ft.}$$

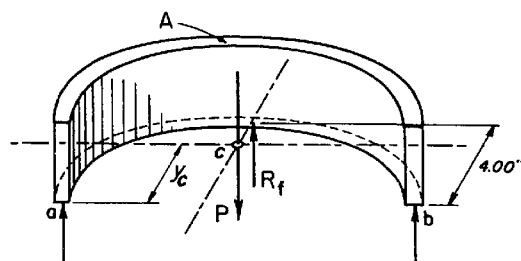


Fig. 48

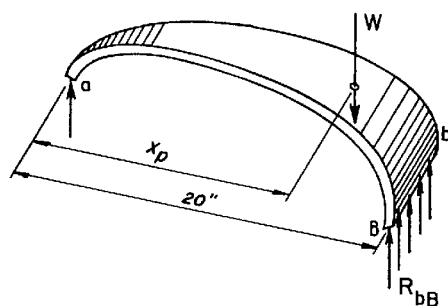
(3) Determine  $x_p$ .

Geometric scale 1 in. = 3 ft.

$$W = 490 \quad R_{bB} = 347$$

$$490 x_p = (347)(20)$$

$$x_p = 14.15 \text{ in.}$$

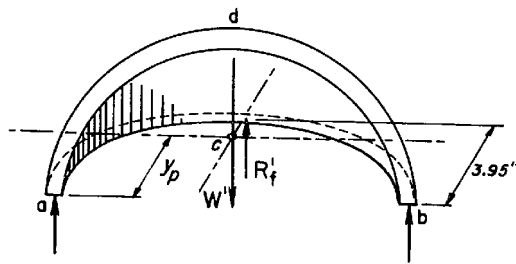


For prototype,

$$x_p = (14.15)(3.00) = 42.45 \text{ ft.}$$

Fig. 49

- (4) Determine  $y_p$ . Geometric scale 1 in. = 3.75 ft.



$$W' = 317 \quad R_f' = 261$$

$$317 y_p = (261)(3.95)$$

$$y_p = 3.26 \text{ in.}$$

For prototype,

$$y_p = (3.26)(3.75) = 12.21 \text{ ft.}$$

Fig. 50

- (5) Compute  $Q_x$ ,  $J_x$ ,  $Q_y$ ,  $J_y$ ,  $J_{xy}$ ,  $J_{x_0}$ ,  $J_{y_0}$ .<sup>(10)</sup>

$$(a) \quad Q_x = y_c \int ds = (10.55)(72.75) = 769$$

$$(b) \quad \frac{J_x}{Q_x} = y_p \therefore J_x = Q_x y_p = (769)(12.21) = 9,400$$

$$(c) \quad Q_y = x_c \int ds = (30)(72.75) = 2,183$$

$$(d) \quad \frac{J_y}{Q_y} = x_p \therefore J_y = Q_y x_p = (2,183)(42.45) = 92,500$$

$$(e) \quad J_{xy} = x_c y_c \int ds = (30)(10.55)(72.75) = 23,050$$

$$(f) \quad J_{x_0} = J_x - y_c^2 \int ds = 9,400 - (10.55^2)(72.75)$$

$$J_{x_0} = 1,270$$

$$(g) \quad J_{y_0} = J_y - x_c^2 \int ds = 92,500 - (30^2)(72.75)$$

$$J_{y_0} = 27,025$$

<sup>(10)</sup> Several of these quantities are not required in Example 7 but are used in other examples.

The deflections of the cantilever arch will be computed in tabular form. Deflections correspond to the bending moments in the conjugate beam caused by the unit loads shown in Figs. 43, 44 and 45. The arch is subdivided into eleven equal elements  $\Delta s$  (see Fig. 42) and their mid-point coordinates  $x_0$  and  $y_0$  are scaled from the drawing.

$$\Delta s = \frac{\int ds}{11} = \frac{72.75}{11} = 6.61 \text{ ft.}$$

Mid-Point Coordinates

Point	1	2	3	4	5	6	7	8	9	10	11
$x_0$	-29.30	-25.10	-19.35	-13.10	-6.55	0	symmetrical				
$y_0$	-7.37	-2.34	+0.95	2.95	4.10	4.45					



Influence Values for  $V_o$  and  $V_a$

Point	$x_o$	1	2	3	4	5	6(*)
1	29.30	$29.30 \times 0 = 0$	$29.30 \times 4.20 = 123.0$	$29.30 \times 9.95 = 292.0$	$29.30 \times 16.20 = 475.0$	$29.30 \times 22.75 = 666.0$	$29.30 \times 29.30 = 860.0$
2	25.10		$25.10 \times 0 = 0$	$25.10 \times 5.75 = 144.5$	$25.10 \times 12.00 = 302.0$	$25.10 \times 18.55 = 466.0$	$25.10 \times 25.10 = 631.0$
3	19.35			$19.35 \times 0 = 0$	$19.35 \times 6.25 = 121.0$	$19.35 \times 12.80 = 248.0$	$19.35 \times 19.35 = 375.0$
4	13.10				$13.10 \times 0 = 0$	$13.10 \times 6.55 = 85.7$	$13.10 \times 13.10 = 171.5$
5	6.55					$6.55 \times 0 = 0$	$6.55 \times 6.55 = 42.9$
6	0						$0 \times 0 = 0$
$\Sigma$		0	123.0	436.5	898.0	1465.7	2080.4
$V_o = \Delta s \Sigma \div J_{y_o}$		0	$\frac{6.61 \times 123.0}{27025} = 0.030 \uparrow$	$\frac{6.61 \times 436.5}{27025} = 0.107 \uparrow$	$\frac{6.61 \times 898.0}{27025} = 0.220 \uparrow$	$\frac{6.61 \times 1465.7}{27025} = 0.358 \uparrow$	$\frac{6.61 \times 2080.4}{27025} = 0.509 \uparrow$
$V_a = -(V_o - 1)$ $= 1 - V_o$		1.000 $\uparrow$	0.970 $\uparrow$	0.893 $\uparrow$	0.780 $\uparrow$	0.642 $\uparrow$	0.491 $\uparrow$

(\*)Note -  $V_a$ -values for unit load acting at points 7, 8, 9, 10, 11 and 12 are obtained from load acting at the symmetrically located point to the left of crown-point 6, and  $\Sigma V = 0$ .

Influence Values for  $H_o$  and  $H_a$

Point	$y_o$	1	2	3	4	5	6
1	-7.37	$-7.37 \times 0 = 0$	$-7.37 \times 4.20 = -30.95$	$-7.37 \times 9.95 = -73.33$	$-7.37 \times 16.20 = -119.39$	$-7.37 \times 22.75 = -167.67$	$-7.37 \times 29.30 = -215.94$
2	-2.34		$-2.34 \times 0 = 0$	$-2.34 \times 5.75 = -13.47$	$-2.34 \times 12.00 = -28.08$	$-2.34 \times 18.55 = -43.41$	$-2.34 \times 25.10 = -58.73$
3	+0.95			$+0.95 \times 0 = 0$	$+0.95 \times 6.25 = +5.94$	$+0.95 \times 12.80 = +12.16$	$+0.95 \times 19.35 = +18.38$
4	2.95				$2.95 \times 0 = 0$	$2.95 \times 6.55 = 19.32$	$2.95 \times 13.10 = 38.65$
5	4.10					$4.10 \times 0 = 0$	$4.10 \times 6.55 = 26.86$
6	4.45						$4.45 \times 0 = 0$
$\Sigma$		0	-30.95	-86.80	-141.53	-179.60	-190.78
$H_o = \Delta s \Sigma \div J_{x_o}$		0	$\frac{6.61 \times (-30.95)}{1270} = 0.161$	$\frac{6.61 \times (-86.80)}{1270} = 0.452$	$\frac{6.61 \times (-141.53)}{1270} = 0.737$	$\frac{6.61 \times (-179.60)}{1270} = 0.935$	$\frac{6.61 \times (-190.78)}{1270} = 0.994$
$H_a = -H_o$		0	0.161	0.452	0.737	0.935	0.994


# Influence Values for $M_o$

Point	1	2	3	4	5	6
1	$1 \times 0 = 0$	$1 \times 4.20 = 4.20$	$1 \times 9.95 = 9.95$	$1 \times 16.20 = 16.20$	$1 \times 22.75 = 22.75$	$1 \times 29.30 = 29.30$
2		$1 \times 0 = 0$	$1 \times 5.75 = 5.75$	$1 \times 12.00 = 12.00$	$1 \times 18.55 = 18.55$	$1 \times 25.10 = 25.10$
3			$1 \times 0 = 0$	$1 \times 6.25 = 6.25$	$1 \times 12.80 = 12.80$	$1 \times 19.35 = 19.35$
4				$1 \times 0 = 0$	$1 \times 6.55 = 6.55$	$1 \times 13.10 = 13.10$
5					$1 \times 0 = 0$	$1 \times 6.55 = 6.55$
6						$1 \times 0 = 0$
$\Sigma$	0	4.20	15.70	34.45	60.65	93.40
$M_o = \Delta s \Sigma \ddot{A}$	0	$\frac{6.61 \times 4.20}{72.75} = -0.38$	$\frac{6.61 \times 15.70}{72.75} = -1.43$	$\frac{6.61 \times 34.45}{72.75} = -3.14$	$\frac{6.61 \times 60.65}{72.75} = -5.52$	$\frac{6.61 \times 93.40}{72.75} = -8.49$

## Summary - Influence Values for Neutral-Point Reactions

Point	1	2	3	4	5	6	7	8	9	10	11
$V_o$	0	0.030	0.107	0.220	0.358	0.509	0.642	0.780	0.893	0.970	1.000
$H_o$	0	-0.161	-0.452	-0.737	-0.935	-0.994	-0.935	-0.737	-0.452	-0.161	0
$M_o$	0	-0.38	-1.43	-3.14	-5.52	-8.49	not required				



Summary - Influence Values for  $V_a$ ,  $H_a$ ,  $M_a$  

Point	1(*)	2	3	4	5	6	7	8	9	10	11(*)
$V_a$	1.000	0.970	0.893	0.780	0.642	0.491	0.358	0.220	0.107	0.030	0
$H_a$	0	0.161	0.452	0.737	0.935	0.994	0.935	0.737	0.452	0.161	0
$M_a$	-0.70	-1.92	-1.24	+0.64	2.69	4.26	4.66	4.34	2.99	1.18	0

(\*) Values slightly in error due to the use of concentrated loads on conjugate beam.

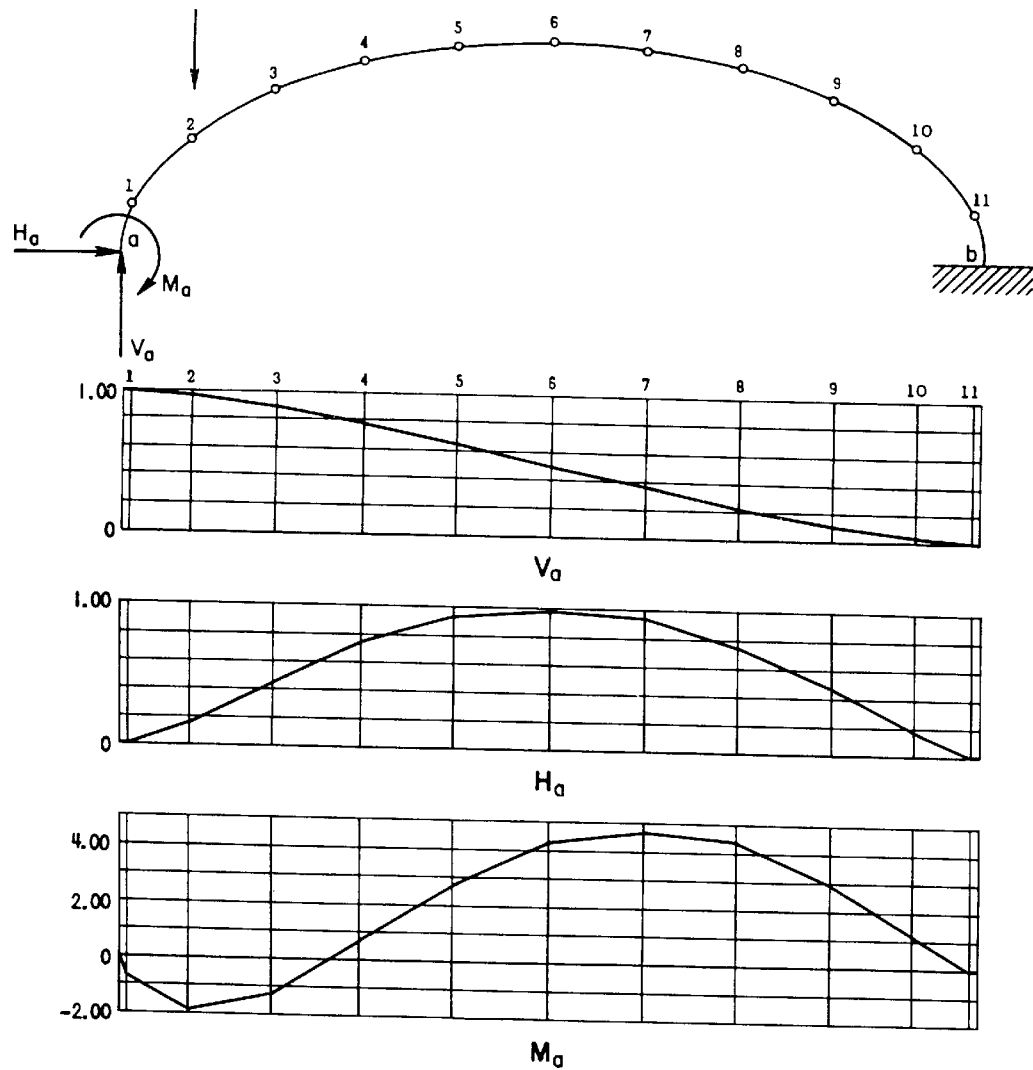


Fig. 52

10. Discussion of the Semi-Experimental Method. - It is quite obvious from the preceding example that in order to determine the influence values for reactions a considerable amount of numerical work is required in addition to the experimental part of the solution. The effort can be significantly reduced by subdividing the arch into fewer elements. In general for an arch of practical proportions eight or even six subdivisions will give sufficiently close results.

For a given number of subdivisions the accuracy of the semi-experimental results depends on that of  $A$ ,  $J_x$ ,  $J_y$  and the other experimentally evaluated arch properties. The influence values for reactions obtained in Example 7 and values found in a purely analytic solution are compared below.

TABLE IV

Point	1	2	3	4	5	6	7	8	9	10	11	Average % Error(*)
$V_a$ (Exper.)	1.000	0.970	0.893	0.780	0.642	0.491	0.358	0.220	0.107	0.030	0	0.99
$V_a$ (Theor.)	1.000	0.970	0.895	0.784	0.648	0.500	0.352	0.216	0.105	0.030	0	
% Error	0	0	0.22	0.51	0.93	1.80	1.70	1.85	1.90	0	0	
$H_a$ (Exper.)	0	0.161	0.452	0.737	0.935	0.994	0.935	0.737	0.452	0.161	0	2.14
$H_a$ (Theor.)	0	0.162	0.460	0.752	0.965	1.040	0.965	0.752	0.460	0.162	0	
% Error	0	0.62	1.74	1.99	3.10	4.41	3.10	1.99	1.74	0.62	0	
$M_a$ (Exper.)	-0.70	-1.92	-1.24	+0.64	2.69	4.26	4.66	4.34	2.99	1.18	0	6.67
$M_a$ (Theor.)	-0.70	-1.90	-1.17	+0.73	2.92	4.58	5.25	4.67	3.18	1.20	0	
% Error	0	1.05	5.98	12.31	7.87	6.97	11.22	7.05	5.97	1.67	0	

(\*) Does not include points 1 and 11.



#### IV - THE EFFECT OF IMPRESSED DISTORTIONS IN SYMMETRICAL ARCHES

The foundations of an arch may settle, tilt and spread, thereby causing moments in the structure. Shrinkage or expansion resulting from a temperature change, and rib shortening due to direct stress change the free length of the arch. The effect of such impressed distortions can be studied by various methods as is shown in the following cases.

1. Lineal Displacement. Rotation of Abutments Prevented. - The effect of a lineal relative displacement  $\Delta$  of abutments a and b is represented in the column analogy method by a tilting moment  $\Delta$  about the centroidal axis parallel to the direction of the displacement. Accordingly in Fig. 54 the

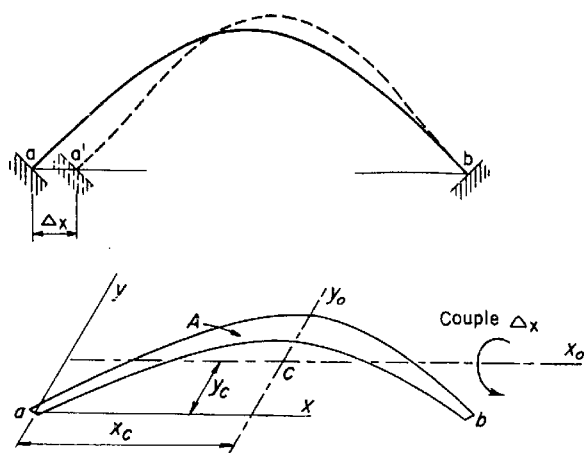


Fig. 54

fixed end moment at a caused by an impressed horizontal displacement  $\Delta_x$  is

$$M_a^{\Delta_x} = f_a = \frac{\Delta_x}{J_{x_o}} y_c \quad \text{Eq. 66}$$

Since

$$J_{x_o} = J_x - A y_c^2 = A y_c (y_p - y_c),$$

Eq. 66 may be written in the form

$$M_a^{\Delta_x} = \frac{\Delta_x}{A (y_p - y_c)} \quad \text{Eq. 67}$$

Similarly, for a vertical relative displacement  $\Delta y$ ,

$$M_a^{\Delta y} = \frac{\Delta y}{J_{y_0}} x_c = \frac{\Delta y}{A(x_p - x_c)} \quad \text{Eq. 68}$$

In either case, because of the symmetry of the arch, the moments at the far end b are equal to those at a.

2. Rotation. Translation of Abutments Prevented. - A rotation  $\theta_a$  of abutment a induces a fixed end moment at a

$$M_a^{\theta_a} = \theta_a S_a \quad \text{Eq. 69}$$

which follows directly from the definition of the stiffness factor  $S_a$ . At b, the moment is

$$M_b^{\theta_a} = C_{ab} M_a^{\theta_a} = \theta_a (S_a C_{ab}) \quad \text{Eq. 70}$$

3. Thrust Stiffness. - In the analysis of continuous arches on elastic piers by the moment distribution method it is necessary to know the so-called thrust stiffness of the arches bridging each pair of adjoining piers. In Fig. 55a, the thrust stiffness  $T_s$  is defined as the horizontal force at a required to induce a unit horizontal displacement of the arch abutment, both ends remaining restrained against rotation. From Eq. 66, the fixed end moment induced by this displacement is

$$M_a^{\Delta x=1} = \frac{1}{J_{x_0}} y_c \quad \text{Eq. 71}$$



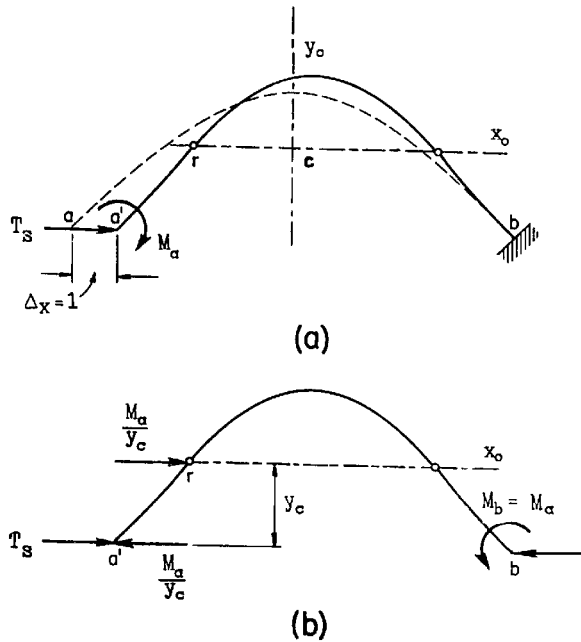


Fig. 55

The fixed end moment  $M_a$  in Fig. 55a may be replaced by the couple  $M_a = \frac{M_a}{y_c} y_c$ , shown in Fig. 55b. At point  $r$ , located on the  $x_0$ -axis, the bending moment is zero.<sup>(11)</sup> From the condition of equilibrium of the segment  $a' - r$  of the arch taken as a free body it is seen that the thrust stiffness is

$$T_s = \frac{M_a}{y_c}$$

Substituting from Eq. 71, the last equation becomes

$$T_s = \frac{I}{J_{x_0}} = \frac{I}{A y_c (y_p - y_c)} \quad \text{Eq. 72}$$

<sup>(11)</sup> The stress at point  $r$  of the analogous column section, and hence the moment in the arch, are zero.

Example 9. - The elliptical arch analyzed in Examples 6 and 7 will be investigated for the effects of settlement and rotation of an abutment, temperature change<sup>(12)</sup>, and rib shortening. The thrust stiffness will be also determined.

Assume the following arch data:

$$E = 2,000,000 \text{ psi.} = 288 \times 10^6 \text{ psf.}$$

$$I = 0.667 \text{ ft.}^4 \text{ (constant)}$$

$$\text{Coefficient of thermal expansion } \alpha = 6 \times 10^{-6} \text{ per 1 deg.}$$

From Example 7,

$$J_{x_0} = 1,270 (\text{rel.}) = \frac{1,270}{288 \times 10^6 \times 0.667} = 6.6 \times 10^{-6} (\text{abs.})$$

$$J_{y_0} = 27,025 (\text{rel.}) = \frac{27,025}{288 \times 10^6 \times 0.667} = 1.409 \times 10^{-4} (\text{abs.})$$

From Example 6,

$$S_a = \frac{9.77}{A} (\text{rel.}) = \frac{9.77 \times 288 \times 10^6 \times 0.667}{72.75} = 2.58 \times 10^7 (\text{abs.})$$

(a) Settlement of Abutment a. The springing moment will be found for a settlement  $\Delta_y = 1$  in. of the left abutment. (Eq. 68)

$$M_a^{\Delta_y=1} = \frac{\frac{1}{12}}{1.409 \times 10^{-4}} \times 30 = 17,750 \text{ lb-ft.} \quad (13)$$

The crown ( $x_0 = 0$ ) moment is zero.

---

<sup>(12)</sup> See "Statically Indeterminate Structures" by L.C. Maugh, Example 47, page 229.

<sup>(13)</sup> Signs will be discussed in article 4.

(b) Rotation of Abutment a. The moment at the left-hand springing will be found for a  $0.1^\circ = 0.001745$  rad. rotation of the left abutment.

(Eq. 69)

$$M_a^{\theta_a} = (0.001745)(2.58 \times 10^7) = 45,100 \text{ lb-ft.}$$

(c) Temperature Change. The springing and crown moments caused by a 50-degree temperature rise will be determined.

The effective change in free span is

$$\Delta L = L \alpha T = (60)(6 \times 10^{-6})(50) = 0.018 \text{ ft.}$$

(Eq. 66)

$$M_a^{\Delta x = \Delta L} = \frac{0.018}{6.6 \times 10^{-6}} \times 10.55 = 28,800 \text{ lb-ft.} \downarrow$$

$$M_{\text{crown}}^{\Delta x = \Delta L} = \frac{0.018}{6.6 \times 10^{-6}}(15 - 10.55) = 12,120 \text{ lb-ft.} \uparrow$$

(d) Rib Shortening. The springing and crown moments will be determined from the effect of an average compression stress  $s = 100$  psi. over the entire length of the arch.

The effective change in free span is

$$\Delta L = \frac{S}{E} L = \frac{100 \times 144}{288 \times 10^6} \times 60 = 0.003 \text{ ft.}$$

(Eq. 66)

$$M_a^{\Delta x = \Delta L} = \frac{0.003}{6.6 \times 10^{-6}} \times 10.55 = 4,800 \text{ lb-ft.} \downarrow$$

$$M_{\text{crown}}^{\Delta x = \Delta L} = \frac{0.003}{6.6 \times 10^{-6}} (15 - 10.55) = 2,020 \text{ lb-ft.}$$

(e) Thrust Stiffness. The thrust stiffness of the arch is (Eq. 72)

$$T_s = \frac{I}{6.6 \times 10^{-6}} = 151,400 \text{ lb.}$$

4. Discussion. - In Example 9 moments induced by impressed distortions were found for the springing and crown sections. Moments at other points of the arch can be determined just as readily by using the respective column analogy formulae with the proper values of  $x_0$  and  $y_0$  substituted.

The signs of the moments are best determined by reverting to the neutral-point concept, illustrated in Fig. 56 for the effect of a temperature change or other virtual or real horizontal displacement. A temperature rise would

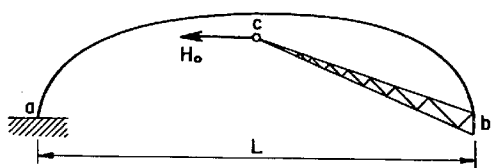


Fig. 56

tend to lengthen the span  $L$  of the arch by causing the cantilever end  $b$  to move to the right. The neutral-point force  $H_0$  preventing this move-

ment acts to the left. At the left springing its moment is positive (beam sign convention), causing tension in the inside fibers. At the crown-point the bending moment is negative, causing compression in the inside fibers. For a temperature drop the bending moment signs would be reversed.

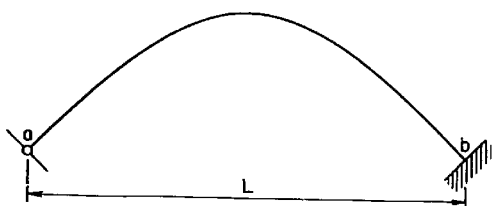
The qualitative effects of other impressed distortions are analyzed in a similar manner.

A comparison of experimental and analytic results and per cent errors are shown in the table below. Both sets of values are in excellent agreement.

TABLE V

Distortion and Effect	Exper.	Theor.	% Error	Average % Error
Settlement at <u>a</u> $M_a$	17,750	17,490	1.49	1.17
Rotation at <u>a</u> $M_a$	45,100	45,660	1.22	
Temperature Change $M_a$ $M_{\text{crown}}$	28,800 -12,120	29,050 -11,900	0.86 1.85	
Rib Shortening $M_a$ $M_{\text{crown}}$	-4,800 2,020	-4,850 1,985	1.03 1.76	
Horizontal Translation $T_s$	151,400	151,400	0	

5. Arch Fixed at One End and Hinged at the Other. Solution by the Method of Least Work. - The arch shown in Fig. 57



will be investigated for the effect of lineal displacements induced at hinge a.

Fig. 57

(a) Horizontal Displacement. In Fig. 58 the strain-energy in the arch distorted as a result of an impressed horizontal

displacement  $\Delta_x$  is

$$U = \int_{a'}^b \frac{M^2 ds}{2EI}$$

in which  $M = Hy - Vx$   
is the bending moment at  
any point  $k (x, y)$ .

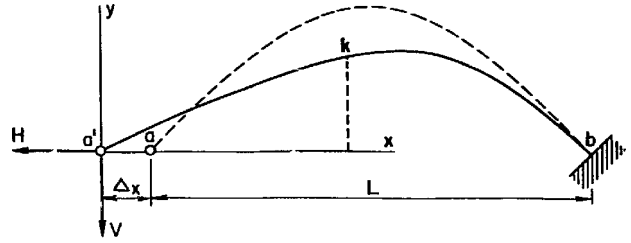


Fig. 58

By Castigliano's second theorem,

$$\frac{\partial U}{\partial V} = \Delta_y = 0 = \int_{a'}^b \frac{M}{EI} \frac{\partial M}{\partial V} ds = \int_{a'}^b \frac{(Hy - Vx)(-x)}{EI} ds$$

$$0 = -HJ_{xy} + VJ_y$$

whence

$$V = H \frac{J_{xy}}{J_y} \quad \text{Eq. 73}$$

$$\frac{\partial U}{\partial H} = \Delta_x = \int_{a'}^b \frac{(Hy - Vx)(y)}{EI} ds = HJ_x - VJ_{xy}$$

Solving the last equation and Eq. 73 for  $H$  and  $V$ ,

$$\left. \begin{aligned} H &= \frac{J_y}{J_x J_y - J_{xy}^2} \Delta_x \\ V &= \frac{J_{xy}}{J_x J_y - J_{xy}^2} \Delta_x \end{aligned} \right\} \quad \text{Eqs. 74}$$

The fixed end moment at b is

$$M_b = -(-VL) = \frac{J_{xy}L}{J_x J_y - J_{xy}^2} \Delta_x \quad \text{Eq. 75}$$

(b) Vertical Displacement. Fig. 59 shows arch  $a - b$  distorted along the curve  $a' - b$  as a result of an impressed vertical displacement  $\Delta y$ .

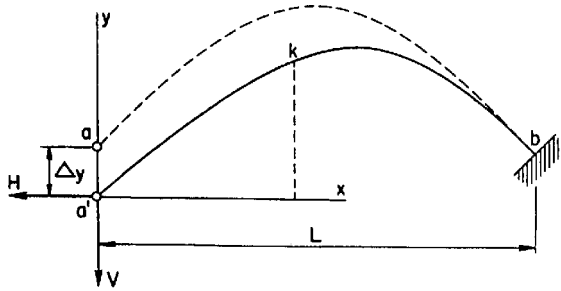


Fig. 59

$$U = \int_{a'}^b \frac{M^2 ds}{2EI}$$

$$M = Hy - Vx$$

$$\frac{\partial U}{\partial H} = \Delta_x = 0 = \int_{a'}^b \frac{M}{EI} \frac{\partial M}{\partial H} ds = \int_{a'}^b \frac{(Hy - Vx)(y)}{EI} ds$$

$$0 = HJ_x - VJ_{xy}$$

$$\frac{\partial U}{\partial V} = \Delta_y = \int_{a'}^b \frac{(Hy - Vx)(-x)}{EI} ds = -HJ_{xy} + VJ_y$$

$$\left. \begin{aligned} V &= \frac{J_x}{J_x J_y - J_{xy}^2} \Delta_y \\ H &= \frac{J_{xy}}{J_x J_y - J_{xy}^2} \Delta_y \end{aligned} \right\}$$

Eqs. 76

$$M_b = H\Delta_y - VL = \frac{J_{xy}\Delta_y^2 - J_x L \Delta_y}{J_x J_y - J_{xy}^2} \quad \text{Eq. 77}$$

6. Arch Hinged at Both Ends. Solution by the Method of Real Work. - A two-hinged arch will be investigated for the effect of lineal displacements induced at hinge a.

(a) Horizontal Displacement. Fig. 60 shows arch a - b and its distorted shape a' - b, caused by an impressed displacement  $\Delta_x$ .

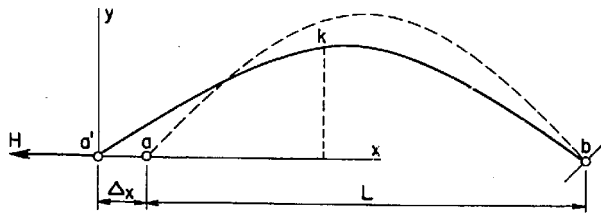


Fig. 60

The external work done by force  $H$  effecting the displacement is equal to the strain-energy stored in the arch. Neglecting the effect of normal and shearing stresses, the work done is

$$\frac{1}{2} H \Delta_x = \int_{a'}^b \frac{M^2 ds}{2EI} = \int_{a'}^b \frac{H^2 y^2}{2EI} ds = \frac{1}{2} H^2 J_x$$

whence

$$H = \frac{\Delta_x}{J_x} \quad \text{Eq. 78}$$

(b) Vertical Displacement. In Fig. 61, hinge a of arch a - b

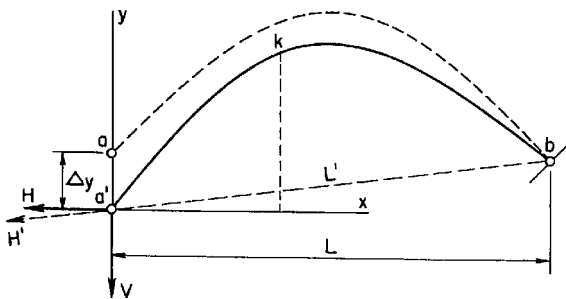


Fig. 61

is displaced vertically to position a'. Since the moment at b is zero, force  $H'$ , the resultant of reactions  $H$  and  $V$  (not drawn to scale), must pass through both a' and b. It follows that the distorted arch in Fig. 61



is in the same condition as arch  $a' - b$  in Fig. 60. Applying Eq. 78 to the arch in Fig. 61,

$$H' = \frac{L' - L}{J_x} = \frac{\sqrt{L^2 + \Delta_y^2} - L}{J_x}$$

The horizontal and vertical components of  $H'$  are

$$\left. \begin{aligned} H &= \frac{\sqrt{L^2 + \Delta_y^2} - L}{J_x} \cdot \frac{L}{\sqrt{L^2 + \Delta_y^2}} = \frac{L}{J_x} \left[ 1 - \frac{L}{\sqrt{L^2 + \Delta_y^2}} \right] \\ V &= \frac{\sqrt{L^2 + \Delta_y^2} - L}{J_x} \cdot \frac{\Delta_y}{\sqrt{L^2 + \Delta_y^2}} = \frac{\Delta_y}{J_x} \left[ 1 - \frac{L}{\sqrt{L^2 + \Delta_y^2}} \right] \end{aligned} \right\} \text{Eqs. 79}$$

7. Discussion. - An inspection of articles 5 and 6 shows that the effects of impressed lineal displacements can be readily evaluated if the arch properties  $J_x$ ,  $J_y$  and  $J_{xy}$  are known. The experimental determination of these quantities was illustrated in Example 7. The relationships between moment and angle change for the arches investigated in articles 5 and 6 was treated earlier in this paper in conjunction with the stiffness and modified stiffness factors.

## V - CONCLUSION

The paper presents a fairly exhaustive study of the various beam and arch constants required for the purposes of structural analysis by the Cross method of moment distribution.

The focal point of interest is the parameter  $J/Q$  and its direct or indirect occurrence in each of the moment distribution constants. Its relationship to the centroid of the pressure and load solids and, particularly, the manner of its evaluation by weighing constitute what is believed to be an original contribution to experimental structural analysis. The derivations of the various working formulae follow standard methods of analysis and no originality is claimed for them.

It would appear that the merits of the methods of solution presented herein and of the paper itself are as follows:

(a) In general the carry-over and stiffness factors for beams with variable moment of inertia can be determined rapidly and reliably by fashioning the pressure solid, and weighing its reactions, etc.

(b) The concept of the three-dimensional conjugate beam (pressure solid) is helpful in visualizing and understanding the relationships between the moments of inertia of a member and its carry-over, stiffness and other factors. In preliminary analytic work, the concept permits a rough

visual estimate of the carry-over and stiffness factors (the solid may be sketched and the location of its center of gravity guessed at). The moment-area method and the two-dimensional conjugate beam load-diagrams are not conducive to making such an estimate.

(c) In any typical problem of indeterminate analysis and design the moments of inertia of the component members are unknown at the outset. Successive analyses involve changes of the originally assumed structural sections, arrangement of cover plates, knees, or percentage of steel. A new set of calculated factors is therefore required in each successive try.

It is an easy matter to change the  $1/EI$ -values of the pressure solid by cutting or sanding. Since the reactions can be weighed rapidly, the evaluation of each new set of factors is a matter of several minutes only.

(d) With the exception of influence lines for reactions, each solution carried out by the methods described herein is numerically independent of its purely analytic counterpart. In the case of influence lines, the tabular calculations, although cumbersome, are of an elementary nature.

(e) The paper embodies a noteworthy simplification of the notation used in most standard textbooks in that integrals are replaced by symbols  $J$ ,  $Q$ ,  $j$ ,  $q$ , etc. This simplified notation results in a more workable and meaningful

appearance of each formula. For example, the stiffness factor,  $k C_{1-2}$ , for a haunched beam, equal to  $S_a$  adopted in this paper, is such that <sup>(14)</sup>

$$C_{1-2} = \frac{L^2 \int_0^L x^2 \left( \frac{I_0}{I} \right) dx}{\left[ \int_0^L (L-x) \left( \frac{I_0}{I} \right) dx \right] \left[ \int_0^L x^2 \left( \frac{I_0}{I} \right) dx \right] - \left[ \int_0^L x \left( \frac{I_0}{I} \right) dx \right] \left[ \int_0^L (Lx - x^2) \left( \frac{I_0}{I} \right) dx \right]}$$

In contrast, Eq. 10 of the present paper expresses the same stiffness factor in the form

$$S_a = \frac{1}{A - \frac{Q^2}{J}}$$

---

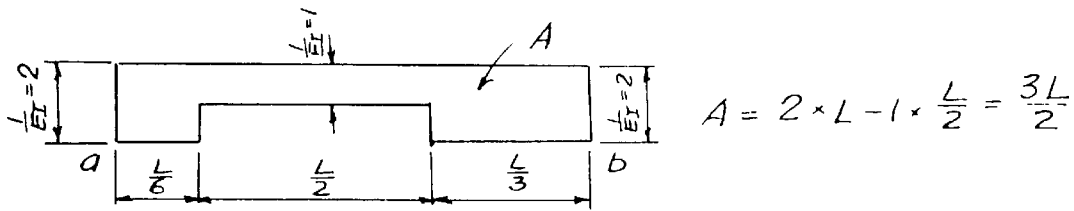
<sup>(14)</sup> See "Analysis of Statically Indeterminate Structures" by J.I. Parcel & R.B.B. Moorman, page 275.

## APPENDIX

Analytic Solutions of Examples 1 to 9

# Example 1- Deepened Beam

(a) Solution by Eqs. 4 & 10



$$Q_a = 2L \times \frac{L}{2} - 1 \times \frac{L}{2} \times \frac{5L}{12} = \frac{19L^2}{24}$$

$$J_a = \frac{1}{12} \times 2 \times L^3 + (2 \times L) \left( \frac{L}{2} \right)^2 - \left[ \frac{1}{12} \times 1 \times \left( \frac{L}{2} \right)^3 + 1 \times \frac{L}{2} \times \left( \frac{5L}{12} \right)^2 \right]$$

$$= \frac{L^3}{6} + \frac{L^3}{2} - \frac{L^3}{96} - \frac{25L^3}{288} = \frac{41L^3}{72}$$

$$C_{ab} = \frac{Q_a}{J_a} L - 1 = \frac{\frac{19L^2}{24}}{\frac{41L^3}{72}} - 1 = \frac{57}{41} - 1 = 0.39$$

$$S_a = \frac{1}{A - \frac{Q_a^2}{J_a}} = \frac{1}{\frac{3L}{2} - \frac{\left( \frac{19L^2}{24} \right)^2}{\frac{41L^3}{72}}} = \frac{1}{\frac{3L}{2} - 1.1L}$$

$$= \frac{2}{3L - 2.2L} = \frac{2}{0.8L} = \frac{2.50}{L} \text{ (rel.)}$$

$$Q_b = 2L \times \frac{L}{2} - 1 \times \frac{L}{2} \times \frac{7L}{12} = \frac{17L^2}{24}$$

$$J_b = \frac{1}{12} \times 2 \times L^3 + (2 \times L) \left( \frac{L}{2} \right)^2 - \left[ \frac{1}{12} \times 1 \times \left( \frac{L}{2} \right)^3 + 1 \times \frac{L}{2} \times \left( \frac{7L}{12} \right)^2 \right]$$

$$= \frac{L^3}{6} + \frac{L^3}{2} - \frac{L^3}{96} - \frac{49L^3}{288} = \frac{35L^3}{72}$$

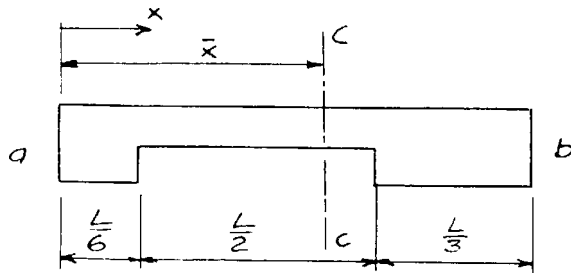
$$C_{ba} = \frac{Q_b}{J} L - 1 = \frac{\frac{17L^3}{24}}{\frac{35L^3}{72}} - 1 = 1.455 - 1 = 0.455$$

$$S_b = \frac{1}{A - \frac{Q_b^2}{J_b}} = \frac{1}{\frac{3L}{2} - \frac{\left(\frac{17L^2}{24}\right)^2}{\frac{35L^3}{72}}} = \frac{1}{\frac{3L}{2} - 1.031L} =$$

$$= \frac{2}{3L - 2.062L} = \frac{2}{0.938L}$$

$$S_b = \frac{2.13}{L} \text{ (rel.)}$$

(b) Solution by Column Analogy Method



$$A = 2L - 1 \times \frac{L}{2} = \frac{3L}{2}$$

$$\sum (\Delta A) x = 2L \times \frac{L}{2} - 1 \times \frac{L}{2} \times \frac{5L}{12} = \frac{19L^2}{24}$$

$$\bar{x} = \frac{Q_a}{A} = \frac{\frac{19L^2}{24}}{\frac{3L}{2}} = \frac{19L}{36}$$

$$J_c = \frac{1}{12} 2 \times L^3 + 2L \left(\frac{L}{36}\right)^2 - \left[ \frac{1}{12} 1 \times \left(\frac{L}{2}\right)^2 + 1 \times \frac{L}{2} \left(\frac{4L}{36}\right)^2 \right]$$

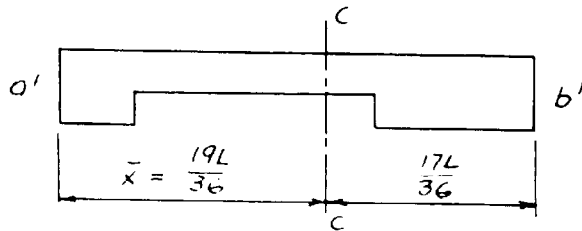
$$J_c = \frac{131L^3}{864}$$

$$S_a = M_a = \frac{1}{\frac{3L}{2}} + \frac{(1) \left( \frac{19L}{36} \right)^2}{\frac{131L^3}{864}} = \frac{2}{3L} + \frac{1.838}{L}$$

$$S_a = \frac{2.505}{L} \text{ (rel.)}$$

$$M_b = \frac{1}{\frac{3L}{2}} - \frac{(1) \frac{19L}{36} \times \frac{17L}{36}}{\frac{131L^3}{864}} = \frac{2}{3L} - \frac{1.642}{L} = -\frac{0.975}{L}$$

$$C_{ab} = -\frac{M_b}{M_a} = -\frac{-0.975}{2.505} = +0.389$$



$$S_b = M_{b'} = \frac{1}{\frac{3L}{2}} + \frac{(1) \left( \frac{17L}{36} \right)^2}{\frac{131L^3}{864}} = \frac{2}{3L} + \frac{1.47}{L}$$

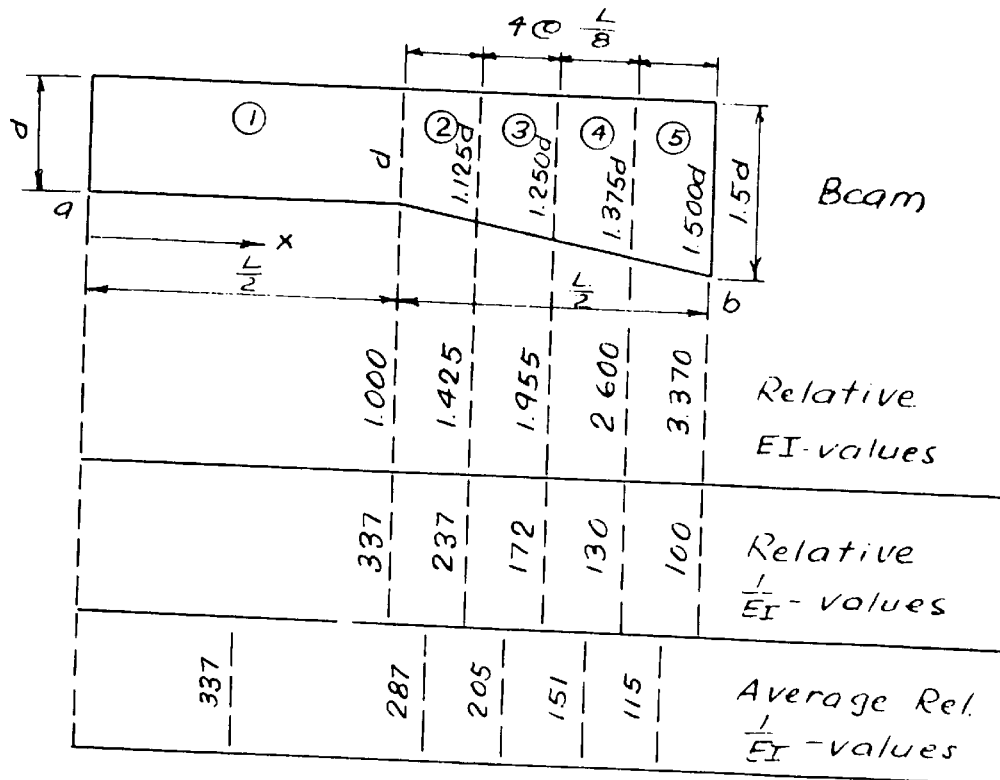
$$S_b = \frac{2.137}{L} \text{ (rel.)}$$

$$C_{ba} = -\frac{M_{a'}}{M_{b'}} = -\frac{M_b}{M_{b'}} = -\frac{-0.975}{2.137} = +0.456$$



# Example 2- Haunched Beam

(a) Solution by Eqs. 4 & 10



Part	Avg. $\frac{1}{EI}$	$\frac{x}{L}$	$\frac{x^2}{L^2}$	$\frac{A}{L}$	$\frac{Ax}{L^2}$	$\frac{Ax^2}{L^3}$	$\frac{J_c}{L^3}$
1	337	0.2500	0.063	168.5	42.1	10.6	3.51
2	287	0.5625	0.317	35.9	20.2	11.4	0.05
3	205	0.6875	0.473	25.6	17.6	12.1	0.03
4	151	0.8125	0.661	18.9	15.4	12.5	0.03
5	115	0.9375	0.880	14.4	13.5	12.7	0.02
$\Sigma =$				263.3	108.8	59.3	3.64

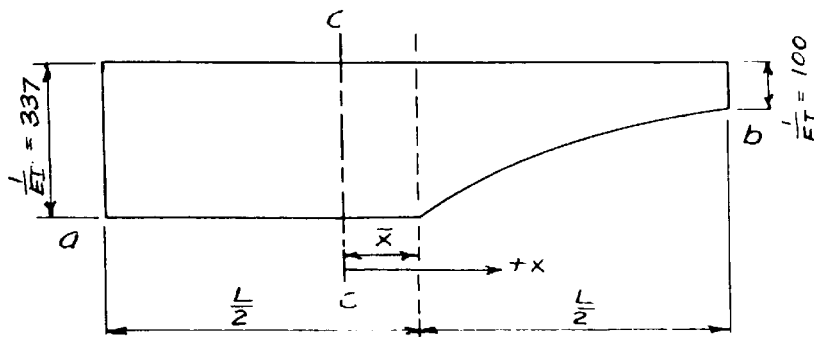
$$J_o = \Sigma J_y + \Sigma Ax^2 = 3.64 L^3 + 59.3 L^3$$

$$J_o = 62.94 L^3$$

$$C_{ob} = \frac{Q_a}{J_a} L - 1 = \frac{108.8 L^3}{62.94 L^3} - 1 = 1.73 - 1 = 0.73$$

$$S_a = \frac{1}{A - \frac{Q_a^2}{J_a}} = \frac{1}{263.3L - \frac{(108.8L^2)^2}{62.94L^3}} = \frac{1}{75.2L} = \frac{0.0133}{L}$$

(b) Solution by Column Analogy Method



Part	Avg. $\frac{1}{EI}$	$\frac{A}{L}$	$\frac{x}{L}$	$\frac{x^2}{L^2}$	$\frac{Ax}{L^2}$	$\frac{Ax^2}{L^3}$	$\frac{J_c}{L^3}$
1	337	168.5	-0.2500	0.0625	-42.12	10.52	3.51
2	287	35.9	0.0625	0.0039	+2.24	0.14	0.05
3	205	25.6	0.1875	0.0352	4.80	0.90	0.03
4	151	18.9	0.3125	0.0976	5.91	1.85	0.03
5	115	14.4	0.4375	0.1920	6.30	2.76	0.02
$\Sigma =$		263.3			-22.87	16.17	3.64
							19.81

$$\bar{x} = \frac{-22.87L^2}{263.3L} = -0.087L$$

$$J \text{ corrected to centroid: } 19.810 L^3$$

$$- (263.3 L)(0.087 L)^2 = \frac{-1.995 L^3}{17.815 L^3 = J_c}$$

$$S_a = M_a = \frac{1}{263.3 L} + \frac{(1)(0.413 L)^2}{17.82 L^3}$$

$$S_a = \frac{0.0038}{L} + \frac{0.0096}{L} = \frac{0.0134}{L} \text{ (rel.)}$$

$$M_b = \frac{1}{263.3 L} - \frac{(1)(0.413 L)(0.587 L)}{17.82 L^3}$$

$$M_b = \frac{0.0038}{L} - \frac{0.0136}{L} = \frac{-0.0098}{L}$$

$$C_{ab} = -\frac{M_b}{M_a} = \frac{-0.0098}{0.0134} = +0.731$$

$$S_b = -M'_b = \frac{1}{263.3 L} + \frac{(1)(0.587 L)^2}{17.82 L^3} =$$

$$S_b = \frac{0.0038}{L} + \frac{0.0194}{L} = \frac{0.0232}{L} \text{ (rel.)}$$

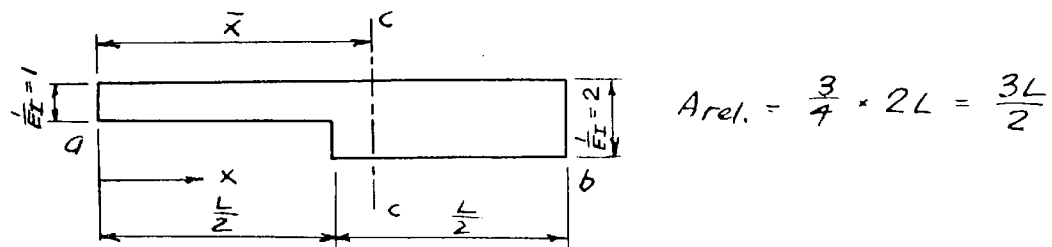
$$M'_a = \frac{1}{263.3 L} - \frac{(1)(0.587 L)(0.413 L)}{17.82 L^3} =$$

$$= \frac{0.0038}{L} - \frac{0.0136}{L} = -\frac{0.0098}{L}$$

$$C_{ba} = -\frac{-0.0098}{0.0232} = +0.422$$

### Example 3- Deepened Beam

Solution by Column Analogy Method



$$Q_a = 2L \times \frac{L}{2} - 1 \times \frac{L}{2} \times \frac{1}{4} = \frac{7L^2}{8}$$

$$\bar{x} = \frac{\frac{7L^2}{8}}{\frac{3L}{2}} = \frac{7L}{12}$$

$$J_c = \frac{1}{12} 2L^3 + 2L \left(\frac{L}{12}\right)^2 - \frac{1}{12} 1 \left(\frac{L}{2}\right)^3 - 1 \times \frac{L}{2} \left(\frac{L}{3}\right)^2$$

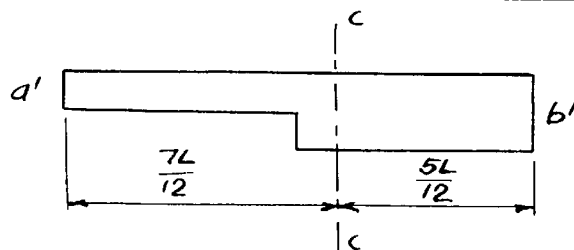
$$J_c = \frac{11L^3}{96}$$

$$S_a = M_a = \frac{1}{\frac{3L}{2}} + \frac{(1) \frac{7L}{12} \times \frac{7L}{12}}{\frac{11L^3}{96}} = \frac{2}{3L} + \frac{98}{33L}$$

$$S_a = \frac{3.64}{L} \text{ (rel.)}$$

$$M_b = \frac{1}{\frac{3L}{2}} - \frac{(1) \frac{7L}{12} \times \frac{5L}{12}}{\frac{11L^3}{96}} = \frac{2}{3L} - \frac{70}{33L} = -\frac{1.454}{L}$$

$$C_{ab} = -\frac{M_b}{M_a} = -\frac{-1.454}{3.64} = +0.40$$



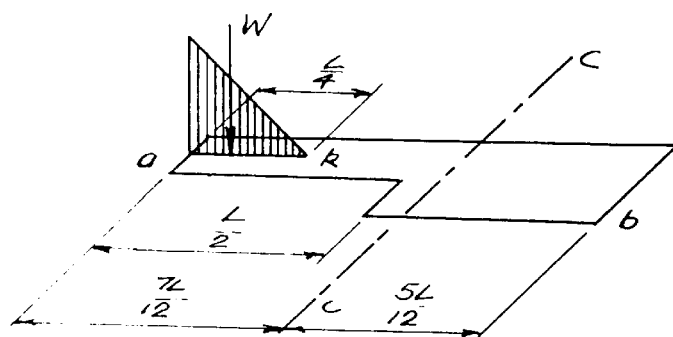
$$S_b = M_b'$$

$$S_b = \frac{1}{\frac{3L}{2}} + \frac{(1) \frac{5L}{12} \times \frac{5L}{12}}{\frac{11L^3}{33L}} = \frac{2}{3L} + \frac{50}{33L} = \frac{2.18}{L} (\text{rel.})$$

$$M'_a = M_b = - \frac{1.454}{L}$$

$$C_{ba} = - \frac{M'_a}{M'_b} = - \frac{-1.454}{2.18} = + 0.667$$


---



$$W = \frac{1}{2} \times \frac{L}{4} \times \frac{PL}{4} = \frac{PL^2}{32}$$

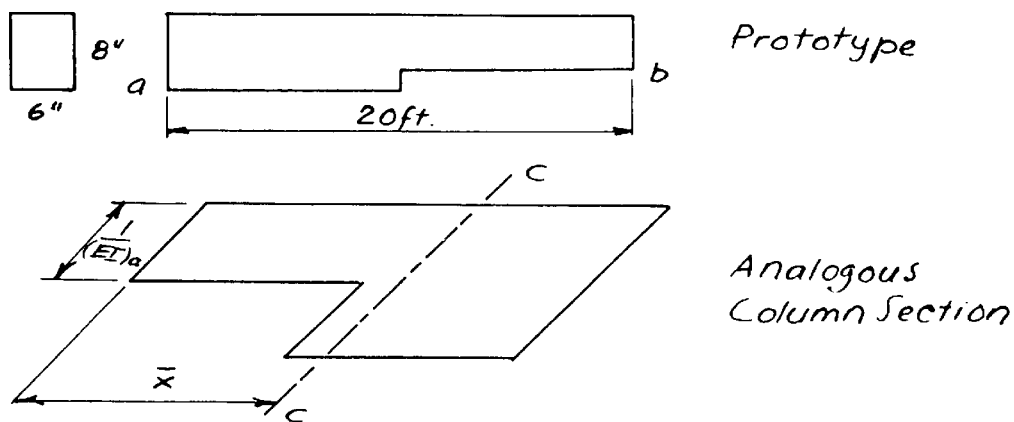
$$M_o = - (P) \frac{L}{4} + \frac{\frac{PL^2}{32}}{\frac{3L}{2}} + \frac{\frac{PL^2}{32} \times \frac{L}{2} \times \frac{7L}{12}}{\frac{11L^3}{96}} =$$

$$M_o = - \frac{PL}{4} + \frac{PL}{48} + \frac{7PL}{88} = - \frac{79PL}{528} = - 0.1495 PL$$

$$M_b = 0 + \frac{\frac{PL^2}{32}}{\frac{3L}{2}} - \frac{\frac{PL^2}{32} \times \frac{L}{2} \times \frac{5L}{12}}{\frac{11L^3}{96}}$$

$$M_b = \frac{PL}{48} - \frac{5PL}{88} = - \frac{19PL}{528} = - 0.036 PL$$

Example 4 - Deepened Beam (refer to Ex. 3).



From Ex. 3 :  $\bar{x} = \frac{7L}{12}$

$$J_c = \frac{11L^3}{96} \text{ (rel.)}$$

$$S_a = \frac{3.64}{L}, C_{ab} = 0.40, S_b = \frac{2.18}{L}, C_{ba} = 0.667$$

$$(EI)_a = 2,000,000 \times \frac{1}{12} 6 \times 8^3 = 5.12 \times 10^8 \text{ lb-in.}^2$$

$$(a) S_a = \frac{3.64 \times 5.12 \times 10^8}{240} = 7,770,000 \text{ lb-in.}$$

$$S_a = 647,000 \text{ lb-ft.}$$

$$S_b = \frac{2.18 \times 5.12 \times 10^8}{240} = 4,650,000 \text{ lb-in.}$$

$$S_b = 388,000 \text{ lb-ft.}$$

$$(b) \bar{x} = \frac{7L}{12} = \frac{7 \times 240}{12} = 140 \text{ in.}$$

$$J_c = \frac{11 \times 240^3}{96} \times \frac{1}{5.12 \times 10^8} = 3.09 \times 10^{-3} \frac{\text{in}}{\text{lb}}$$

$$M_a^A = \frac{A}{J_c} \bar{x} = \frac{0.5 \times 10^3}{3.09} \times 140 = 22,600 \text{ lb-in.}$$

$$M_a^A = 1,880 \text{ lb-ft.}$$

$$M_b^A = \frac{L - \bar{x}}{\bar{x}} M_a = \frac{240 - 140}{140} \times 1,880 = 1,344 \text{ lb-ft.}$$

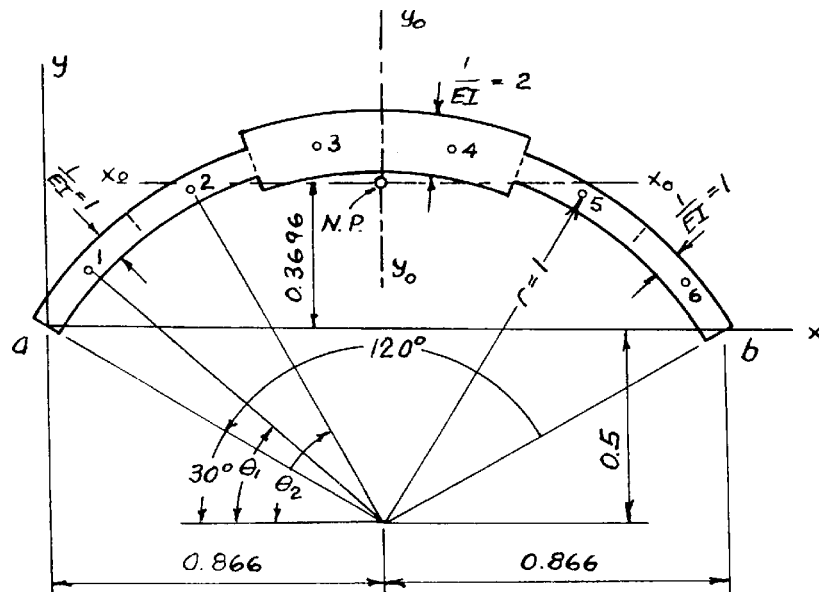
$$(c) M_a^\theta = \theta_a S_a = 0.00349 \times 647,000 = 2,260 \text{ lb-ft.}$$

$$M_b = M_a C_{ab} = 2,260 \times 0.40 = 904 \text{ lb-ft.}$$

$$(d) V = \frac{M_a + M_b}{L} = \frac{1,880 + 1,344}{20} = 161.2 \text{ lb.}$$

$$S_s = \frac{161.2 \text{ lb}}{0.5''} = 322.4 \frac{\text{lb}}{\text{in}}$$

### Example 5- Deepened 120° Circular Arch



See Table on the following page.

$$\bar{y} = \frac{\sum \frac{ds}{EI} y}{\sum \frac{ds}{EI}} = \frac{6.9568}{8} = 0.8696$$

$$M_a = S_a = \frac{1}{8} + \frac{(1)(0.866)^2}{1.7940} + \frac{(1)(0.3696)^2}{0.15622}$$

$$M_a = 0.125 + 0.420 + 0.875 = 1.42$$

In terms of any geometrically similar area  $A$ ,

$$M_a = \frac{1.42}{A} \times 8 = \frac{11.36}{A}$$

$$M_b = 0.125 - 0.418 + 0.875 = 0.582$$

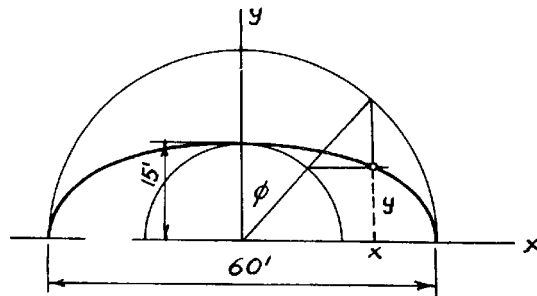
$$C_{ab} = C_{ba} = - \frac{0.582}{1.42} = -0.411$$

Table of Arch Properties ( $r=1$ )

Pt.	$\frac{ds}{EI}$	$\theta$	$x_o = \cos \theta$	$x_o^2$	$y = \sin \theta$	$y_o = \bar{y} - y$	$y_o^2$	$\frac{ds}{EI} y$	$J_{x_o}$	$J_{y_o}$
1	1	40°	-0.7660	0.5868	0.6428	-0.2268	0.05150	0.6428	0.05150	0.5868
2	1	60°	-0.5000	0.2500	0.8660	-0.0036	0.00001	0.8660	0.00001	0.2500
3	2	80°	-0.1736	0.0301	0.9848	+0.01152	0.01330	1.9696	0.02660	0.0602
4	2	100°	+0.1736	0.0301	0.9848	+0.1152	0.01330	1.9696	0.02660	0.0602
5	1	120°	0.5000	0.2500	0.8660	-0.0036	0.00001	0.8660	0.00001	0.2500
6	1	140°	0.7660	0.5868	0.6428	-0.2268	0.05150	0.6428	0.05150	0.5868
$\Sigma =$	8			1.7338			0.12962	6.9568	0.15622	1.7440



Example 6- Elliptical Arch (see L.C. Maugh, "Statically Indeterminate Structures," pages 220 to 228).



$$x = 30 \sin \phi$$

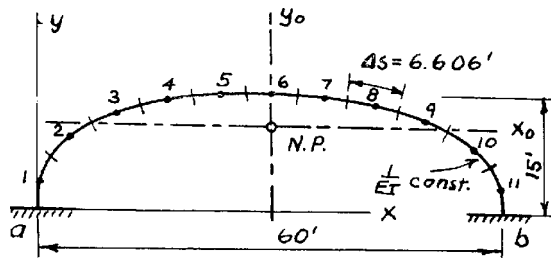
$$y = 15 \cos \phi$$

$$\begin{aligned} ds &= \sqrt{(dx)^2 + (dy)^2} = \sqrt{900 \cos^2 \phi + 225 \sin^2 \phi} d\phi \\ &= 15 \sqrt{4 \cos^2 \phi + \sin^2 \phi} d\phi = 30 \sqrt{1 - \frac{3}{4} \sin^2 \phi} d\phi \\ S &= (2)(30) \int_0^{\frac{\pi}{2}} \sqrt{1 - \frac{3}{4} \sin^2 \phi} d\phi \end{aligned}$$

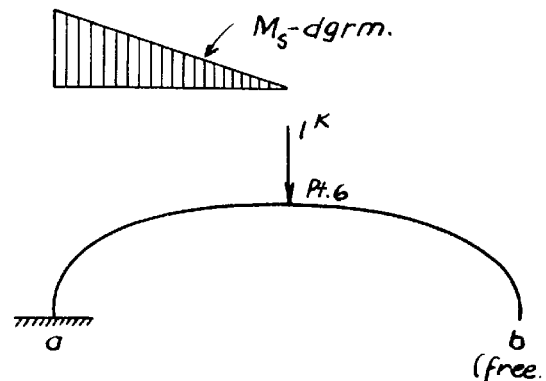
From Table of Elliptic Integrals, for  $k^2 = \frac{3}{4}$ ,

$$S = 60 \times 1.2111 = 72.666 \text{ ft.}$$

The arch rib will be subdivided into 11 equal elements  $\Delta s = \frac{72.666}{11} = 6.606 \text{ ft.}$



Arch Data



Statically Determinate Arch &  $M_5$  diagram

Arch Properties (relative values for  $\frac{\Delta S}{EI} = 1$ ). See Table on the following page.

$$A = \sum \frac{\Delta S}{EI} = 11$$

$$Q_x = \sum \frac{y \Delta S}{EI} = 117.08$$

$$Q_y = \sum \frac{x \Delta S}{EI} = 330.00$$

$$J_x = \sum \frac{y^2 \Delta S}{EI} = 1,438.26$$

$$J_y = \sum \frac{x^2 \Delta S}{EI} = 14,054.86$$

$$J_{xy} = \sum \frac{xy \Delta S}{EI} = 3,512.41$$

$$J_{x_0} = \sum \frac{y_0^2 \Delta S}{EI} = 192.11$$

$$J_{y_0} = \sum \frac{x_0^2 \Delta S}{EI} = 4,154.86$$

$$V = \sum \frac{M_s \Delta S}{EI} = 94.23$$

$$M_{x_0} = \sum \frac{M_s y_0 \Delta S}{EI} = 195.68$$

$$M_{y_0} = \sum \frac{M_s x_0 \Delta S}{EI} = 2,078.80$$

Location of Neutral Point N.A. -

$$\bar{x} = \frac{60}{2} = 30 \text{ ft. by symmetry}$$

$$\bar{y} = \frac{Q_x}{A} = \frac{117.08}{11} = 10.64 \text{ ft.}$$

$$\begin{aligned} (a) \quad S_a = M_a &= \frac{1}{A} + \frac{(\bar{x})^2}{J_{y_0}} + \frac{(\bar{y})^2}{J_{x_0}} \\ &= \frac{1}{11} + \frac{(30)^2}{4,154.86} + \frac{(10.64)^2}{192.11} \end{aligned}$$

$$S_a = 0.091 + 0.216 + 0.590 = 0.897 \therefore$$

$$S_a = \frac{0.897}{A} \times 11 = \frac{9.867}{A}$$

Table of Arch Properties

Pt.	$\frac{4\Delta}{EI}$	x	x <sup>2</sup>	y	y <sup>2</sup>	x <sub>0</sub>	y <sub>0</sub>	x <sub>0</sub> <sup>2</sup>	y <sub>0</sub> <sup>2</sup>	xy	$\frac{M_x \Delta S}{EI}$	$\frac{M_y \Delta S}{EI}$	$\frac{M_z \Delta S}{EI}$
1	1	0.70	0.49	3.18	10.11	-29.30	-7.46	858.49	55.65	2.23	-29.30	858.49	+218.58
2	1	4.90	24.01	8.21	67.40	-25.10	-2.43	630.01	5.90	40.23	-25.10	630.01	+61.10
3	1	10.65	113.42	11.50	132.25	-19.35	+0.86	374.42	0.74	122.48	-19.35	374.42	-16.65
4	1	16.90	285.61	13.50	182.25	-13.10	+2.86	171.61	8.18	228.15	-13.10	171.61	-37.45
5	1	23.45	549.90	14.65	214.62	-6.55	+4.01	42.90	16.08	343.54	-6.55	42.90	-26.30
5 $\frac{3}{4}$	0.5					-1.65	+4.34				-0.83	1.37	-3.60
6	1	30.00	900.00	15.00	225.00	0	+4.36	0	19.01	450.00			
7	1	36.55	1335.90	14.65	214.62	+6.55	+4.01	42.90	16.08	535.46			
8	1	43.10	1857.61	13.50	182.25	13.10	+2.86	171.61	8.18	581.85			
9	1	49.35	2435.42	11.50	132.25	19.35	+0.86	374.42	0.74	567.53			
10	1	55.10	3036.01	8.21	67.40	25.10	-2.43	630.01	5.90	452.37			
11	1	59.30	3516.49	3.18	10.11	29.30	-7.46	858.49	55.65	188.57			
$\Sigma$	11 <sup>1)</sup>	330.00	14,054.86	117.08	1,438.26			4,154.86	192.11	3,512.41	-94.23	2,078.80	+195.68

1) Does not include Pt. 5  $\frac{3}{4}$

$$M_b = 0.091 - 0.216 + 0.590 = 0.465$$

$$C_{ab} = - \frac{M_b}{M_a} = - \frac{0.465}{0.897} = - 0.517$$


---

(b) (Eq. 61)

$$S_a' = \frac{L^2}{J_{y_0} - \frac{J_{x_0 y_0}^2}{J_{x_0}}}$$

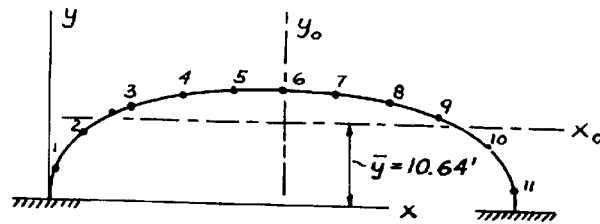
Since the centroid of area  $A$  shifts to the location of the hinge at  $b$ , and because of the symmetry of the arch,

$$\left. \begin{aligned} J_{y_0} &= J_b = J_y = 14,054.86 \\ J_{x_0 y_0} &= J_{a-b,b} = J_{xy} = 3,512.41 \\ J_{x_0} &= J_{a-b} = J_x = 1,438.26 \end{aligned} \right\} \text{ for } \frac{\Delta S}{EI} = 1$$

$$\begin{aligned} S_a' &= \frac{(60)^2}{(14,054.86 - \frac{(3,512.41)^2}{1,438.26}) 6,606} \\ &= \frac{3,600}{(14,054.86 - 8,600) 6,606} = \frac{3,600}{36,100} \end{aligned}$$

$$S_a' = 0.0996$$

# Example 7- Influence Lines for Reactions (Refer to Ex. 6).



## Load-Point Coordinates

Pt.	1	2	3	4	5	6	7, etc.
$x_0$	-29.30	-25.10	-19.35	-13.10	-6.55	0	symmetrical
$y_0$	-7.46	-2.43	+0.86	2.86	4.01	4.36	"

## Influence Values for $V_0$ & $V_a$

Pt.	$x_0$	1	2	3	4	5	6
1	29.30	$29.30 \cdot 0 = 0$	$29.30 \cdot 4.20 = 123.0$	$29.30 \cdot 9.95 = 292.0$	$29.30 \cdot 16.20 = 475.0$	$29.30 \cdot 22.75 = 666.0$	$29.30 \cdot 29.30 = 860.0$
2	25.10		$25.10 \cdot 0 = 0$	$25.10 \cdot 5.75 = 144.5$	$25.10 \cdot 12.00 = 302.0$	$25.10 \cdot 18.55 = 466.0$	$25.10 \cdot 25.10 = 631.0$
3	19.35			$19.35 \cdot 0 = 0$	$19.35 \cdot 6.25 = 121.0$	$19.35 \cdot 12.80 = 248.0$	$19.35 \cdot 19.35 = 375.0$
4	13.10				$13.10 \cdot 0 = 0$	$13.10 \cdot 6.55 = 85.7$	$13.10 \cdot 13.10 = 171.5$
5	6.55					$6.55 \cdot 0 = 0$	$6.55 \cdot 6.55 = 42.9$
6	0						$0 \cdot 0 = 0$
$\Sigma$		0	123.0	436.5	898.0	1465.7	2080.4
$V_0 = \frac{\Sigma}{J_{x_0}}$		0	$\frac{123.0}{4154.86} = 0.030 \uparrow$	$\frac{436.5}{4154.86} = 0.105 \uparrow$	$\frac{898.0}{4154.86} = 0.216 \uparrow$	$\frac{1465.7}{4154.86} = 0.352 \uparrow$	$\frac{2080.4}{4154.86} = 0.500 \uparrow$
$V_a = 1 - V_0$		1.000 $\uparrow$	0.970 $\uparrow$	0.895 $\uparrow$	0.784 $\uparrow$	0.648 $\uparrow$	0.500 $\uparrow$

## Influence Values for $H_0$ & $H_a$

Pt.	$y_0$	1	2	3	4	5	6
1	7.46	$-7.46 \cdot 0 = 0$	$-7.46 \cdot 4.20 = -31.4$	$-7.46 \cdot 9.95 = -74.4$	$-7.46 \cdot 16.20 = -121.0$	$-7.46 \cdot 22.75 = -170.0$	$-7.46 \cdot 29.30 = -219.0$
2	-2.43		$-2.43 \cdot 0 = 0$	$-2.43 \cdot 5.75 = -14.0$	$-2.43 \cdot 12.00 = -29.2$	$-2.43 \cdot 18.55 = -45.1$	$-2.43 \cdot 25.10 = -61.1$
3	+0.86			$+0.86 \cdot 0 = 0$	$+0.86 \cdot 6.25 = +5.4$	$+0.86 \cdot 12.80 = +11.0$	$+0.86 \cdot 19.35 = +16.7$
4	2.86				$2.86 \cdot 0 = 0$	$2.86 \cdot 6.55 = 18.7$	$2.86 \cdot 13.10 = 37.4$
5	4.01					$4.01 \cdot 0 = 0$	$4.01 \cdot 6.55 = 26.3$
6	4.36						$4.36 \cdot 0 = 0$
$\Sigma$		0	-31.4	-88.4	-144.8	-185.4	-199.7
$H_0 = \frac{\Sigma}{J_{y_0}}$		0	$\frac{-31.4}{192.11} = 0.162 \leftarrow$	$\frac{-88.4}{192.11} = 0.460 \leftarrow$	$\frac{-144.8}{192.11} = 0.752 \leftarrow$	$\frac{-185.4}{192.11} = 0.965 \leftarrow$	$\frac{-199.7}{192.11} = 1.040 \leftarrow$
$H_a = -H_0$		0	0.162 $\rightarrow$	0.460 $\rightarrow$	0.752 $\rightarrow$	0.965 $\rightarrow$	1.040 $\rightarrow$

### Influence Values for $M_o$

Pt.	1	2	3	4	5	6
1	$1 \times 0 = 0$	$1 \times 4.20 = 4.20$	$1 \times 9.95 = 9.95$	$1 \times 16.20 = 16.20$	$1 \times 22.75 = 22.75$	$1 \times 29.30 = 29.30$
2		$1 \times 0 = 0$	$1 \times 5.75 = 5.75$	$1 \times 12.00 = 12.00$	$1 \times 18.55 = 18.55$	$1 \times 25.10 = 25.10$
3			$1 \times 0 = 0$	$1 \times 6.25 = 6.25$	$1 \times 12.80 = 12.80$	$1 \times 19.35 = 19.35$
4				$1 \times 0 = 0$	$1 \times 6.55 = 6.55$	$1 \times 13.10 = 13.10$
5					$1 \times 0 = 0$	$1 \times 6.55 = 6.55$
6						$1 \times 0 = 0$
$\Sigma$	0	4.20	15.70	34.45	60.65	93.40
$M_o - \frac{\Sigma}{4}$	0	$\frac{4.20}{4} = 0.38$	$\frac{15.70}{4} = 1.43$	$\frac{34.45}{4} = 3.14$	$\frac{60.65}{4} = 5.52$	$\frac{93.40}{4} = 8.49$

Example. For load acting at point 6,

$$M_o = +8.49 + (1.040 \times 10.64) + (0.500 \times 30) - (1 \times 30)$$

$$M_o = 8.49 + 11.09 + 15.00 - 30.00 = +4.58 \text{ K-ft.}$$

Load Points 1 to 6 (Refer to Fig. 51a)

Point	1	2	3	4	5	6
$M_o$	0	0.38	1.43	3.14	5.52	8.49
$10.64 H_o$	0	1.72	4.90	8.01	10.29	11.09
$30 V_o$	0	0.90	3.15	6.48	10.56	15.00
$-1(30 + x_o)$	-0.70	-4.90	-10.65	-16.90	-23.45	-30.00
$M_o = \Sigma$	-0.70	-1.90	-1.17	+0.73	2.92	4.58

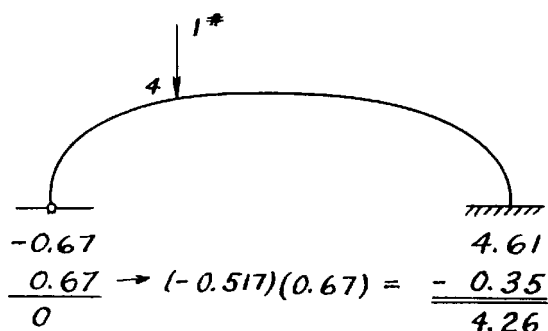
Load Points 7 to 11 (Refer to Fig. 51b)

Point	7	8	9	10	11
$M_b$	2.92	0.73	-1.17	-1.90	-0.70
$-60 V_a$	-21.12	-12.96	-6.30	-1.80	0
$1(30 - x_o)$	23.45	16.90	10.65	4.90	0.70
$M_o = \Sigma$	5.25	4.67	3.18	1.20	0

### Example 8- Fixed End Moment.

From Example 7,  $M_a = 0.67$ ,  $M_b = 4.61$

" " 6,  $C_{ab} = -0.517$



### Example 9- Effect of Impressed Distortions.

For arch data and properties, refer to Example 6.

$$E = 2,000,000 \text{ psi.} = 288 \times 10^6 \text{ psf.}$$

$$I = 0.667 \text{ ft.}^4 \text{ (const.)}$$

$$\alpha = 6 \times 10^{-6} \text{ per } 1^\circ$$

(a) Settlement of lin. at a.

$$M_a^{\Delta y=1} = \frac{\Delta \cdot \bar{X}}{J_{y_0}}$$

$$J_{y_0} = \frac{4,154.86 \times 6.606}{288 \times 10^6 \times 0.667} = 1.43 \times 10^{-4} \text{ (abs.)}$$

$$M_a = \frac{\frac{1}{12} \times 30}{1.43 \times 10^{-4}} = 17,490 \text{ lb-ft.}$$

(b) Rotation of 0.001745 rad. at a.

$$M_a = \frac{\theta_o}{A} + \frac{\theta_o(\bar{x})^2}{J_{y_o}} + \frac{\theta_o(\bar{y})^2}{J_{x_o}}$$

$$A = 11 \times \frac{\Delta S}{EI} = 11 \times \frac{6.606}{288 \times 10^6 \times 0.667} = 3.78 \times 10^{-7}$$

$$J_{x_o} = 192.11 \times \frac{\Delta S}{EI} = 192.11 \times \frac{6.606}{288 \times 10^6 \times 0.667} = 6.6 \times 10^{-6}$$

$$M_a = \frac{0.001745}{3.78 \times 10^{-7}} + \frac{0.001745 \times (30)^2}{1.43 \times 10^{-4}} + \frac{0.001745(10.64)^2}{6.6 \times 10^{-6}}$$

$$M_a = 4,610 + 11,000 + 30,050 = 45,660 \text{ lb-ft.}$$


---

(c) Temperature Change of  $+50^\circ$ .

$$\Delta L = L \alpha T = 60 \times 6 \times 10^{-6} \times 50 = 0.018 \text{ ft.}$$

$$M_a^{\Delta x = \Delta L} = \frac{\Delta L \times \bar{y}}{J_{x_o}} = \frac{0.018 \times 10.64}{6.6 \times 10^{-6}} = 29,000 \text{ lb-ft.}$$

$$M_{\text{crown}}^{\Delta x = \Delta L} = \frac{0.018}{6.6 \times 10^{-6}} (15 - 10.64) = 11,900 \text{ lb-ft.}$$


---

(d) Rib Shortening,  $S = 100 \text{ psi. (comp.)}$

$$\Delta L = \frac{S}{E} L = \frac{100 \times 144}{288 \times 10^6} \times 60 = 0.003 \text{ ft.}$$

$$M_a^{\Delta x = \Delta L} = \frac{0.003}{6.6 \times 10^{-6}} \times 10.64 = 4,840 \text{ lb-ft.}$$

$$M_{\text{crown}}^{\Delta x = \Delta L} = \frac{0.003}{6.6 \times 10^{-6}} \times (15 - 10.64) = 1,985 \text{ lb-ft.}$$


---

(e) Thrust Stiffness

$$T_s = \frac{1}{6.6 \times 10^{-6}} = 151,400 \text{ lb.}$$



BIBLIOGRAPHY

1. Costa, J. J., "Advanced Structural Analysis,"  
Edwards Brothers, Inc., 1953
2. Cross, H. and Morgan, N. D., "Continuous Frames of  
Reinforced Concrete," John Wiley & Sons,  
Inc., 1932
3. Grinter, L. E., "Theory of Modern Steel Structures,"  
Vol. II, The MacMillan Company, 1937
4. "Handbook of Frame Constants," Portland Cement Asso-  
ciation, 1947
5. Maugh, L. C., "Statically Indeterminate Structures,"  
John Wiley & Sons, Inc., 1951
6. Parcel, J. I. and Moorman, R. B. B., "Analysis of  
Statically Indeterminate Structures,"  
John Wiley & Sons, Inc., 1955
7. Sutherland H. and Bowman, H. L., "Structural Theory,"  
John Wiley & Sons, Inc., Third Edition,  
1942

VITA

Name: Otakar Ondra  
Place of Birth: Vítkovice, Czechoslovakia  
Date of Birth: August 5, 1914  
Father's Name: Otakar Ondra  
Mother's Name: Anděla Ondra  
Wife's Name: Sally Ondra

Education

1. Collège Français de Prague, Czechoslovakia, 1929 - 1932;  
B.A., 1932
2. České Vysoké Učení Technické, Prague, Czechoslovakia,  
1932 - 1938; Dipl.Ing. in C.E., 1938
3. Lehigh University, Bethlehem, Pa., 1938 - 1941;  
M.S. in C.E., 1940
4. Columbia University, Teachers College, New York, N.Y.,  
1941 - 1946; M.A. in Pedagogy, 1946
5. České Vysoké Učení Technické, Prague, Czechoslovakia;  
Dr.Techn., 1947
6. Professional Engineer; New York, Ohio, 1952

Membership in Societies

1. The American Society of Civil Engineers; Assoc. Member,  
1947
2. Société des Ingénieurs Civils de France; Member, 1947
3. The Society for the Promotion of Engineering Education;  
Member, 1943
4. The Society of the Sigma Xi, Lehigh Chapter; Associate  
Member, 1943

Membership in Societies, cont.

5. Fritz Engineering Research Society; 1940
6. Chi Epsilon Fraternity, Manhattan College Chapter;  
Honorary Chapter Member, 1952
7. American Rocket Research Association; Honorary Member,  
1954

Publications

1. "Balancing Earthwork by Graphics," The Highway Magazine,  
July - August, 1944
2. "Fundamentals of Engineering Mathematics," Edwards  
Brothers, Inc., 1945

Teaching and Professional Experience

1. Instructor, Assistant Professor, Associate Professor  
of Civil Engineering, Manhattan College, New York,  
N.Y., 1941 to date
2. Consulting Engineer for Associated Steel Mills of Czecho-  
slovakia, 1946 - 1949
3. Consulting Engineer for Department of Highways, British  
Guiana, 1948
4. Engineer in charge of Manhattan College research project  
"Torsional Vibration and Engine Damping," sponsored  
by the Navy Department, 1954 to date.

Address

4645 Arlington Avenue, New York 71, N.Y.